Results in Surfaces and Interfaces 23 (2026) 100750

Contents lists available at ScienceDirect

Results in Surfaces and Interfaces

journal homepage: www.elsevier.com/locate/rsurfi

Review Article

Tribological challenges in ocean energy systems: Failure mechanisms, materials, lubrication strategies, and reliability roadmaps

Rahul Kumar [a,b,*]

[a] Laboratory for Tribology and Interface Nanotechnology, University of Ljubljana, Askerceva 6, SI-1000, Ljubljana, Slovenia
[b] Department of Engineering Sciences and Mathematics, Luleå University of Technology, Luleå, SE 97187, Sweden

A R T I C L E I N F O

Keywords:
Ocean tribology
Marine renewable energy (MRE)
Tribocorrosion
Erosion
Biofouling
Marine lubrication
Offshore reliability
SDGs

A B S T R A C T

The vast renewable energy potential of the oceans remains largely untapped, not due to a lack of energy conversion concepts, but because the moving components of wave, tidal, and current energy systems experience premature failure under the ocean's aggressive tribological environment. This review dissects the coupled (multi-mode) phenomena of friction, wear, lubrication, corrosion, erosion, and biofouling that collectively dictate the reliability of marine energy converters. Moving beyond isolated failure analyses, it establishes a system-level framework that links component function, motion kinematics, and degradation pathways under real oceanic conditions. The synthesis reveals how mechanical stresses, and environmental agents coevolve to form self-reinforcing degradation loops, where corrosion debris, cavitation, and microbial colonization accelerate wear and frictional loss in ways conventional testing cannot replicate. By consolidating these insights, the study formulates the fundamental, unanswered questions that define the frontiers of ocean tribology such as how third-body dynamics, transient electrochemistry, and surface-adherent biofilms interact at the interface to control material durability. Addressing these gaps is pivotal to transforming tribology from an afterthought to a central design principle, enabling durable, predictable, and economically viable marine energy systems.

Abbreviations:

Abbreviation/Symbol	Definition
AISI	American Iron and Steel Institute
AW	Anti-Wear (additives)
COF (μ)	Coefficient of Friction
DLC	Diamond-Like Carbon (coatings)
EAL	Environmentally Acceptable Lubricant
EP	Extreme Pressure (additives)
EPDM	Ethylene Propylene Diene Monomer (rubber)
FKM	Fluorocarbon Elastomer (Viton)
HEES	Hydraulic Environmental Ester Synthetic
HEPG	Hydraulic Environmental Polyalkylene Glycol
HETG	Hydraulic Environmental Triglyceride (vegetable oils)
HNBR	Hydrogenated Nitrile Butadiene Rubber
HSLA	High-Strength Low-Alloy (steels)
HVOF	High-Velocity Oxy-Fuel (thermal spray coating)
i_{corr}	Corrosion Current Density
K	Specific Wear Rate
LCOE	Levelized Cost of Energy
MIC	Microbiologically Influenced Corrosion
MRE	Marine Renewable Energy
MTBF	Mean Time Between Failures
NBR	Nitrile Butadiene Rubber
OCT	Ocean Current Turbines
OTC	Ocean Tribology Center
OWC	Oscillating Water Column
PAG	Polyalkylene Glycol
PCD	Polycrystalline Diamond
PEEK	Polyether Ether Ketone
PET	Polyethylene Terephthalate
PH	Precipitation-Hardened (steels)
PSU	Practical Salinity Units
PTFE	Polytetrafluoroethylene
PTO	Power Take-Off (system)
PU	Polyurethane
PV	Pressure-Velocity limit
Ra	Arithmetic average of Surface Roughness
SCC	Stress Corrosion Cracking
SDG	Sustainable Development Goal
SLIPS	Slippery Liquid-Infused Surface
SRB	Sulfate-Reducing Bacteria

(*continued on next page*)

* Department of Engineering Sciences and Mathematics, Luleå University of Technology, Luleå, SE 97187, Sweden.
E-mail addresses: Rahul.kumar@associated.ltu.se, Rahul.Kumar@fs.uni-lj.si.

https://doi.org/10.1016/j.rsurfi.2026.100750
Received 25 October 2025; Received in revised form 30 January 2026; Accepted 22 February 2026
Available online 23 February 2026

(*continued*)

Abbreviation/Symbol	Definition
TEC	Tidal Energy Converter
TPU	Thermoplastic Polyurethane
TRL	Technology Readiness Level
TTF	Time To Failure
UHMWPE	Ultra-High-Molecular-Weight Polyethylene
VI	Viscosity Index
VIV	Vortex-Induced Vibration
WEC	Wave Energy Converter
ZDDP	Zinc Dialkyldithiophosphate

1. Introduction

Marine renewables are the inevitable frontier for a net-zero 2050, with tidal and wave resources offering energy densities tens to hundreds of times greater than those of solar and wind [1]. However, converting this potential into durable, commercial-scale systems has proven difficult [2,3]. Early prototypes such as Pelamis, etc. encountered recurring mechanical and material failures, where tribological issues i.e. friction, wear, and lubrication breakdown emerged as dominant but insufficiently addressed factor [4–9]. The marine environment amplifies these effects through coupled mechanical and chemical interactions that accelerate degradation beyond standard design expectations [5,7,10–13]. Components that would remain functional for decades on land can deteriorate within months offshore [14–16]. Laboratory studies struggle to reproduce these conditions accurately due to limited understanding of failure mechanisms, scarcity of relevant field data, and inadequate tribological test design [17]. This persistent gap between experimental and operational realities constrains technology readiness (TRL), leading to high maintenance demands, reduced availability, and levelized energy costs (LCOE) that remain uncompetitive with established renewables [17,18]. Hence, developing durable ocean tribological systems, particularly for energy converters, is imperative to accelerate decarbonization and achieve global clean energy targets [19–22]. Fig. 1 schematically outlines the transition from vast ocean energy potential to a reliable, sustainable power generation system.

Unlike wind, solar or hydropower systems, where tribological issues are comparatively well-understood, characterized and mitigated, new entrants i.e. offshore wave and tidal energy converters operate in one of the most mechanically and chemically aggressive environments conceivable: high salinity, variable pH, unsteady hydrodynamic loading, abrasive particulate matter, and biofouling pressures are simultaneously imposed on dynamic interfaces [7,10,12,20]. While hydrodynamic efficiency and structural fatigue receive significant attention, it is often tribology at the interface level that dictates whether a system can operate reliably over extended deployments [10]. Here, the loading regimes are not only cyclic but also highly stochastic in wave energy devices [23,24], bidirectional in tidal turbines [25,26], and continuous but debris-laden in ocean-current systems [27,28]. Many components such as power take-off mechanisms, turbine shafts, blade root interfaces, mooring connections, bearings, and seals operate in either near-dry (splash), boundary or mixed lubrication regimes, often exposed to sediment, seawater chemistry fluctuations, and evolving biofouling layers [6,7,12,29]. Unlike offshore oil and gas systems, where maintenance can be routine and surfaces can be designed for inspection, wave or tidal energy converters are typically deployed for years (typically 25+ years), offshore (6-23 km), fully submerged (0-1000 m), and without easy access [21,30].

Moreover, ocean energy systems present a uniquely coupled multi-degradation environment, a convergence of wear, corrosion, fatigue, cavitation, and biological or organic colonization often acting with nonlinear synergies [12,13,31,32]. This makes component-level failure prediction and materials selection highly nontrivial. For instance, bearings and ocean rods in submerged power take-off (PTO) units undergo reciprocating or oscillatory motion under varying lubrication regimes and may simultaneously face abrasive wear, tribo-corrosion, and seal leakage induced by marine fouling [24,26,33]. Here, surface wear accelerates corrosion (coating failure exposes nascent surface) [34]. Cavitation-induced pitting promotes fatigue [35,36]. Biofouling adds roughness to the surface and alters flow and contact regimes, turning a well-lubricated joint into a partially starved one [13,37]. Similarly, PTO's ocean rod and tidal turbine shafts experience fluctuating torque loads under biofouled and cavitating conditions where the effectiveness of conventional coatings or stainless alloys often proves short-lived [9,31,34,38]. Materials such as duplex steels (ocean rods), bronze alloys, and polymeric seals/bearings have been adapted, but not necessarily optimized, for these environments [15,31,39,40]. Coating solutions like hardfacing, diamond-like carbon (DLC), or thermally sprayed ceramics often face premature failure due to poor adhesion (to the substrate) under wet cyclic conditions, galvanic mismatches, or surface fatigue [15,28,32,41,42]. Fig. 2 shows schematic interplay of materialistic, environmental and tribological factors that govern ocean/marine tribological and energy systems.

Despite this, the design of tribological components in wave and tidal energy systems has largely relied on extrapolations from offshore oil & gas (riser) and naval tribology, domains that lack comparable motion types, frequency spectra, and system architectures. Few standards exist for wear testing in saline, particle-laden fluids with fouling under dynamic load [43–45]. However, tribo-corrosion and bio-tribology (biofouling or organic matter exposure) are still studied mostly in isolation, not as part of integrated mechanical systems [5,6]. As a result, component lifetimes are poorly predicted, maintenance intervals uncertain, and the overall LCOE remains high [46,47].

By addressing multimode-wear coupling, corrosion, biofouling, and lubrication instability, this work directly supports the global transition

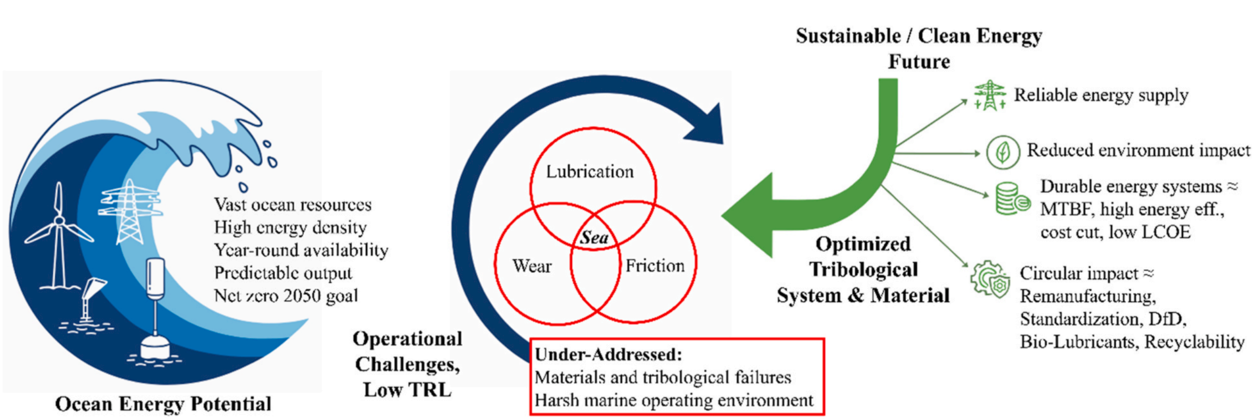

Fig. 1. Bridging the gap from ocean to sustainable energy future.

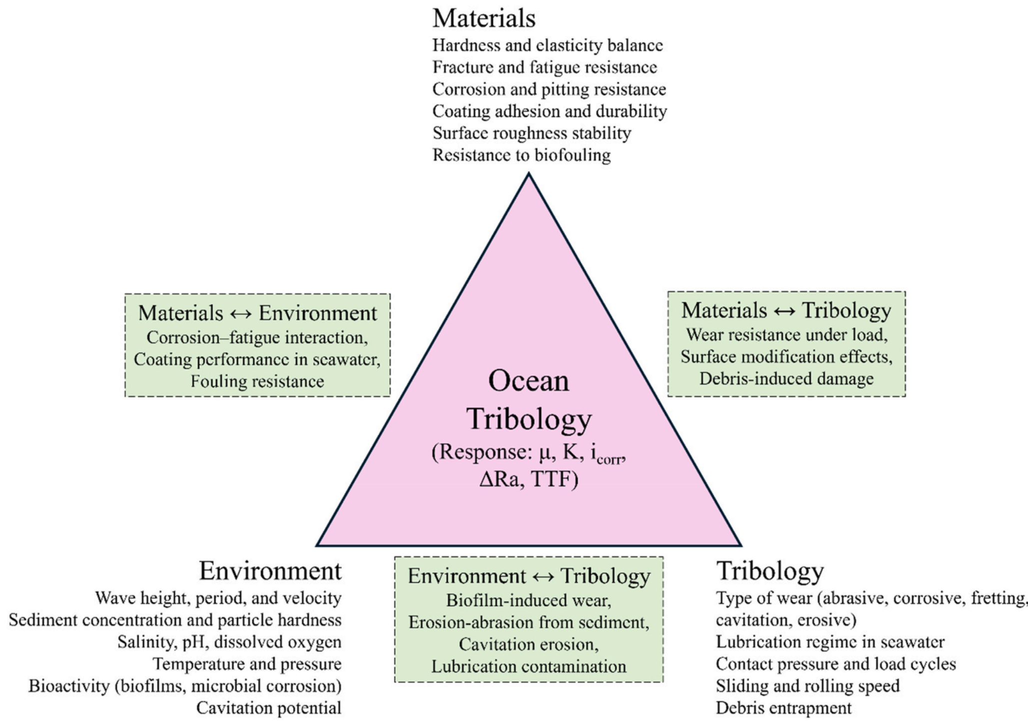

Fig. 2. The ocean tribology response triangle, illustrating the interplay between materials, environment, and tribology that governs the performance and durability of marine energy systems.

to clean power (SDG 7: Affordable and Clean Energy). Enhancing material resilience and reliability in harsh oceanic environments contributes to the development of durable and cost-effective infrastructure (SDG 9: Industry, Innovation, and Infrastructure), a prerequisite for bankable wave and tidal technologies. Reducing unplanned maintenance and extending component lifetimes directly lowers environmental footprint, aligning with sustainable coastal development strategies (SDG 11: Sustainable Cities and Communities). At the same time, improving system longevity and lowering life-cycle emissions strengthen the role of ocean energy in climate mitigation (SDG 13: Climate Action). Finally, the interdisciplinary nature of tribology i.e. spanning materials science, marine engineering, and environmental science exemplifies the partnerships across academia, industry, and policy required to accelerate sustainable deployment (SDG 17: Partnerships for the Goals). The main objectives of this review paper are.

- **Map operational tribology in ocean energy:** Provide a structured analysis of tribological conditions in wave, tidal, and current energy systems, linking component motion, loading modes, and lubrication regimes to specific wear and failure processes.
- **Identify critical degradation couplings:** Highlight the interplay between corrosion, erosion, cavitation, and biofouling, showing where multi-degradation accelerates component failure and compromises reliability.
- **Define performance benchmarks:** Establish quantitative targets for friction, wear, corrosion resistance, and fouling mitigation that can guide material design, surface engineering, and lubricant strategies in marine environments.
- **Show future pathways:** Pinpoint where emerging materials, coatings, and lubricants; along with additive manufacturing and in-situ refurbishment offer the greatest promise, while clarifying where current testing protocols and field data remain insufficient.

2. Methodology of review

This review synthesizes findings from a systematic analysis of 300 cited works. To ensure the synthesis reflects the current state of the art, the review is predominantly built upon contemporary research, with ~84% of the cited literature published within the last decade (2015-2025). To map the research landscape quantitatively, we employed a thematic co-occurrence analysis. Each paper was categorized by its core topics. A single paper was counted in all relevant categories, reflecting the field's interdisciplinary nature. These counts are termed "thematic assignments." A total of ~517 thematic assignments were realized. The prevalence of each research theme is calculated based on its frequency of occurrence (thematic instances).

The data reveals a clear research hierarchy. Corrosion and tribocorrosion constitute the primary challenge in 98 thematic instances (~19.0% of thematic focus), followed by wear and friction (87 instances, ~16.8%), biofouling (62 instances, ~12.0%), and lubrication (58 instances, ~11.2%). The study of multi-degradation synergy is a niche area, covered in only 4 papers (0.8%). For mitigation strategies, research is dominated by coatings and surface engineering (87 instances, ~16.8%) and the development of new materials (77 instances, ~14.9%); while monitoring and digital tribology represents an emerging focus (10 instances, ~1.9%), with most publications post-2017. The remaining (~6.6%) encompass contextual studies on ocean energy policy, fundamental marine science, and other niche topics. Notably, only three papers directly combine "tribology" with "wave" or "tidal" in their titles. This framework objectively highlights the field's priorities, confirming that the direct application of tribology to ocean energy is a nascent synthesis that this review consolidates into a dedicated framework (Fig. 3).

3. Tribological dynamics of ocean energy systems

Ocean energy systems in the current work are categorized into three types: wave energy converters, tidal energy converters, and ocean-current energy converters. Each of these operates in a distinct marine environment, with characteristic flow profiles, system architectures, and tribological demands and the tribological performance cannot be generalized. Tribo-design must therefore be system-specific, and ideally

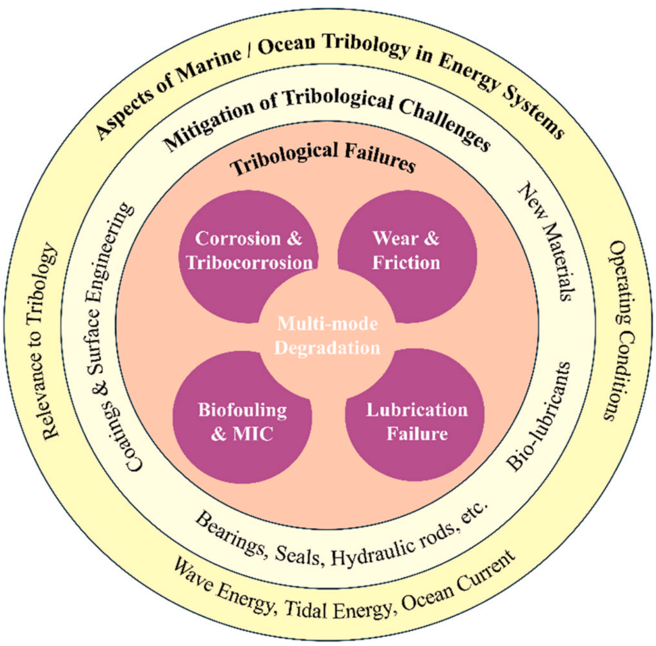

Fig. 3. Schematic framework outlining the key tribological challenges in marine energy systems discussed in this review.

component-specific within each system [17]. While they share exposure to saline conditions, high humidity, and marine fouling, their tribological behavior diverges significantly in how contact mechanics, lubrication conditions, surface interactions, and environmental exposures manifest across key interfaces. These differences are central to how friction, wear, corrosion, and surface fatigue manifest and interact in real components.

3.1. Wave energy converters (WECs)

WECs are categorized by their fundamental operating principle, which dictates their method of energy capture and conversion. The primary archetypes include Point Absorbers, which utilize the heaving motion of a buoy; Oscillating Water Columns (OWCs), which harness wave-induced air pressure changes to drive a turbine; Attenuators, which capture energy from the flexing motion along their multi-segment length; Oscillating Wave Surge Converters, which use the back-and-forth motion of a seabed-mounted flap; and Overtopping Devices, which exploit the potential energy of water stored in an elevated reservoir (Fig. 4). Each of these distinct architectures presents a unique set of engineering challenges, particularly for their moving mechanical components and tribological interfaces [48]. This results in unique sets of tribological interfaces distributed across moving joints, conversion linkages, and structural constraints. Because WECs are typically surface-piercing, these components must function under highly variable environmental conditions exposed to wet-dry cycling, wave impact, and dynamic alignment changes [33]. Fig. 5 depicts different WECs systems and their energy harnessing routes.

Key interfaces in different types of wave energy generation systems include.

- Reciprocating mechanical linkages, including pistons, guide rods, or mechanical arms, transmit heave or pitch motions to PTO systems. These operate at low frequency but with a large amplitude, under alternating loads [52].
- Linear and rotary PTO components (e.g., hydraulic cylinders, ball screws, gears) undergo oscillatory motion in partially submerged or fully immersed conditions [48].
- Bearings and bushings at mechanical pivots, joints, and sliders accommodate bi-directional rotation or translation, often within the splash or intertidal zones [29].
- Sealing elements, including dynamic rod seals, bellows, or sliding O-rings, are located at hydraulic or mechanical interfaces to maintain fluid integrity and isolate moving components from seawater ingress [53].

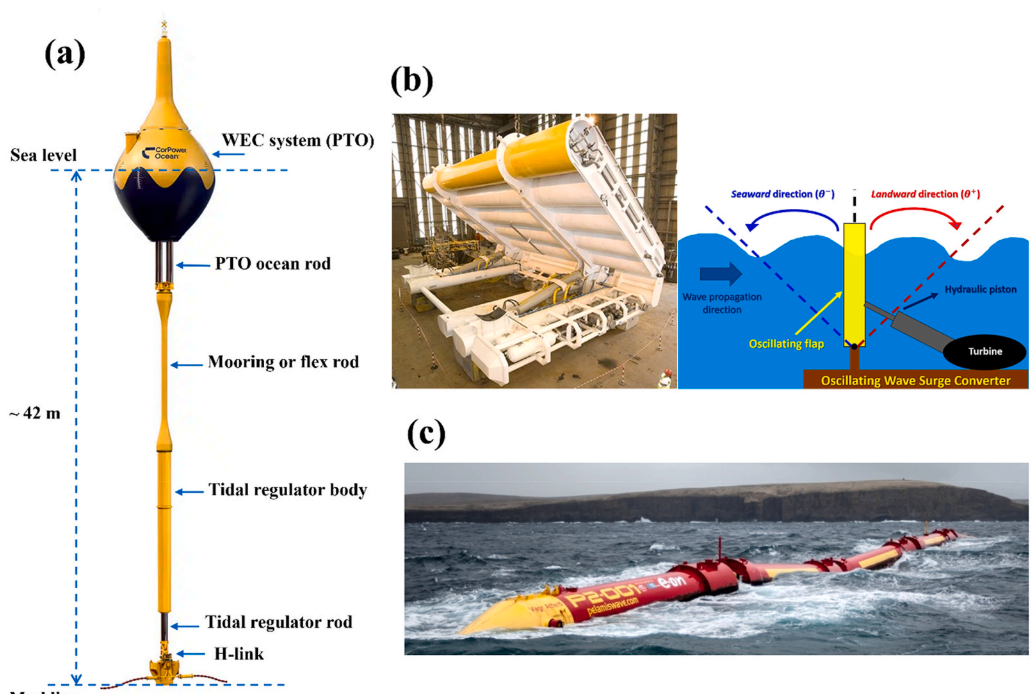

Fig. 4. Typical wave energy converter types: (a) point absorber [49], (b) oscillating wave surge [50], and (c) attenuator [51].

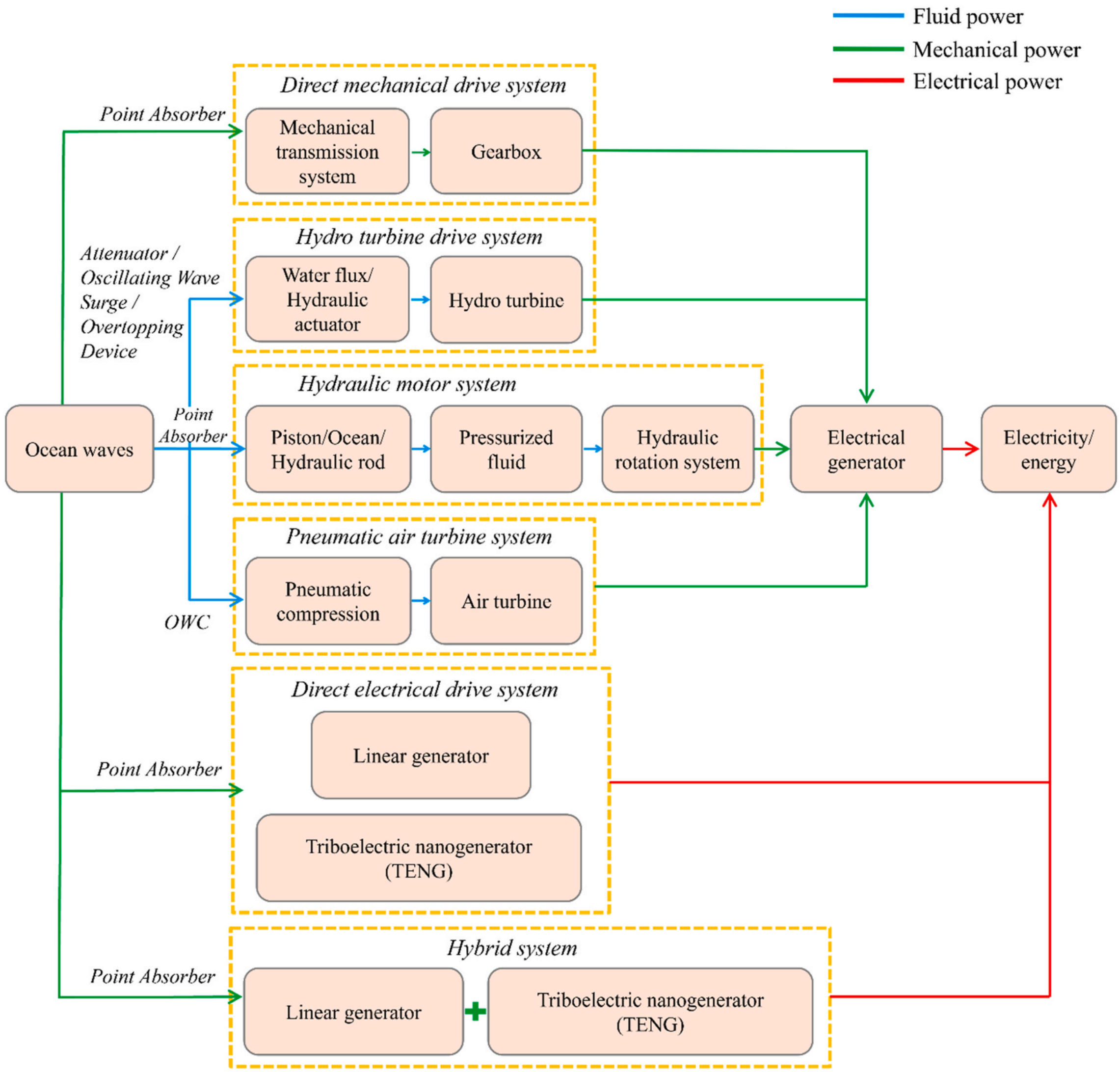

Fig. 5. Flowchart showing types of WECs and their energy production routes from ocean waves.

- Mooring line attachments including swivels, chain connectors, and clevis pins secure the device to the seabed. These interfaces enable compliant motion under wave excitation and tidal drift [42,54].
- Articulated joints, such as hinge assemblies in multi-body attenuators, allow large angular displacements between floating sections and may include low-friction liners or rolling-contact elements [55].
- Guideways or surface slides, especially in shoreline-mounted OWCs or tethered point absorbers, operate at variable immersion depths with constrained lateral motion [48].

3.2. *Tidal energy converters (TECs)*

Tidal energy systems harness the ocean's tides through several distinct technological pathways, each with unique operational principles and engineering challenges as shown in Figs. 6 and 7. One prominent method, tidal stream generation, extracts kinetic energy from horizontal tidal currents using submerged turbines that undergo continuous rotational motion. These systems incorporate hydrodynamic control surfaces for optimization and are mounted on submerged

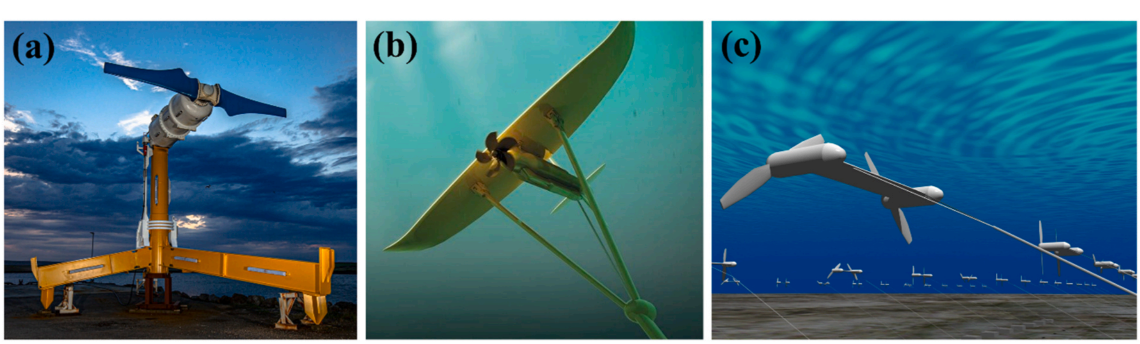

Fig. 6. Showing (a) horizontal-axis tidal turbine, (b) tidal kite driven by ocean tide/or current [56], and (c) floating underwater marine-current turbine [57].

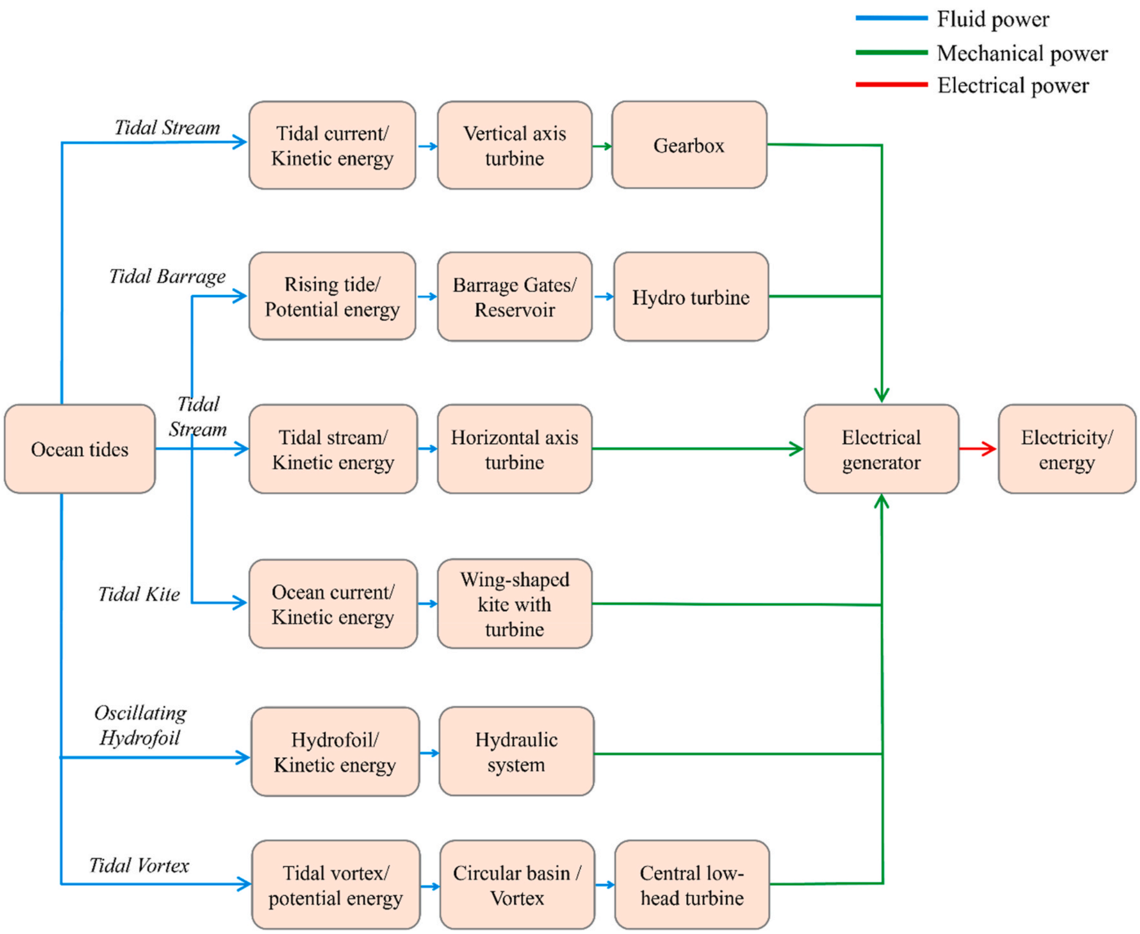

Fig. 7. Flow chart showing types of TECs and energy production routes from ocean tides.

support structures, with critical tribological interfaces spanning power transmission, control mechanisms, and station-keeping elements requiring compact, sealed designs to function in the thermally stable yet hydrodynamically active environments at depths of 10-70 m [24,26]. In contrast, tidal barrages operate on a fundamentally different principle, leveraging potential energy by impounding water behind large dam-like structures and releasing it through low-head hydro turbines, which experience intermittent, bidirectional flow rather than continuous rotation. Similarly, oscillating hydrofoil systems convert kinetic energy not through rotation but via the oscillatory motion of a hydrofoil driving hydraulic pumps, presenting tribological challenges centered on reciprocating rather than rotational components. Another emerging approach, tidal vortex systems, guides water into a controlled whirlpool to drive a central turbine, combining aspects of both potential and kinetic energy conversion with a unique vortex-induced loading profile. These methodological differences directly influence the nature and demand on their tribological systems, from the continuous rotational interfaces in tidal stream devices to the intermittent sliding contacts in barrages and oscillating hydraulics, all requiring robust sealing and corrosion resistance in the harsh marine environment.

Key interfaces in different types of tidal energy generation systems include.

3.2.1. *Tidal current/stream generators*

- Main turbine shafts are supported by bearings operating under continuous rotation, often with variable torque due to tidal speed variation and flow reversal [58].
- Blade pitch control systems, common in axial-flow designs, use actuated splines or hinges to adjust blade angle. These are low-frequency rotary or oscillatory interfaces under internal loading [59].
- Yaw mechanisms, implemented in floating TECs, allow nacelle orientation to align with reversing flows. These may involve slewing rings or rotary bushings [26].
- Gearbox and generator couplings include high-torque transmission elements inside pressurized nacelles, operating at moderate speeds with controlled lubrication [29].
- Dynamic shaft seals at the turbine-hull interface maintain dry internals under hydrostatic pressure and flow-induced vibration [60].
- Foundation or support structure joints, such as bolted flanges or base connectors, allow for assembly flexibility and tolerance management [61].
- Mooring systems, particularly in floating or semi-submersible designs, involve chain connectors, spherical joints, or flexure elements to accommodate tidal drift and structural oscillation [54].

3.2.2. *Tidal barrages and lagoons*

- Low-head turbine bearings and seals for bi-directional flow operation.
- Sluice gate trunnion bearings and hinges supporting massive oscillating gates.
- Sluice gate actuator systems, including hydraulic cylinder rods or screw jacks.
- Gate seals to prevent water leakage around closed gates.

3.2.3. Oscillating hydrofoils and other reciprocating systems

- Main hydrofoil pivot bearings for large-angle oscillatory motion.
- Hydraulic actuator cylinders, including piston rods, liners, and high-pressure seals.
- Hydraulic motor internals (bearings, seals) if used for power generation.

3.2.4. Tidal vortex systems

- Central turbine bearings under vortex-induced loading.
- Guide vane pivot mechanisms and their associated seals.

3.3. Ocean-current turbines (OCTs)

Ocean current energy systems exploit slow but persistent geostrophic flows such as boundary currents (e.g., Gulf Stream). These devices are generally deployed in deep-sea environments, with large, slow-rotating turbines and pressure-tolerant mechanical subsystems [62]. Tribological interfaces here are defined by deep-submerged (500-2000 m) [62], low-frequency operation with near-zero maintenance access.

- Main rotational shafts connect large-diameter rotors to sealed transmission housings, operating at steady, low angular velocities under constant hydrodynamic loads [62].
- Thrust bearings and radial supports manage rotor-induced loads within compact, pressure-isolated housings.
- Blade root connections, which may be rigid or semi-compliant, include splines, keyed hubs, or flexure couplings to manage manufacturing tolerances and long-term loading.
- Deep-sea sealing assemblies, such as metallic bellows, pressure-balanced seals, or compliant polymer barriers, protect internal systems from high hydrostatic loads [63].
- Mooring systems, required to maintain station in deep currents, include high-strength chain or cable connections, ball joints, and tensioned suspension elements designed for minimal structural drift [64].
- Internal mechanical couplings, including reduction gearsets or magnetic couplings, may be housed within flooded or dry enclosures, depending on system design [65].

3.4. Comparative operating conditions

While wave, tidal, and ocean current energy systems all harness marine hydrodynamics, their operating differences are rooted in flow regime, deployment depth, motion type, and environmental coupling that shape the nature of tribological contacts.

WECs operate closest to the ocean surface (0-20 m), where oscillatory energy from wave motion drives reciprocating linkages, sliding joints, and dynamic sealing systems [24]. These devices encounter the broadest range of thermal conditions (5-30 °C), and though the ambient pressure is low (~1-2 bar), components are frequently exposed to wet-dry cycling, impact loads, and surface splash [17]. Particulate exposure from suspended sand or marine debris is moderate, but biofouling is intense due to nutrient-rich and light-penetrated surface layers [66]. These systems are comparatively easier to access, allowing for periodic maintenance, but their interfaces must accommodate high-frequency reversals and structural compliance across mooring and PTO elements.

The tribological landscape of TECs is defined by their core motion i.e. continuous rotation in tidal stream devices, oscillation in hydrofoils, and intermittent operation in barrages and vortex systems. Among TECs, tidal stream devices are submerged in shallow-to-moderate depths (10-70 m), extract energy from bidirectional or unidirectional tidal flows with steady-state or reversing rotational shafts [26]. While flow velocities (1-5 m/s) are lower than wave crest speeds, the energy density remains very high due to flow mass and velocity cube dependence [67]. Tribologically, these rotary-based TECs are defined by continuous rotation in high-load environments, with critical interfaces in pitch mechanisms, yaw bearings, and nacelle-mounted shafts. These devices face elevated sediment loads especially in estuarine and nearshore zones leading to abrasive exposure of blade surfaces, seals, and moving parts. Temperature fluctuations are smaller (typically 5-15 °C) [68], but access limitations and subsea maintenance challenges place high importance on long-life, sealed, and low-maintenance interface designs.

OCTs are typically located at depths of 500-2000 m, operate under the most thermally and hydrodynamically stable conditions, but at the cost of extremely high hydrostatic pressures (50-200 bar). These devices rotate slowly (<0.1 Hz) in low-velocity flows (<1 m/s), targeting continuous base-load generation rather than peak power [69]. Their tribological architecture favors slow-speed, high-reliability components such as deep-sea bearings, thrust supports, and compliant joints often within pressure-compensated housings [62]. Particulate exposure is minimal, and biofouling progresses slowly [70,71], but the primary challenge is inaccessibility. Maintenance must be minimized or eliminated entirely through long-life materials and autonomous operation.

A comparative summary of these parameters is provided in Table 1. Tribologically, WECs are characterized by stochastic oscillatory loading with high risk of boundary film collapse and seal damage from bio-debris. TECs primarily suffer from bidirectional wear, sediment-induced abrasion, and cavitation at blade roots. OCTs experience slow, continuous motion where deep-sea pressure and inaccessibility accelerate long-term tribo-corrosion. Additionally, a relatively less mature, Vortex-Induced Vibration (VIV) based energy systems introduce tribological challenges characterized by high-frequency fretting and small-amplitude fatigue at tethering and pivot points, requiring specialized bearing interfaces capable of resisting rapid, repetitive shear stress in saline environments [72]. Besides, VIV -induced fretting can outpace the re-passivation kinetics of metallic surfaces, leading to localized tribocorrosion and seal degradation even during periods of low wave or tidal activity.

4. Tribological relevance of operating conditions

This section provides a consolidated overview of the measurable operating conditions with data drawn from public-domain sources including experimental deployments (e.g. EMEC, Pelamis, SeaGen), hydrodynamic simulations, as well as validated OEM specifications and oceanographic datasets [51,77,78]. These envelopes represent the tribologically significant boundary conditions for marine energy systems. Fig. 8 shows typical depth profiles of physicochemical parameters (dissolved oxygen, temperature, pH, and salinity) measured at a specific testing site in the Pacific Ocean [79].

Marine tribo-components are immersed in seawater environments exhibiting variable salinity (30-38 PSU), temperatures ranging from −2 to 35 °C depending on deployment zone and depth, and pH conditions typically between 7.5 and 8.4 [11,80,81]. Bioactivity is high in near-surface zones, with dissolved oxygen often exceeding 6 mg/L and suspended particulates reaching up to 500 mg/L in dynamic coastal regions, particularly during storms or spring tides [82,83]. These particulates, primarily composed of silts, quartz, and biogenic debris, infiltrate sealing interfaces and induce erosive wear in dynamic contacts [83]. Hydrostatic pressures are depth-dependent and typically range from 0.1 MPa at the surface to around 20 MPa at 2000 m deployment conditions common in tidal and moored wave systems though pressures exceeding 10 MPa are rare and typically not encountered in current-generation marine energy deployments [81,84–86]. These general parameters are tabulated in Table 2.

WECs are subjected to large, low-frequency oscillations dictated by sea states, with wave heights ranging from 0.5 to over 10 m and typical wave periods between 5 and 20 s [24,52,76]. Such kinematics induces cyclic stroke velocities of 0.2-1.5 m/s in PTO components, particularly

Table 1
Contextual overview of mechanical and environmental boundaries within marine energy systems [24,26,48,62,67–70,73–76].

Parameter	Wave systems	Tidal systems	Ocean-current systems
Energy potential	High	Very High	Low
Flow velocity	3-20 m/s (oscillatory)	1-5 m/s (unidirectional or bidirectional)	0.1-1 m/s (steady state)
Location	Surface/subsurface (0-20 m depth)	Fully submerged (10-70 m depth)	Fully submerged (500-2000 m depth)
Amplitude	1-8 m wave height	0.5-10 m tidal range	-
Frequency of Mechanical Motion	0.05-0.3 Hz (reciprocating, heaving, pitching, surge)	0.05-0.3 Hz (continuous or intermittent rotation)	0.01-0.1 Hz (slow rotation)
Operating pressure	~1-2 bar (near surface)	~2-6 bar (shallow submerged)	~50-200 bar (depth-dependent)
Temperature range	5-30 °C	5-15 °C	2-10 °C (deep sea, stable)
Particulate contamination	Moderate (spray, marine debris)	High (silt, estuarine sediment)	Low (open ocean, but bio-debris)
Biofouling rate	High (algae, barnacles, macrofouling)	Moderate to high (hard fouling species)	High (long-term barnacle accumulation)
Maintenance accessibility	Moderate (surface access possible)	Low (diver/ROV dependent)	Very low (deep-sea, autonomous)

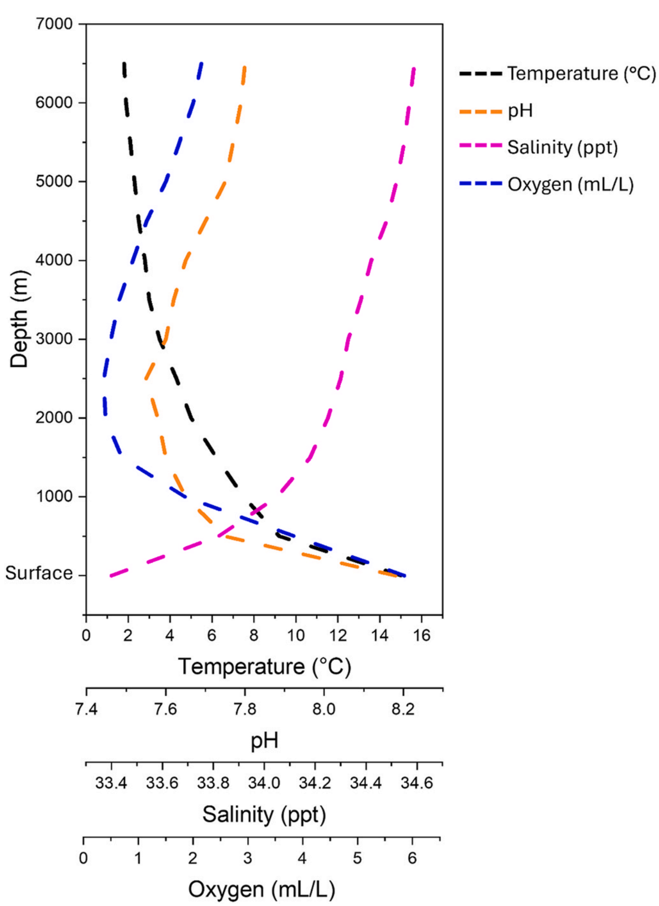

Fig. 8. Vertical profiles of dissolved oxygen, temperature, pH, and salinity versus depth at a Pacific Ocean corrosion test site. Adapted from Ref. [79].

in linear hydraulic systems [75,88]. The associated actuator pressures can exceed 30 MPa during energetic sea states, imposing significant Hertzian contact stresses in internal surfaces, including ocean rod-cylinder interfaces and guide bushings [24,25,31,89,90]. Moreover, the proximity to the air-sea interface enhances oxygen ingress and biofouling load, with marine growth thickness often exceeding 10 mm within weeks [87,91,92]. These key conditions are summarized in Table 3.

TECs operate under quasi-steady unidirectional flow regimes, with peak current velocities between 1 and 5 m/s driving relatively slow rotational speeds in submerged turbines, typically between 10 and 30 RPM [24,67]. Such low-speed, high-load operation promotes boundary and mixed lubrication regimes in main shaft and gearbox bearings [24,26]. Gearbox input torques can reach several hundred kilonewton-meters, particularly in multi-megawatt class turbines [94–96]. Blade pitch systems experience oscillatory actuation synchronized with tidal cycles, often undergoing two to four full angular reversals per tidal period, exposing pitch bearings and actuator seals to oscillatory micro-movements susceptible to fretting [97,98]. Cavitation is a relevant concern on leading edges of turbine blades in fast-flowing sites, with localized negative pressures potentially dropping below 30 kPa in turbulent wake zones [35,99]. The typical envelope for such

Table 2
Environmental conditions shared across marine systems [11,80–83,85–87].

Parameter	Typical range	Relevance to tribology
Seawater temperature	5 °C to 30 °C	Varies with location and depth. Influences lubricant viscosity and corrosion rates.
Salinity (NaCl eq.)	30-38 PSU	High ion concentration drives galvanic and crevice corrosion in submerged tribo-contacts.
Dissolved oxygen	3-10 mg/L	Facilitates corrosion-oxidation mechanisms; varies with depth and biological activity.
PH	7.5-8.4	Marginal alkalinity, local acidification can occur near biofilms or crevice zones.
Suspended particulate load	10-500 mg/L (coastal), 0.1-10 mg/L (deep)	Silt and sand ingress are major sources of third-body abrasion in seals and joints.
Hydrostatic pressure	0.1 MPa (surface) to 20 MPa (2000m)	Governs seal load, lubricant density, cavitation resistance in deep-submerged systems.

Table 3
Operating envelope of WECs and their corresponding tribological relevance [12,24,52,74,76,77,81,84,85,87,92,93].

Parameter	Typical range	Relevance to tribology
Wave height	0.5-10 m (significant), up to 20 m (extreme)	High wave heights drive actuator stroke and joint angular displacement; affect contact force.
Wave period	5-20 s	Determines oscillation frequency of PTO and articulated joints.
PTO stroke velocity	0.2-1.5 m/s	Affects lubrication regime in hydraulic actuators and guides.
PTO pressure (hydraulic)	5-35 MPa	Drives contact stress in piston-cylinder interfaces and seal deformation.
Surface water speed	0.5-3 m/s (horizontal motion)	Influences erosion rate of surface-exposed coatings and mooring fatigue.
Biofouling growth rate	1-10 mm/month	Alters surface roughness, promotes underfilm corrosion, and increases seal preload.
Temperature cyclic amplitude	±5-10 °C per day	Thermal cycling causes expansion/contraction of seals and lubrication viscosity shifts.

systems is presented in Table 4.

OCTs are characterized by slow and more constant flow velocities (0.5-2.5 m/s), longer deployment durations, and deeper immersion, often exceeding 50 m [69]. These systems experience reduced mechanical cycling but are more susceptible to long-term degradation such as biofouling-induced surface roughening, coating delamination, and corrosion under biofilms [70,91,92]. Shaft speeds are usually below 20 RPM, placing them again in low-speed tribological regimes [102,103]. Pressure compensators in such systems operate under swing ranges of 0.2 to 0.5 MPa, influencing dynamic seal behavior and lubricant pressurization [14,104]. Notably, biofouling thicknesses in unmaintained deployments can exceed 25 mm within a year, modifying fluid-structure interactions and acting as a precursor for underfilm corrosion and sealing failures [70,105–107]. These conditions are tabulated in Table 5.

5. Tribological interfaces, motion regimes, and degradation pathways

5.1. System-level overview of tribological contacts

Degradation in marine energy converters originates at functional interfaces where global hydrodynamic loads translate into localized motion, pressure, and reactivity. Across converter architectures, Table 6 integrates these interfaces to trace the degradation sequence from system → component → motion → failure → cause.

Linear actuators, pistons, and sliding seals operate under reciprocating motion where boundary-mixed transitions and salt ingress promote adhesive wear, tribo-corrosion, and fatigue cracking [17]. Articulated connectors and hinged joints exhibit multi-axis oscillation, generating fretting and galling when lubrication replenishment is limited [12]. Mooring chains and shackles endure cyclic tensile loading with micro-slip, dominated by abrasive and fretting wear [54].

In tidal turbines, continuous rotation sustains hydrodynamic films but in chemically aggressive lubrication regimes: main bearings experience salt-induced micropitting and corrosion fatigue; gear trains scuff and micro-pit under high Hertzian stresses; pitch and yaw bearings develop boundary wear and false brinelling under limited-angle oscillation [24,96,120]. Deep ocean-current turbines further face quasi-static seal degradation under hydrostatic pressure [60], leading to adhesive and corrosive wear and gradual coating delamination under cyclic pressure and bio-colonization [9,100].

Across all systems, lubricant contamination through emulsified seawater, particulates, or microbial ingress accelerates additive depletion, viscosity loss, and tribo-corrosive reactions [6,121–123]. The resulting mechanisms converge into a motion-linked hierarchy of risk through: (i) reciprocating and oscillatory interfaces → film rupture, fretting, tribo-corrosion; (ii) continuous rotation → micropitting, scuffing, lubricant breakdown; and (iii) quasi-static seals → adhesive and abrasive wear under pressure-driven micro-slip.

Abrasive wear is pervasive, where sand, silt, and bio-debris gouge polymers and scar metallic counterfaces [112]. At low speed and high load, adhesive wear dominates as film collapse exposes asperities, leading to plowing and thermal softening [124]. In submerged components, even trace seawater ingress (<500 ppm) promotes tribo-corrosion, where oxide film removal during motion exposes reactive substrate, accelerating localized corrosion. Fretting and false brinelling are characteristic of slow or micro-motion joints such as mooring links, blade-hub splines, and yaw bearings [42]. High-speed components such as impellers and shafts additionally suffer cavitation erosion from vapor-bubble collapse [35,113].

Biofouling further amplifies these modes by modifying surface chemistry, promoting crevice corrosion beneath colonies, and introducing abrasive particulates upon detachment [37,71]. Coating delamination under cyclic hydrodynamic load remains the most frequent secondary failure [12].

Table 4
Operating envelope of TECs and their corresponding tribological relevance [24,26,67,87,91,94–96,98–101].

Parameter	Typical range	Relevance to tribology
Tidal flow velocity	1-5 m/s (peak), 2.5 m/s average	Directly correlates with shaft speed and bearing load.
Turbine RPM	5-30 RPM, variable	Low-speed rotation, prone to boundary/mixed lubrication challenges.
Gearbox input torque	50-500 kNm	Determines Hertzian contact stresses in gear flanks.
Blade pitch actuation frequency	2-4 per tidal cycle	Governs number of oscillation cycles in pitch bearings.
Cavitation onset pressure	<20-30 kPa local (depending on profile)	Drives pitting and surface fatigue on blade edges and high-speed seals.
Immersion depth	5-40 m (nearshore), up to 60 m (offshore)	Influences cooling, corrosion rate, and fouling composition.
Operating cycle duration	6-12 h per tide; continuous	High-duty operation exposes rolling/sliding contacts to fatigue within one tidal cycle.

Table 5
Operating envelope of OCTs and their corresponding tribological relevance [12,14,28,62,69,70,94,102,104,106,108–111].

Parameter	Typical range	Relevance to tribology
Current velocity (deep ocean)	0.01-0.1 m/s	Lower than tidal; translates to slower component cycling but longer exposure duration.
System deployment duration	1-3 years (before retrieval)	Extended duration exposes coatings and materials to cumulative degradation.
Shaft speed	5-20 RPM	Similar tribological regime to tidal, but with reduced speed variance.
Pressure compensator swing	±0.2-0.5 MPa	Affects sealing dynamics and lubrication flow in submerged housings.
Biofouling thickness (unmaintained)	5-25 mm after 12 months	Alters surface hydrodynamics and contributes to underfilm corrosion and seal failure.

5.2. Tribo-corrosion and chemical-mechanical degradations

Corrosion in marine systems rarely occurs in isolation; it interacts with wear (tribological phenomena), to define true tribo-corrosive behavior [12,32]. The following mechanisms dominate across alloys and components in seawater service.

- Uniform Corrosion- Even dissolution over exposed metal surfaces, typically limited by diffusion through corrosion product films. It defines baseline material loss and modifies surface roughness and frictional behavior in uncoated steel housings and mooring elements [79,125].
- Pitting Corrosion- Localized perforation of passive films (penetration of barrier), accelerated by chloride enrichment and acidification within pits. In marine bearings and shafts, pit initiation often precedes rolling-contact fatigue or scuffing due to local stress concentration [43].
- Crevice Corrosion- Attack confined to occluded zones such as bolted flanges, seal lips, and gasketed interfaces where oxygen depletion and chloride accumulation create anodic microenvironments. Once initiated, crevice corrosion is self-propagating and particularly problematic beneath biofouling layers or sediment deposits [12,125].
- Galvanic Corrosion- Occurs when dissimilar metals (e.g., stainless-bronze couplings, steel-aluminum housings) are electrically coupled in seawater. The less noble material becomes anodic, accelerating localized attack near mechanical junctions or fasteners [41].

Table 6
Tribological components, motion regimes, dominant degradation mechanisms, and amplifying factors in wave, tidal, and ocean-current systems [5,6,9,10,12,13,17,24,27,34,35,37,42,43,60,66,71,92–94,97,112,113–119].

System	Tribological Component	Primary Motion Type	Dominant Degradation Modes	Key Amplifying Factors
Wave	PTO linear actuator (piston rod/slide)	Linear reciprocation	Erosion-abrasion, coating delamination, tribo-corrosion	Seawater ingress through cracks, bidirectional loading, biofilm thickening
Wave	Linear bearings	Linear reciprocation/oscillation	Abrasive wear, adhesive wear, hydrolysis degradation	Oscillatory reversal, poor lubrication or passive film renewal, sand embedment
Wave, Tidal, Ocean Current	Gearbox/speed increaser internals	Rotational sliding and rolling (high-speed)	Micropitting, scuffing, false brinelling, surface fatigue	Contamination, pressure cycling, mixed-regime loading
Wave	Inter-body hinge joints (attenuator)	Low-frequency, large-angle oscillation	Galling, fretting fatigue	Creep, cyclic loading, corrosion attack
Wave	Flap hinge (oscillating wave surge converter)	High-force oscillation	Fretting, adhesive wear, coating fatigue	High contact stress, oscillatory reversal, poor lubrication replenishment
Tidal	Oscillating hydrofoil pivot bearing	Large-angle oscillation	Fretting corrosion, adhesive wear	Bidirectional motion, lubricant starvation, surface fatigue
Tidal	Barrage sluice gate trunnion	Intermittent oscillation	Abrasive wear, corrosion fatigue	Flow variation, cyclic load, stagnant film renewal
Tidal & Ocean Current	Main rotor shaft bearings	Continuous rotation (bidirectional for tidal, unidirectional for ocean current)	Corrosive wear, cavitation erosion, third-body abrasion	Pressure and temperature differential, lubricant oxidation, seawater attack
Wave, Tidal, Ocean Current	Blade pitch/control bearings	Intermittent or slow oscillation	Micro-slip, false brinelling, fretting corrosion	Torque fluctuation, slow-speed reversal, poor relubrication
Wave, Tidal, Ocean Current	Yaw and orientation bearings (slewing rings)	Intermittent rotation	Tribo-fatigue, boundary wear, creep	Load spikes, stick–slip behavior, poor lubrication management
Tidal, Ocean Current	Blade–hub connection (splines, keyed hubs)	Micro-motion under torque	Micro-motion wear, fretting corrosion, joint loosening	Torque cycling, thermal mismatch, dry contact
Wave, Tidal, Ocean Current	Mooring system connections (chains, ball joints, flexures)	Oscillatory micro-slip and articulation	Fretting wear, corrosion, cold welding	Tension cycling, trapped biofilm under links
Wave, Tidal, Ocean Current	Dynamic shaft seals	Rotary sliding/reciprocating sliding	Abrasive wear, extrusion, hydrolysis, plasticization	Pressure pulsation, particulate ingress, microbial attack
Ocean Current	Pressure-balanced deep-seal assemblies	Static or quasi-static under pressure cycling	Adhesive wear, polymer creep, tribo-corrosion	High hydrostatic pressure, low-velocity interface, seawater ingress
Ocean Current	Thrust bearing assembly	Continuous rotation under high axial load	Pitting, corrosion fatigue, oil–water emulsion degradation	High axial load, lubricant–water interaction, poor film stability
Wave, Tidal, Ocean Current	Protective coatings	—	Delamination, fatigue cracking, erosion	Flow separation, cavitation, adhesion mismatch with biofilms
Wave, Tidal, Ocean Current	Sliding cylinders/alignment units	Low-speed reciprocation/quasi-static	Adhesive wear, particulate abrasion, tribo-corrosion	Biofouling, seawater ingress, high-pressure interfaces

- Stress Corrosion Cracking (SCC)- Arises from the combined effect of tensile stress and corrosion, common in high-strength stainless steels and weld heat-affected zones under hydrostatic pressure or vibration-induced stress [12,115].
- Intergranular Corrosion- Localized attack along grain boundaries, often due to chromium carbide precipitation in improperly heat-treated austenitic steels used in shafts or pins. Though less common in marine energy hardware, it can be critical at weld seams [32,125].
- Hydrogen Embrittlement- Possible in high-strength steels under cathodic charging or corrosion, where atomic hydrogen diffuses into the lattice, reducing ductility and promoting crack initiation in bolts or fasteners under tension [126].
- Dezincification (dealloying) or Selective Leaching- In copper-based alloys (brasses, bronzes), selective loss of zinc or tin weakens structural integrity of bushings or thrust washers [117,125].
- Filiform Corrosion- Superficial under-coating attack forming filamentary paths, typically non-structural but indicative of coating porosity or adhesion failure, serving as a precursor to delamination [127,128].

These mechanisms operate concurrently within tribological contacts, where wear debris, oxide films, and corrosion products form a dynamic third-body layer [9,32]. This layer modulates friction and wear but also serves as a reactive medium [129]. For example, in stainless steel-polymer sliding pairs, corrosion debris can embed in soft counterfaces, increasing abrasive wear; in bronze-steel journal bearings, galvanic coupling accelerates local oxidation and scuffing [32,34,41,115,117,130]. Thus, corrosion not only removes material but continuously alters interfacial chemistry and topography, redefining the tribological regime itself [12].

While corrosion phenomena are classically associated with metallic degradation, polymeric elements in marine tribosystems such as seals, liners, and bearing cages (eg. EPDM, NBR, PTFE, PEEK, PET, or PU) undergo analogous chemo-mechanical deterioration through hydrolysis, environmental stress cracking, hydrogen-induced chain scission, or plasticization due to cathodic hydrogen evolution or ion exchange at the polymer-metal sliding interface [131,132]. These mechanisms, though non-electrochemical, often act synergistically with metallic corrosion, jointly dictating system-level reliability. Table 7 summarizes how classical electro-chemical corrosion in metals and chemo-mechanical degradation in polymers co-exist within marine components.

5.3. Lubricant degradation and boundary film disruption

Lubricant failure in ocean energy systems is a primary initiator of catastrophic component wear [14]. The degradation pathways such as viscosity loss from thermal cycling, additive depletion, and water emulsification are accelerated by the marine setting, while system failures like filter blockage and oil starvation directly translate the external environment's harshness into internal mechanical damage [139,140].

Across components such as PTO actuators, gearbox bearings, shaft

Table 7
Electro-chemical corrosion mechanisms in metals and chemo-mechanical degradation in polymeric marine components [12,32,61,79,93,115,117,127,131–138].

Degradation Type	Triggering Environmental/ Mechanical Conditions	Susceptible Materials/ Interfaces	Impact on Tribological Performance	Representative Marine Components
Uniform Corrosion	Continuous seawater immersion, dissolved oxygen presence, stable pH	Carbon steels, low-alloy steels, Cu-Ni alloys	Gradual wall thinning, surface roughening, loss of dimensional control	Structural frames, shafts, housings
Pitting Corrosion	Chloride-induced passive film rupture, stagnant zones	Stainless steels (304, 316), Al alloys	Rapid localized penetration, initiation of fatigue cracks, lubricant contamination	Shafts, bolts, bearing races
Crevice Corrosion/Crevice-Induced Polymer Degradation	Restricted electrolyte flow, oxygen depletion, microbial growth	Austenitic steels, Ti alloys, NBR, EPDM elastomers	Local acidification, seal swelling and cracking, loss of sealing integrity	O-rings, shaft seals, gasketed joints
Galvanic Corrosion	Electrical coupling of dissimilar metals in seawater	Carbon steel coupled with Cu-Ni or Ti alloys	Preferential attack on less noble alloy, interfacial pitting, coating breakdown	Fasteners, flanges, composite hubs
Stress-Corrosion Cracking/ Environmental Stress Cracking in Polymers	Combined tensile stress and chloride or oil exposure	High-strength steels, PTFE, polymers, glass-filled polymers	Brittle fracture, crack propagation, loss of dimensional or mechanical stability	Fasteners, polymer bearings, sliding liners
Hydrogen Embrittlement/ Hydrogen-Induced Chain Scission in Polymers	Cathodic protection, galvanic coupling, nascent hydrogen at metal-polymer interfaces	High-strength steels, Ni alloys, PU, Elastomers	Reduced ductility or elasticity, premature cracking, seal compression set	Bolts, shaft seals, polymer couplings
Intergranular Corrosion/Grain Boundary Weakening	Sensitization due to thermal cycling, weld heat-affected zones	Austenitic stainless steels (>0.03% C), some Ni alloys	Subsurface cracking, loss of load-bearing cross-section, coating disbondment	Weld joints, heat-affected zones during repair of ocean rods
Dealloying (e.g., De-zincification)	Selective dissolution of active alloying elements	Brasses, bronzes (Cu-Zn, Cu-Sn)	Porous residue formation, loss of strength and sealing surfaces	Bearings, valve bodies, couplings
Filiform Corrosion/Coating Undermining	Moisture ingress beneath organic coatings or paints	Painted steels, Zn- or Al-coated substrates	Threadlike corrosion under films, localized coating delamination	External casings, housings, fasteners
Hydrolysis (Polymers)	Long-term seawater exposure, elevated temperature, cyclic stress	Polyesters, polyamides, PU elastomers	Chain scission, loss of strength and elasticity, microcracking	Sliding seals, bearing cages, flexible connectors
Oxidative Degradation	UV exposure, oxygen-rich environment, shear heating	EPDM, NBR, PU, silicone	Surface embrittlement, color change, cracking, debris generation	External seals, exposed flexible joints
Plasticization	Ion exchange, oil absorption, long-term seawater contact	NBR, PVC, silicone rubbers	Softening, swelling, dimensional change, lubricant incompatibility	Static seals, gaskets, vibration dampers

seals, and structural joints, lubricant performance degrades due to an interplay of mechanical shearing, pressure cycling, thermal gradients, and seawater contamination, all of which compromise boundary film formation and persistence [139,140]. For instance, In PTO hydraulic rams, emulsified lubricants impair pressure transmission and cause non-uniform loading on bearings, promoting localized adhesive and abrasive wear [141]. Yaw and pitch bearings, exposed to slow oscillation and often marginal lubrication, show progressive tribo-fatigue and fretting corrosion, particularly where lubricant starvation prevents oxide film recovery [130,142]. Tidal gearbox bearings, cycling between high torque loads and standstill, develop micro-pits and varnish deposits due to oxidative lubricant degradation and boundary starvation at rolling element contacts [98,142].

Typically, a seawater ingress, whether through shaft seals, elastomeric interfaces, or condensation under pressure-temperature cycling, introduces ionic species (Cl^-, SO_4^{2-}), oxygen, and water molecules directly into the lubricant medium. Even minute levels <500 ppm of seawater in synthetic gear oils have been shown to accelerate hydrolytic degradation, additive depletion, and emulsification, leading to a rapid loss in load-carrying capacity [122,143]. Interfaces exposed to such conditions suffer from increased micropitting, surface fatigue, and corrosion pitting, often under misclassified boundary or mixed regimes [144,145].

Under cyclic shear especially in gearbox oils or oscillatory hydraulic actuators the viscosity index modifiers and anti-wear additives (e.g., ZDDP, esters, amines) undergo thermomechanical breakdown [145–147]. This not only leads to viscosity loss but also alters the tribochemical interface, encouraging metal-to-metal contact [148]. In the presence of oxygen and seawater, oxidation products such as acids, sludge, and varnish form and precipitate, particularly at low-flow or stagnant regions within lubricant delivery paths [149]. This alters frictional behavior, increases torque draw, and enhances surface fatigue initiation.

In regimes where full-film hydrodynamics cannot be sustained such as low-speed oscillation (e.g., in pitch/yaw bearings), intermittent motion (e.g., mooring line shackles), and stop-start cycles (e.g., wave energy pistons) [150]. In such conditions, the replenishment of boundary films becomes non-trivial [151]. Neverthless, surface-active additives fail to regenerate tribofilms once disrupted by water/oxygen-rich environments due to depletion and hence, inactivity and loss of protection leading to high friction/wear [152].

Lubricant degradation indirectly impacts tribological reliability through elastomer compatibility issues [153]. Swollen seals due to plasticization by degraded base oils, or shrinkage due to water ingress, compromise dynamic sealing performance [154]. This enhances lubricant leakage and contaminant ingress, creating a positive feedback loop of degradation [155]. Fig. 9 classifies key lubrication failure modes in oceanic systems.

5.4. Biofouling influenced tribological interactions

Marine biofouling is not merely a surface contamination problem, but it actively transforms the frictional environment, alters wear mechanisms, and accelerates degradation modes [12,71]. The colonization of components by microorganisms, algae, barnacles, and biofilms leads to a dynamic interface evolution, often turning inert surfaces into chemically reactive, mechanically abrasive, or physically obstructive zones [7,12,156,157]. For instance, Pitch and yaw bearings operating under tidal reversals often accumulate marine growth near raceways. The presence of hard-shelled organisms promotes fretting, false brinelling, and torque non-uniformity during actuation [7,34,158]. Hydraulic cylinder (ocean) rods in wave energy converters face biofilm buildup that disrupts seal dynamics, leading to ingress of seawater and sand, and initiating coating failure and tribo-corrosion [12]. Mooring chains resting on the seabed form bio-layers under compressive contact, which trap moisture and acids, accelerating fretting corrosion and reducing fatigue life [93]. Other ways it can be tribologically detrimental are.

5.4.1. Altering surface topography and contact mechanics

On components such as pitch bearings, sliding cylinder rods, and

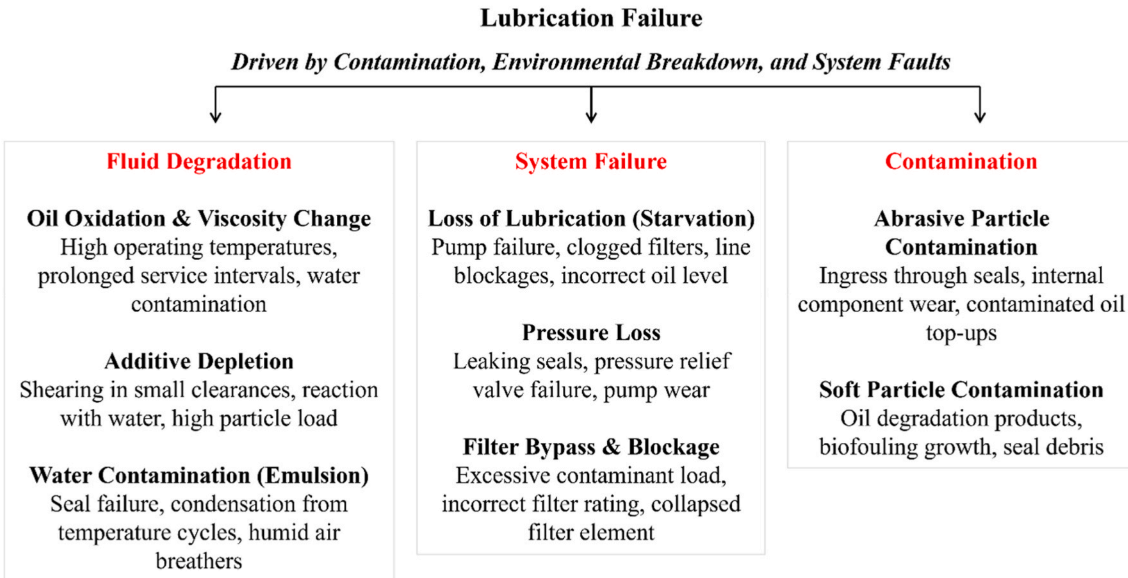

Fig. 9. Classification of lubrication failure modes and their associated faults in ocean tribological systems.

hinge joints, biofouling introduces localized roughness, high spots, and soft matter asperities, modifying the effective tribological contact [12,93,158]. This disrupts lubrication regimes, particularly under boundary and mixed lubrication, where film thickness is already marginal [37]. Fouling deposits act as third bodies, altering contact stress distributions and promoting stick-slip behavior, especially under oscillatory or low-speed motion [34].

5.4.2. *Abrasive debris and shear-induced delamination*

Fouling layers, when partially detached during operation (e.g., by pressure reversal or mechanical motion), create irregular debris that acts like abrasive slurry [10,159]. This is critical in linear seals, piston rods, and mooring interfaces, where barnacle fragments or filamentous organisms infiltrate contact zones. The abrasive nature of biogenic material combined with hard shell microstructures and embedded sediment grains can lead to severe scratching, coating delamination, and even counterface gouging, particularly on polymer-metal interfaces.

5.4.3. *Chemical microenvironments and localized corrosion*

Biofilms induce heterogeneous electrochemical conditions on metallic surfaces [107,160]. Their metabolic byproducts such as organic acids, sulfides, and extracellular enzymes create micro-acidic or reducing environments. In shaft bearings, bolt joints, and structural hinges, this leads to crevice corrosion, under-deposit pitting, and in some alloys, microbial-induced stress corrosion cracking [161]. Moreover, galvanic effects can intensify if fouling interface dissimilar metals under conductive saline conditions [41].

5.4.4. *Lubricant degradation and fouling-promoted starvation*

Fouling also indirectly accelerates tribological failure by interfering with lubricant retention and delivery [162]. Hydrophilic biofilms can isolate lubricant droplets or create capillary bridges that displace oil films [163]. In submerged bearings and gear seals, this causes localized lubricant starvation, surface drying, and eventual transition to adhesive wear. Fouling can also plug lubrication ports, further impairing film reformation in dynamic contacts.

5.5. *Erosion–corrosion interactions*

Erosion-corrosion is a subject within the broader area of tribo-corrosion which covers all aspects of tribologically (mainly mechanically) induced interactions with electrochemical processes [27]. Erosion-corrosion material degradation is governed by a non-linear synergistic coupling where the total material loss (T) is deconstructed into three distinct components via the fundamental equation $T = E_0 + C_0 + S$ [27]. Here, E_0 represents the baseline material removal from pure mechanical actions such as solid particle impingement or cavitation bubble collapse measured in an inert, non-corrosive environment. Conversely, C_0 is the material dissolution rate from pure electrochemistry, measured under static, non-eroding conditions. The critical term, S, quantifies the synergy, which is the non-additive, extra material loss resulting from the interplay of these mechanisms. This synergy itself can be partitioned into ΔCe, the corrosion-enhanced erosion where dissolution weakens the material microstructure (e.g., grain boundaries), facilitating mechanical removal, and ΔEc, the erosion-enhanced corrosion where mechanical depassivation continuously creates fresh, active anodic surfaces, drastically increasing dissolution currents [164,165]. In operational marine systems, it is this synergistic component S, not E_0 or C_0, that frequently dominates the total degradation.

The primary mechanism is mechano-electrochemical [27,32]: the mechanical removal of the protective passive film by sediment impacts or cavitation bubbles. This depassivation creates a fresh, active anode, with the anodic dissolution current density increasing from passive state. Furthermore, the plastic deformation from impact creates a work-hardened, metastable sub-layer that is electrochemically more active than the bulk material, establishing a micro-galvanic cell. This is critically evident on tidal turbine blades, where the leading edge and root experience localized flow acceleration, leading to synergy-dominated wear rates exceeding 1.2 mm/yr and compromising aerodynamic performance and structural integrity [166].

The operational risk is defined by the erosive severity and is proportional to particle kinetic energy [28]. The transition between degradation regimes is not linear but follows a characteristic trajectory (Fig. 10), where a critical velocity demarcates the safe, passive-film-dominated regime from the unsafe, synergy-dominated regime. For hydraulic rod cylinders in WECs, the reciprocating motion creates a continuously refreshed tribological interface that effectively lowers this practical critical velocity. For Super Duplex Stainless Steel (UNS S32760), it can fall to 5-7 m/s due to the inability to form a stable repassivation film under reciprocating sliding and particle impingement [167], forcing the component into the mechanical impact-enhanced corrosion regime depicted in Fig. 10.

Fig. 11 maps the interaction regimes between flow conditions and corrosion mechanisms that lead to erosion-corrosion [27]. The most

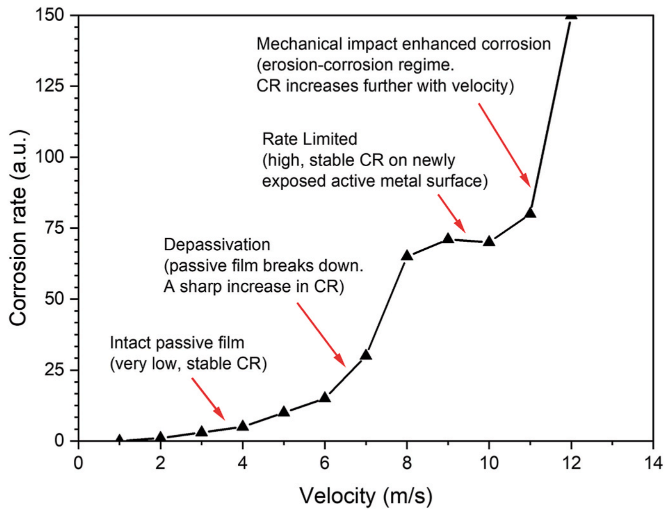

Fig. 10. The transition of corrosion rate (arbitary unit) with flow velocity for a passive metal. Adapted from Ref. [27].

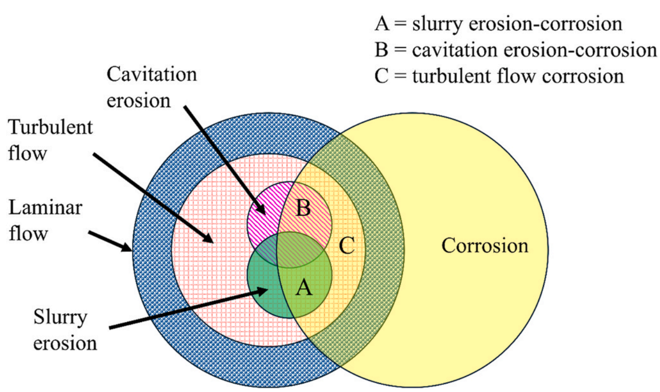

Fig. 11. Schematic of erosion-corrosion regimes identifying synergistic interaction zones: (a) Slurry erosion-corrosion, (b) Cavitation erosion-corrosion, and (c) Flow-accelerated corrosion. Adapted from Ref. [27].

severe material degradation occurs in two primary zones: Region A, where turbulent slurry flow coincides with corrosion (solid particle impingement: mechanical abrasion continuously depassivates the surface, leading to massive synergistic mass loss, e.g., abrasive wear on turbine blade roots and ocean rods); and Region B, where hydrodynamically driven cavitation and corrosion interact synergistically (cavitation-corrosion: bubble collapse jets fracture the passive film and plastically deform the substrate, creating intense local galvanic cells, e.g., on the suction side of turbine blades). A third zone, Region C, results from turbulent flow accelerating corrosion (flow-accelerated corrosion) [flow-accelerated corrosion: purely hydrodynamic dissolution/thinning of the passive film without mechanical damage). While solids in laminar flow can theoretically cause erosion-corrosion if their kinetic energy exceeds the material's yield strength, this is less common.

Material selection is a direct response to these mechanisms. The long-term consequence is tribo-corrosive fatigue [32]. On submerged mooring connectors and pitch bearing raceways, the cyclic loading superimposed on the synergy loop leads to crack initiation at dissolution pits, reducing high-cycle fatigue life by an order of magnitude [168]. A related failure mode, third-body electrochemistry, occurs in these same pitch bearings, where corrosion products (such as Fe_2O_3) become abrasive particulates, grinding away lubricant films and accelerating wear in a self-perpetuating loop [130].

Therefore, mitigation requires a systems approach and moving from passive materials to active design [28]. This includes the application of laser-clad Ni-Cr-B-Si coatings on high-wear regions of tidal turbine hubs and the development of predictive models that integrate real-time sediment data from enabling condition-based maintenance before synergistic failure initiates.

5.6. *Multi-mode and synergistic degradations*

Marine components rarely fail due to a single isolated mechanism. Instead, they undergo interactive degradation, where mechanical, chemical, and biological processes co-evolve and amplify one another [9,34,38]. Such multi-mode failures are not merely additive, but they are synergistic, resulting in wear rates, friction escalation, or material damage that far exceed the sum of individual modes [31]. Notably, a critical distinction from the magnitude of individual effects observed in idealized laboratory tests.

In polymer-lined bushings and linear bearings, for instance, abrasive wear from entrained particulates opens microchannels that allow seawater ingress [58,169]. This leads to hydrolysis, which in turn alters surface polarity and hardness, intensifying abrasion and promoting tribo-chemical pitting [15]. The softened surface (such as seals) is then vulnerable to adhesive smearing during bidirectional motion, completing a degradation loop where wear begets more wear [60]. Similarly, in gearboxes, shaft couplings or coatings, fretting wear at spline or interference fits removes protective films, exposing fresh metal [130]. These nascent surfaces undergo corrosion attack under alternating load and saline exposure, weakening microstructure and accelerating contact fatigue [170]. In dynamic load zones, such as yaw and pitch bearings, false brinelling from vibration combines with micro-slip corrosion, creating oxide debris that further promotes abrasion and lubricant starvation [122,130].

Fig. 12 illustrates the possible mass exchange pathways within a tribocorrosion system incorporating a third body [123]. The primary surface is considered a ductile, passive metal, while the counterface is a hard, inert material (such as, erodent). In such a system, wear debris may detach from the metallic surface and, particularly in regions where the passive film is disrupted, oxidize into ionic species, represented as pathways 2 and 9 in Fig. 12. Alternatively, detached fragments may remain confined within the contact zone, acting as a third body rather than being expelled, corresponding to pathway 3. Once trapped, these particles can evolve along two routes: either they fragment further into smaller debris eventually leaving the contact (pathway 5), or they are mechanically transferred onto one of the contacting surfaces (pathways 4 and 6) [171]. During this cycle of fragmentation and transfer, unprotected metallic regions within the third body can also oxidize to ionic forms (pathway 8). At equilibrium, the system establishes a dynamic mass balance across all these pathways, defining the steady state tribocorrosion condition.

The synergy extends to previously discussed erosion-corrosion and tribo-bio-chemical feedback loops [31]. For instance, biofilms influenced tribology e.g., in mooring chain articulations or sliding seals) alter local pH, foster crevice corrosion, and release biogenic debris [42]. These changes disturb contact mechanics by modifying friction, film formation, and asperity deformation [168]. Hence, what defines multi-mode degradation in marine tribology is not just the diversity of mechanisms but their spatial and temporal entanglement where one initiates, another accelerates, and a third transforms the failure pathway entirely [31]. Fig. 13 shows a degradation flowchart illustrating the multimode failure.

6. Materials and surface engineering strategies for protection

In marine energy systems, material selection and surface engineering must address the simultaneous presence of corrosive fluid environments, cyclic mechanical loading, and mixed mode tribological interactions. The challenge is compounded by site-specific variability in seawater chemistry, biological activity, and sediment content. Achieving these

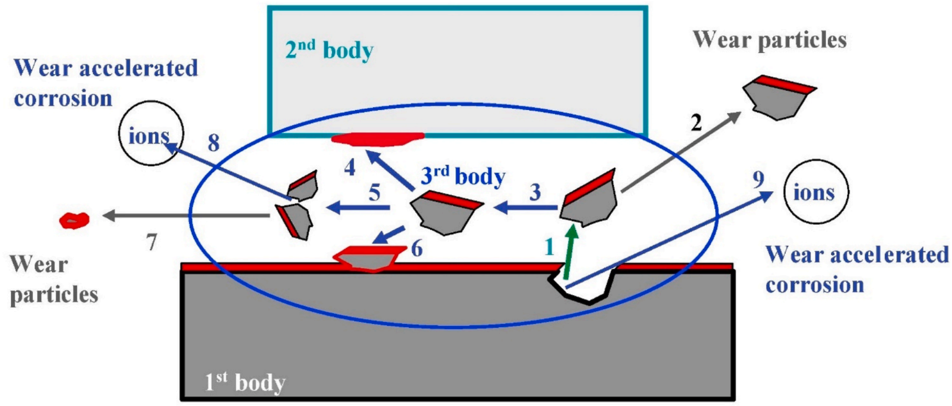

Fig. 12. Representation of possible mass flows in a tribocorrosion system. The arrows trace possible pathways explained in the text. Reproduced with permission from Ref. [123].

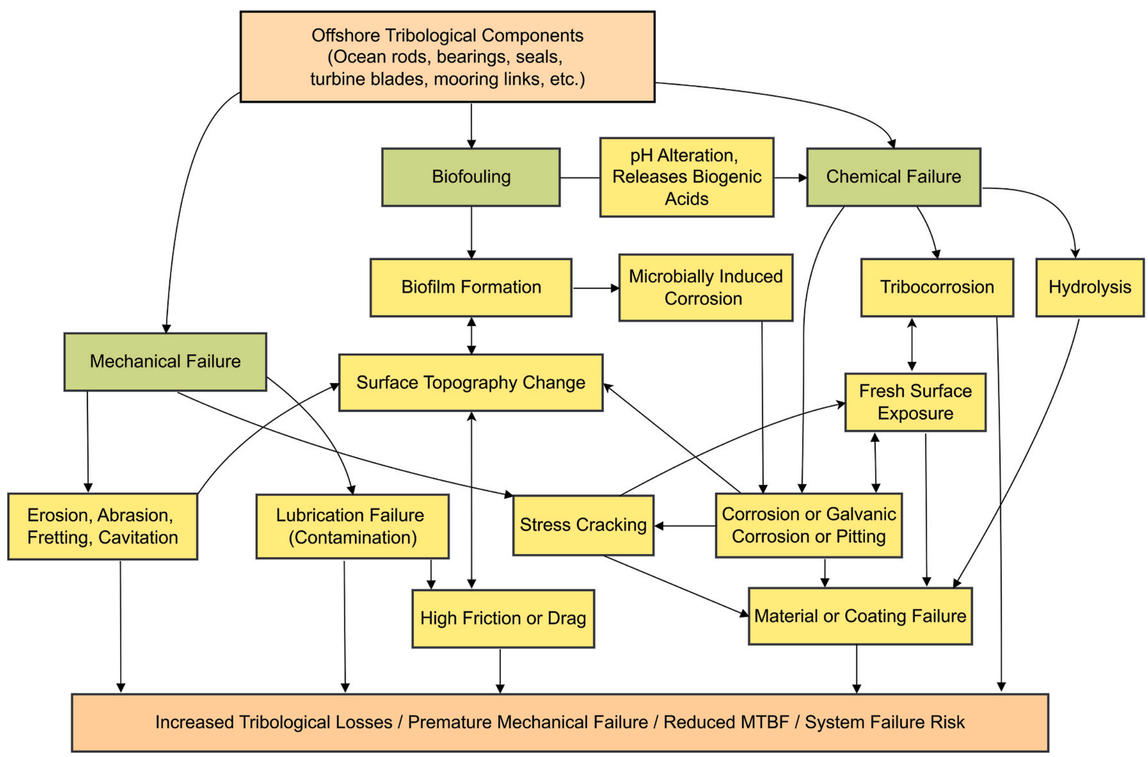

Fig. 13. Flowchart illustrating the multimode degradation cycle of offshore tribological components. The interconnecting arrows represent synergy vectors, illustrating how primary stressors do not act in isolation but instead feed subsequent failure mechanisms.

calls for a multiscale, multiphase materials strategy that considers mechanical wear, seawater chemistry, biofouling, and dynamic loads. Advances in surface engineering, material hybridization, and bio-inspired coatings are promising. However, field-proven durability under real marine loading remains the final criterion, making careful material selection a critical step in system reliability.

6.1. Materials for ocean rods and hydraulic cylinders

Reciprocating components such as ocean rods, hydraulic cylinders, piston rods, and PTO sliders operate in highly tribological aggressive zones including splash exposure, salt-laden mist, abrasive particulates, and microbial colonization [9,12]. Their primary failure modes, including biofouling-induced corrosion, tribocorrosion (erosion-corrosion), pitting, abrasive scoring from contaminated seals, coating fatigue, etc. are intrinsically linked to the constant battle against microbial colonization, suspended abrasives, seawater corrosion, and cyclic side-loading from wave action. Materials for these parts must meet a demanding multi-property envelope: high hardness and wear resistance, strong corrosion and microbially influenced corrosion (MIC) resistance, compatibility with elastomeric seals, and surface finishes that minimize abrasive/adhesive wear. Fig. 14 shows the key failure pathways for hydraulic rods and linear actuators.

Carbon and low-alloy steel have been widely used in marine service, mainly because of their cost effectiveness. Based on the findings summarized in Table 8, alloying elements influence MIC susceptibility in steels in markedly different ways [136]. Carbon shows inconsistent effects. Some studies relate higher C content to increased MIC rates in sulfate-reducing bacteria (SRB) environments, while others report no clear correlation under soil or *E. coli* exposure [172–175]. Copper can be either neutral or beneficial depending on content and steel type: low levels (0.08-0.44 wt%) in API 5LX had minimal impact, whereas higher

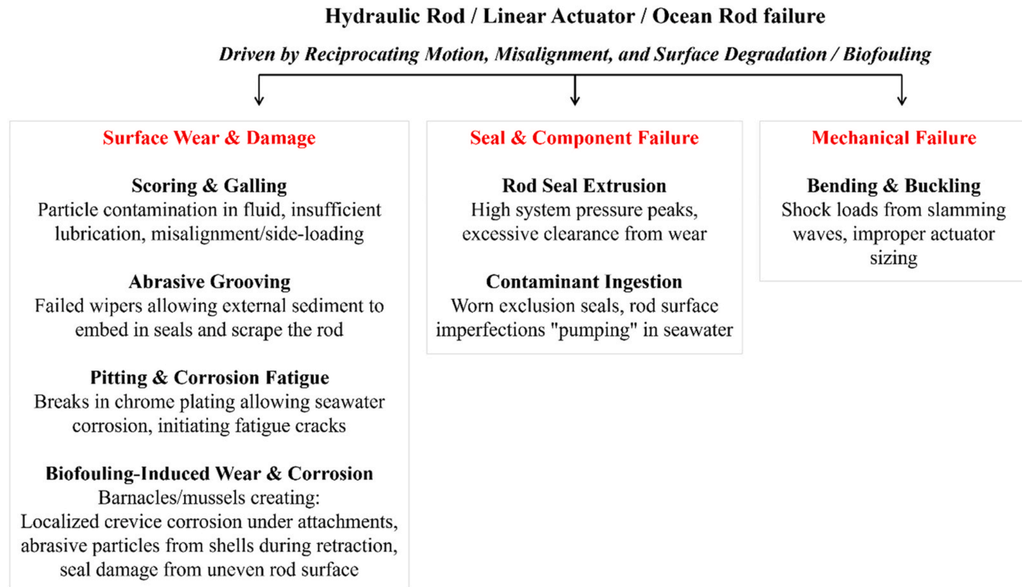

Fig. 14. Key failure pathways for hydraulic rods and linear actuators.

Table 8
Effects of alloying element additions on the susceptibility of steels to MIC. MIC-promoting indicates that susceptibility to MIC increases with higher alloy content, whereas MIC-inhibiting denotes a reduction in susceptibility as alloy content increases.

Alloying Element	Steel Grades	Alloying Levels (wt.%)	Microorganisms	MIC Trend	Ref.
Carbon (C)	K1878, K1063, S2684, K795, V2170, V2179; 1010, 1020, 1030, 1045; A179, A516-70, A106-B; Q235, X65, X70, X80	0.06-0.94	*E. coli*, *D. desulfuricans*, mixed SRB	neutral for K, S, V, Q, X series, MIC-promoting in others	[172–175]
Copper (Cu)	API 5 LX; Carbon steel; Corten steel; X80 steel; BR5 mooring chain steel; HSLA; AISI 8630	0.002-2.0	*P. aeruginosa*, SRB, natural marine consortia	MIC-inhibiting	[134,135, 176–180]
Sulfur (S)	AISI 8630	0.007-0.023	Tap/cooling water, natural consortia	MIC-promoting	[111,182]
Cerium (Ce)	AISI 8630	0.0-0.015	Tap/cooling water, natural consortia	MIC-inhibiting	[111,182, 184]
Chromium (Cr)	Pipeline steels	<0.01-4.62	*Desulfovibrio* spp.	MIC-inhibiting	[181]
Nickel (Ni)	HSLA	4.78-7.23	*H. titanicae*	MIC-inhibiting	[177]
Molybdenum (Mo)	Low-C steels	0-1.0	*P. aeruginosa*	MIC-promoting	[183]

contents (1.0-2.0 wt%) in X80, HSLA, and AISI 8630 steels improved MIC resistance via protective Cu_2O/CuO film formation [134,135, 176–179]. Sulfur consistently worsens MIC resistance, with elevated S contents in AISI 8630 correlating with increased corrosion in various microbial environments [180,181]. In contrast, small additions of Cerium (0.01-0.015 wt%) reliably reduce MIC susceptibility in 8630 steels [182]. Chromium up to ~5 wt% in pipeline steels suppress SRB activity and biofilm development, lowering MIC rates [136]. Nickel in the range of 5-7 wt% enhances MIC resistance in HSLA steels by forming stable Ni-rich oxides. Molybdenum, however, at ~1 wt% in low-carbon

Table 9
MIC susceptibility vs. marine service suitability for steels [11,80,110,111,134,136,173,175,180,182,185,186].

Steel type/Grades	Key alloying additions	MIC susceptibility	Marine suitability (bare)	Recommended use	Protection strategy
Low-carbon steels (1010-1045, Q235, A179, A516)	Minimal alloying	High	Avoid as bare rod/slider material	Non-wetted structural frames, enclosed linkages	Full barrier coating (HVOF, epoxy), oil isolation
HSLA/Pipeline steels (X65-X80, API 5LX)	Variable Cu, Ni, Mo	Medium-High	Avoid for continuous splash/ submersion	Jack-up leg braces, internal supports	Coating + cathodic protection; seal from seawater
Low-alloy steels (AISI 8630)	Cu, Cr, Ni, Ce	Medium-Low (with beneficial alloying)	Conditional	Mooring-chain pins, PTO sliders (with coating)	HVOF WC-Co, Ni-P, laser-clad Inconel
Martensitic stainless (AISI 420, X46Cr13)	High Cr	Low-Medium	Suitable for moderate splash; not continuous immersion	Piston rods, pump shafts	Duplex coating system for immersion service
Duplex/Super-duplex stainless (S32205, S32760)	High Cr, Mo, Ni	Low	Preferred	Continuous-service rods, sliders, shafts	Optional thin-film coating for wear zones
Precipitation-hardened stainless (17-4 PH, 15-5 PH)	Cr, Ni, Cu	Low-Medium	Preferred with coating	High-load rods, slider rails	Hard coating over base
Austenitic stainless (316L, 304)	High Cr, Ni	Low	Preferred as corrosion-resistant substrate	Coated rods, non-wear-critical parts	Hard coating to address low base hardness

steels promote biofilm formation by *P. aeruginosa* and accelerates pitting, increasing MIC vulnerability [183].

Low-carbon steel (e.g., 1010-1045, Q235, A179, A516) and conventional HSLA or pipeline steels (e.g., X65-X80, API 5LX) as shown in Tables 8 and 9, exhibit poor chloride or pitting resistance and high MIC susceptibility when uncoated, despite low cost and good bulk strength [172,180]. They can be used as structural substrates for shielded or oil-isolated internals, or for non-wetted ocean components (e.g., load frames, internal linkages) where coatings or claddings are intact but are avoided as exposed ocean rod materials.

Alloyed low-alloy steel (e.g., AISI 8630) with beneficial additions (Cu, Cr, Ni, Ce) offer improved MIC resistance but remain vulnerable to pitting (localized penetration of passive films barrier, Fig. 15) in seawater [111,136]. They are viable for reciprocating parts only with engineered surface protection such as HVOF WC-Co, electroless Ni-P, or laser-clad Inconel overlays, and are well suited for marine shafts, mooring-chain pins, or PTO slider tracks with controlled sealing and coating systems.

Martensitic stainless steels (AISI 420, X46Cr13) provide high surface hardness (>50 HRC) and moderate chloride resistance suitable for moderate-splash rods, though not for continuous immersion without coating but are to a larger extent preferred for bare exposure in marine splash service [110,187]. They exhibit high corrosion rates >1 mm/year once localized attack initiates, making them unsuitable for permanent immersion.

Duplex and super-duplex stainless steels (UNS S32205, S32760, S32750) deliver high PREN (>40) and yield strength, making them robust for rods, sliders, and pump shafts in high-chloride environments [185,186]. Moreover, they are strong candidates for exposed rods where welding/fabrication capabilities exist. Duplex 2205 (S32205) offers excellent pitting resistance (<0.1 mm/year), while Super Duplex 2507 (S32750) provides superior performance, reducing localized corrosion rates to <0.01 mm/year [79,125].

Precipitation-hardened stainless steels (17-4 PH, 15-5 PH) are attractive for rods due to their good strength, higher hardness after aging (HRC ~40-46), acceptable corrosion resistance with penetration rates ranging from 0.1 to over 1 mm/year (depending on the specific environment and heat treatment) in many marine contexts but still benefit from coatings in highly erosive/splash zones [79].

Austenitic stainless steel 316L shows low corrosion (<0.01 mm/year) but is highly susceptible to crevice corrosion, with penetration rates within the crevice capable of exceeding 1-5 mm/year. They usually have low hardness (~150-250 HV) and are ideal as corrosion-resistant substrates for hard coatings in tribologically active parts [186].

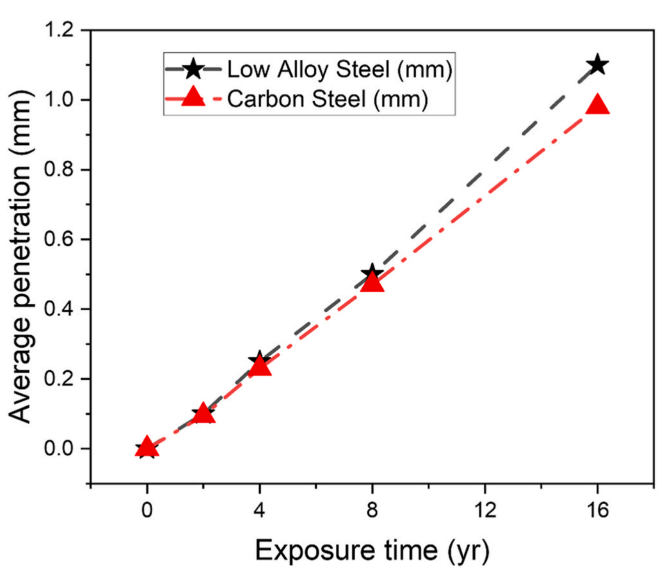

Fig. 15. Long-term corrosion penetration trends of carbon and low-alloy steels in a seawater environment. Adapted from Ref. [125].

Proven surface engineering strategies include thermal spray or high velocity oxygen-fuel (HVOF) carbides (WC-Co, Cr_2O_3-NiCr), ceramic oxides (Cr_2O_3), electroless Ni-P, physical vapor deposition (PVD) coatings (CrN, DLC), and laser-clad Ni superalloys (Inconel 625/718) with hardness >500-600 HV [188]. Ni-based overlays provide dual benefits of chloride/MIC resistance and wear durability, with minimal substrate dilution [189]. While HVOF WC-Co gives excellent erosion-abrasion resistance but needs a corrosion barrier (seal or Ni bondcoat) to avoid porosity leading to undercut corrosion [186].

The same substrate/coating principles apply to other reciprocating or sliding marine parts i.e. winch drums, jack-up leg guides, fairlead sheaves, and splash-zone hydraulic actuators, where the load, wear, and biofouling profiles mirror those of ocean rods. Material choices must be adapted to the exposure zone (submerged, tidal, splash) and integrated with replaceable sacrificial layers or sleeves to extend service intervals.

Seal compatibility and finish control remain critical across all applications, with target Ra <0.2 μm for dynamic seals and coating chemistries tuned to minimize elastomer abrasion.

6.2. Materials for bearings

Bearings are critical to minimizing frictional losses and maintain alignment in ocean energy converters, especially within PTO systems, gearbox units, yaw drives, and articulated linkages. Their performance is challenged by high static and dynamic loads, low-frequency reciprocating or rotating motion, variable lubrication regimes, and the presence of water, silt, or bio-organic contaminants. Bearing types typically include hydrodynamic journal and thrust bearings, sliding bushings, and rolling-element bearings (e.g., spherical or tapered roller bearings in gearboxes). Their performance is critically limited by failure modes that transcend pure cyclic fatigue. The dominant mechanisms including abrasive wear from suspended sediments, white etching cracks from hydrogen embrittlement, and false brinelling from wave-induced vibrations are direct consequences of the synergistic relationship between mechanical stress and the corrosive, particulate-laden marine environment. Fig. 16 shows the key failure mechanisms in ocean energy bearing systems.

Tribologically, these bearings routinely transition from hydrodynamic to boundary/mixed lubrication regimes during slow oscillation, start-stop cycles, and low-velocity actuation. These transitions induce shear stress surges and collapse of lubricating films, thereby demanding materials and coatings that can maintain low friction and resist wear under film-starved conditions. Contact pressures exceeding 30 MPa over extended lifetimes (up to 30-40 years) are not uncommon, especially in hydrodynamic sliding interfaces [150].

Traditionally, self-lubricated bronze bearings (e.g., Cu-Sn-Pb or Cu-Al alloys) have been employed for their conformability and seizure resistance [160]. Self-lubricating bearings eliminate external lubrication altogether and are widely employed nowadays with or without external lubrication [190]. However, optimization needs to be met based on type of operating conditions. For instance, polymeric hydrobearings operate primarily through self-lubrication and the formation of transfer films on metallic counterfaces, enabling polymer/metal tribopairs to replace traditional metal/metal contacts under boundary and mixed lubrication conditions. Engineered polymers such as PTFE, PET, and multiscale composite materials exhibit dry friction coefficients in the range of 0.10-0.15 and withstand static pressures up to 60 MPa while maintaining dimensional stability in seawater [150,191–193]. Transfer film formation, which critically reduces wear and sliding power consumption, is highly sensitive to sliding speed, normal load, surface roughness, and temperature [194,195]. Adhesion-driven mechanisms including van der Waals, Coulombic, and chemical bonding form cohesive junctions at the polymer-metal interface, with film thickness increasing with sliding speed due to frictional heating and decreasing with higher load due to

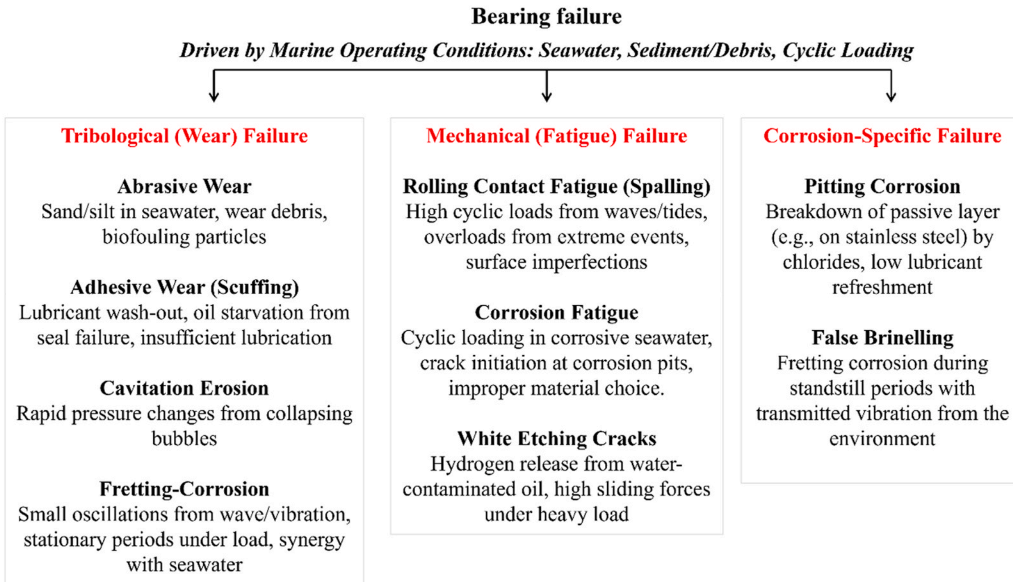

Fig. 16. Key failure mechanisms of bearings in ocean tribological systems.

compaction. Marine-grade high-performance commercial composites such as Orkot®, Deva®, ThorPlas®, and Vesconite® leverage these mechanisms while providing low wear, high load capacity, and self-lubrication, illustrating that the tribological effectiveness of polymeric hydrobearings is dictated by the synergy between material properties, interfacial adhesion, and operating conditions rather than low friction alone [33,150,193,195]. Fig. 17 shows the typical dry friction and wear rate for self-lubricating bearing materials. Table 10 lists different bearings materials employed in offshore sliding contacts.

DLC coatings on steel substrates are being explored for small bearing components operating under dry or water-lubricated conditions [204]. These coatings offer ultralow friction (<0.08) and high hardness (>15 GPa), though their brittleness and substrate adhesion under cyclic loading remain concerns.

A polycrystalline diamond (PCD) bearing shaft (17-4 PH 1150 stainless steel bushing with a ring of ten evenly spaced PCD inserts on the inner face), developed by US Synthetic for the RivGen Power System, was evaluated against Vesconite (self-lubricating thermoplastic),

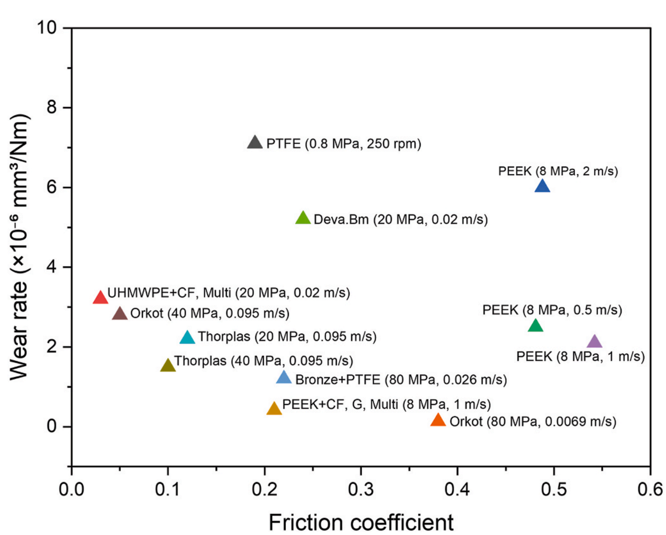

Fig. 17. Dry friction and wear rate for self-lubricating bearing materials. Data points are labelled with material, contact pressure and sliding speed [150,192,194,196,197].

Columbia Industrial Products (CIP) composite with solid lubricant (laminated composite material made of textiles impregnated with thermo setting resins and solid lubricants), and Feroform T814 (composite material made from woven fiber bonded with resin with PTFE as a friction modifier) under 60 h of freshwater operation at loads from 250 N to 2650 N [112]. PCD bearings consistently showed the lowest coefficient of friction (COF: 0.019-0.020), followed by Vesconite (0.134-0.160), Feroform (0.200-0.209), and CIP (0.227-0.231). Wear measurements at the far, centre, and drive-side positions revealed (total) minimal wear for PCD (≤0.04 mm), moderate wear for Feroform, higher wear for CIP, and the greatest wear for Vesconite. It was observed that the integration of PCD bearing technology in the RivGen Power System enables a fluid-cooled bearing-shaft assembly that eliminates the need for seals, reduces component weight, and removes dependence on lubricants and routine maintenance [112]. The diamond-based material offers exceptional resistance to sediment and abrasive particles, while its sliding-element surface sustains higher loads, exhibits minimal wear, and delivers an exceptionally low friction coefficient of 0.01 (Fig. 18).

6.3. Materials for seals

The primary function of a seal is to preserve a pressure and contaminant barrier under persistent micro-motion, pressure cycling, and particulate challenge [53,58]. The overriding tribological requirement is very low wear and extrusion resistance that preserves lip geometry and contact pressure over long time at low sliding speeds [89]. Friction control is important to avoid heat generation and secondary wear, but sealing fails first when volumetric or abrasive wear exceeds the tolerance for leakage [60]. Their primary failure modes, including biofouling-induced crevice corrosion, abrasive scoring from contaminated seals, and coating fatigue, are intrinsically linked to the constant battle against microbial colonization, suspended abrasives, and cyclic side-loading from wave action. This functional hierarchy dictates material choices, counterface finishes, and lubricant compatibility in ways that differ from bearings or sliding bushings [53,89,205–207]. Fig. 19 shows the primary failure modes for dynamic seals in marine environments.

For dynamic elastomeric seals on reciprocating rods and slow rotary shafts, the materials in reliable use are hydrogenated nitrile rubber for oil and EAL service [60], fluoroelastomers for chemically aggressive oils [208], and EPDM (Ethylene Propylene Diene Monomer rubber) for water exposure [209]. HNBR offers a good balance of tear resistance,

Table 10
Bearings employed in offshore sliding contacts [29,33,88,112,179,198–203].

Bearing material type	Examples	Why suited
Bronze-based bearings	Tin-bronze (Cu-Sn), Aluminium-bronze (Cu-Al-Fe), Manganese-bronze	High load capacity, good conformability, excellent seizure resistance, good corrosion resistance in seawater due to stable oxide films; well-established in propeller shafts, rudder bearings.
Tin-based Babbitt bearings	ASTM B23 Grades 2 & 3	Excellent embeddability for debris, conformability to shaft misalignment, low friction, moderate corrosion resistance in oil-lubricated housings; suited for slower-speed shaft journals.
Polymer composite bearings	Vesconite Hilube, Orkot Marine, Thordon Blue, Deva.tex 552	Dimensional stability in seawater, low coefficient of friction against stainless steel or Inconel shafts, good wear resistance under boundary/ mixed lubrication, chemical inertness, no need for oil lubrication; suited for mooring or rod bearings/guides.
Elastomeric bearings	Nitrile rubber (NBR), Neoprene, Polyurethane	Good vibration damping, tolerance to misalignment, resilience under shock loads, moderate wear resistance, corrosion immune.
Lignum vitae - natural wood bearings	Genuine lignum vitae (Guiacum spp.)	Self-lubricating from guaiacum, durable over decades, oil-free, stable low friction; renewable and biodegradable.
Textured bronze/ polymer hybrid bearings	Deva.bm, custom grooved bronze liners	Combines high load-bearing bronze matrix with embedded solid lubricants or polymer inlays; surface texturing enhances hydrodynamic film formation in water-lubricated service, reduces start-stop wear, and improves debris flushing.
PCD bearings	17-4 PH 1150 stainless steel bushing with a ring of ten evenly spaced PCD inserts on the inner face	Eliminates seals, reduces weight, removes need for lubricants and maintenance, resists abrasion from sediment, supports higher loads, minimizes wear, and achieves a low friction coefficient of 0.01.
Hybrid ceramic rolling elements	Si_3N_4 hybrid bearings in sealed housings	Low rotational inertia of Si_3N_4; low density reduces skidding at low speed, good dry-running survivability in transient starved states; seals critical; not suited for direct water lubrication; used for gearbox and generator bearings in sealed housings within nacelles/hulls.

abrasion resistance, and thermal stability with many EALs, provided peroxide cure systems are used to limit hydrolysis and permanent set [114]. Conventional FKM grades provide excellent oil and ozone resistance and low gas permeability, yet they are vulnerable to hot aqueous media and can blister or soften in water-rich environments [208]. Perfluoroelastomers extend fluid compatibility and temperature limits but are seldom justified for large marine actuators because modulus, abrasion resistance, and cost do not align with silt-laden service [208]. EPDM remains the most water-compatible of the common elastomers, showing low swell and good steam resistance, but it should not be used with

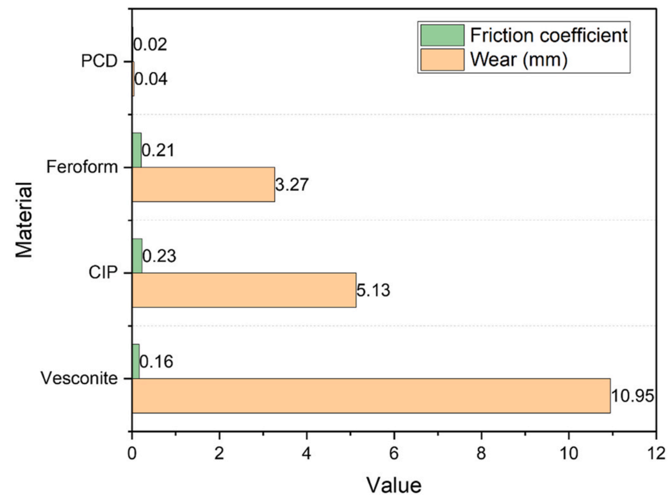

Fig. 18. Abrasion performance of hydrobearing materials over 60 h of freshwater operation, comparing PCD bearing shaft (17-4 PH 1150 stainless steel bushing with ten evenly spaced PCD inserts) with Vesconite (self-lubricating thermoplastic), CIP composite with solid lubricant (laminated textile-resin composite), and Feroform T814 (woven fiber-resin composite with PTFE friction modifier) [112].

hydrocarbon oils and certain PAGs [210,211]. Where cutting abrasion from silt dominates, cast polyurethane and thermoplastic polyurethane lips and wipers are preferred due to high tear strength, rebound resilience, and excellent resistance to particle cutting [60,212]. Polyether-based TPUs are selected over polyester types to resist hydrolysis in seawater [60]. In elastomer systems formulation and cure are as important as base polymer because modulus, crosslink density, filler hardness, and plasticizer chemistry determine abrasion rate, compression set, and cold set at low duty speeds [153,208]. Table 11 lists commonly used rubber materials for ocean rod seals, showing their operating temperature ranges (dynamic/static) and compatibility with key hydraulic fluids. It provides a quick reference for selecting materials suitable for marine hydraulic applications.

Fig. 20 presents the volume change rate (VCR) and hardness change rate (HCR) of different rubber materials in various lubricants [213]. Values are expressed in percentage (%) and retain their signs, so positive values indicate swelling or hardening, and negative values indicate shrinkage or softening. This table allows direct comparison of how each lubricant affects each rubber, providing insight into material-lubricant compatibility and tribological performance for ocean rod seal applications. For lubricating oil, MVQ shows the best compatibility, while EPDM performs the worst. FKM and PTFE are compatible with hydraulic oil. Ideally, sealing materials should combine high compatibility with properties like density and strength, but no material fully meets all requirements. In practice, selection must consider the specific usage conditions, material properties, and detailed performance needs [154, 207,213,214].

PTFE-based seals occupy a separate class that trades elastic conformity for very low friction and outstanding chemical inertness [215]. Pure PTFE creeps under sustained load and can cold flow at the heel of the lip, so fillers such as glass, carbon, graphite, bronze, and MoS_2 are used to suppress deformation and reduce wear [216,217]. Glass-filled PTFE is durable but can abrade shafts; carbon-filled and graphite-filled PTFE are less aggressive to the counterface and give lower dry friction [218]. Because PTFE lacks elasticity, spring energizers in 301 or 316 stainless steel or in nickel-based alloys for chloride service are used to maintain contact force as surfaces wear [219]. These spring-energized PTFE lips are proven in slow rotary seals for tidal main shafts and in reciprocating scrapers on exposed piston rods where oil carry-over must be minimal [220]. Friction is low enough to limit thermally driven

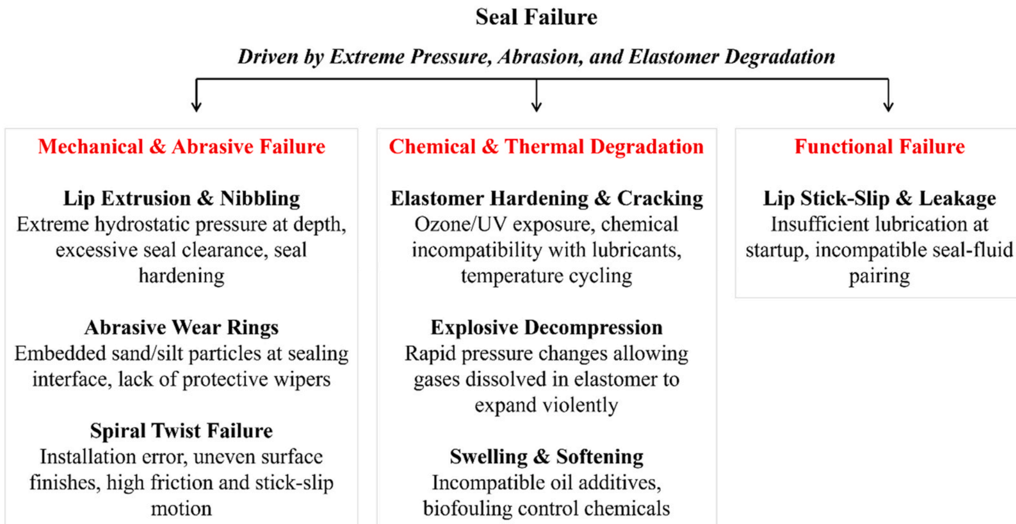

Fig. 19. Primary failure modes of dynamic seals in ocean tribological systems.

Table 11
Rubber material properties & hydraulic oil compatibility [154,213,214].

Material (Full Name + Abbr.)	Use Temp (Dynamic/Static °C)	Ordinary Mineral Oil	Water Glycol Oil	Phosphate Oil	Water-in-Oil Emulsion
Natural Rubber (NR)	60/−30~90	Incompatible	Compatible	Incompatible	Incompatible
Silicone Rubber (MVQ)	170/−60~260	Compatible	Compatible	Incompatible	Compatible
Nitrile Rubber (NBR)	80/−30~120	Compatible	Compatible	Incompatible	Compatible
Chloroprene Rubber (CR)	80/−40~120	Compatible	Compatible	Incompatible	Compatible
Fluororubber (FKM)	150/−20~200	Compatible	Compatible	Compatible	Compatible
Polyurethane Rubber (PUR)	60/−30~80	-	-	-	-
Ethylene Propylene Diene Monomer Rubber (EPDM)	70/−50~150	Incompatible	Compatible	Compatible	Incompatible
Acrylate Rubber (ACM)	80/−30~150	-	-	-	-

hydrolysis in elastomers upstream, but careful selection of energizer alloy avoids crevice corrosion and loss of load under stagnant seawater [221].

Where leakage tolerance is essentially zero and duty is continuous rotation, marine systems rely on mechanical face seals [206]. Hard pairs such as reaction-bonded silicon carbide against silicon carbide or tungsten carbide against silicon carbide dominate in water service due to high hardness, corrosion stability, and resistance to silt-assisted abrasion [222]. Resin-impregnated carbon graphite used against a ceramic counterface can provide excellent run-in and thermal management at low PV [222], but carbon can oxidize or show accelerated wear in aerated warm water [223]. Double-seal arrangements with a clean barrier fluid and pressurization are standard for submerged tidal shafts to prevent seawater ingress; the barrier fluid choice must be compatible with EAL mandates and the elastomeric secondary seals [223–225]. Modern faces often incorporate engineered micro-texturing or shallow spiral grooves to generate hydrodynamic lift at very low speed, which stabilizes friction and reduces start-stop torque without compromising leakage at rest [118,226–228]. Coatings such as PCD, DLC and tetrahedral amorphous carbon further reduce water friction and mitigate tribo-corrosion at mixed lubrication, provided adhesion and residual stress are controlled on hard ceramic substrates [222,229–231].

Counterface engineering is inseparable from seal material performance [205,232]. For dynamic lips on rods and shafts, a plateau-honed or finely ground finish with Ra on the order of 0.1 to 0.3 μm and controlled skewness avoids boundary film starvation while preventing abrasive plowing of the lip [232]. The hardness of the counterface should exceed about 55 HRC for steels or 600 HV for coated rods to resist grooving by embedded particles [12,233]. Corrosion-resistant substrates such as 17-4 PH or duplex stainless provide bulk strengtDEGBRh and chloride resistance, while coatings such as HVOF WC-Co, Cr_3C_2-NiCr, electroless Ni-P, or laser-clad Ni-based superalloys supply wear resistance and maintain a stable tribochemical interface to the elastomer [12,28,38,177,186,189,232,234]. Seal-shaft galvanic couples must be considered where metallic energizers or springs meet coated shafts. Non-conductive spacer rings and compatible alloys eliminate inadvertent galvanic pathways that accelerate micro-pitting under the lip.

Silt, biofilm, and salt crystals are the signature third bodies in marine sealing, and they dictate lip geometry and auxiliary elements more than base chemistry [12,232,235]. Primary lips are paired with sacrificial scrapers and debris excluders in tougher TPU or filled PTFE, staged inboard to outboard to shed particulates before they reach the pressure lip [235,236]. Labyrinths and slingers reduce direct spray and lower the particulate flux at the sealing interface. Biofilm growth raises viscous drag and elevates mixed-regime torque; once detached it becomes abrasive [12,37]. Smooth, low-energy external surfaces and periodic, non-toxic cleaning protocols mitigate both effects without introducing chemistries that would harm the lip or the environment. Where the application allows, seawater-lubricated seals with hydrodynamic features on the lip can run successfully with friction coefficients below 0.1 at low PV, but this requires highly wear-resistant lip materials and hard, corrosion-free counterfaces [212,220,229].

Compatibility with lubricants is a decisive constraint in offshore renewables because EALs, PAGs, and water-rich fluids are widely adopted [154]. HNBR shows generally good compatibility with saturated esters and many PAGs; FKM compatibility is fluid-grade dependent and can degrade in hot water or with certain bio-esters; EPDM is reserved for aqueous systems [154,214,237]. PTFE is broadly compatible with both EALs and water, which is one reason spring-energized PTFE seals are a default choice for barrier-fluid mechanical seals [224]. Additive packages in EALs alter boundary film chemistry at the lip; zinc-free anti-wear

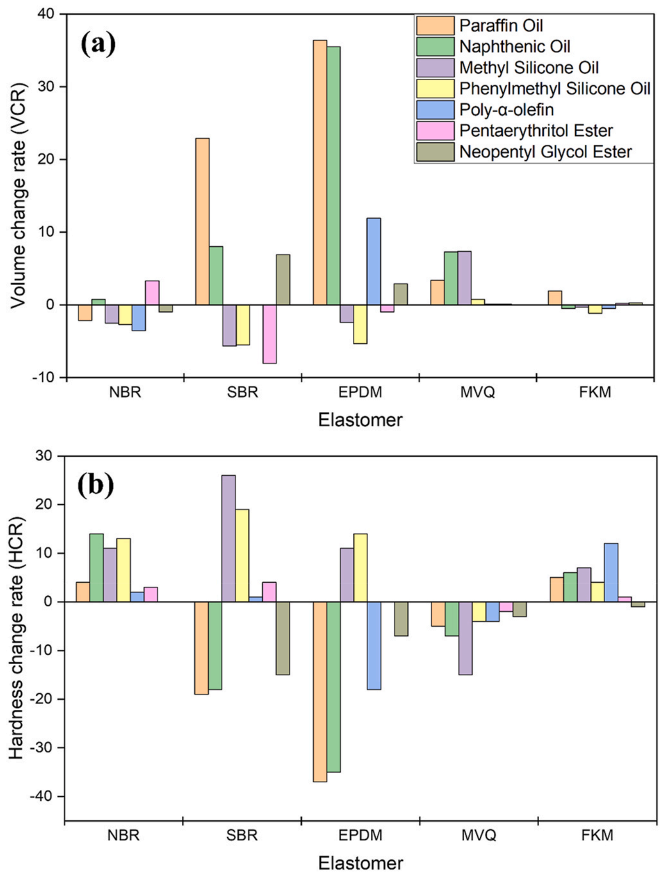

Fig. 20. Effect of different lubricants on rubber/elastomers. Positive values indicate swelling or hardening, negative values indicate shrinkage or softening, showing the relative impact of each lubricant on (a) volume change rate, and (b) hardness change rate. Adapted from Ref. [213].

packages and calcium-based detergents can either stabilize or destabilize transfer films depending on lip polymer and counterface finish, which argues for application-specific screening rather than generic approval lists [238–240].

State-of-the-art practice integrates materials with surface geometry and system controls. Textured faces and lips create controlled micro-hydrodynamic pressure at low speeds [227]. Segmented and split-construction faces simplify underwater replacement without shaft withdrawal. Composite lips that laminate TPU for tearing or abrasion resistance with PTFE or UHMWPE for low friction are entering service in reciprocating scrapers [241,242]. Metal-energized PTFE step seals with PEEK anti-extrusion rings have extended pressure capability well above 20 MPa in water service while preserving low leakage [221]. In every case the successful solution is system-specific i.e. seal compound and architecture are co-designed with the rod or shaft coating [205,232], the expected particulate exposure [243], the lubricant or barrier fluid chemistry [224], and the duty cycle [229]. The outcome to optimize is not minimum friction but minimum leakage over life at an acceptably low and stable friction that does not self-accelerate wear. Table 12 summarizes the strengths, limitations, and typical applications of various seal materials in ocean tribological systems.

6.4. *Lubrication strategy*

Fig. 21 shows the differently lubricated friction and wear rate for several self-lubricating bearing materials. Marine deployments increasingly default to environmentally acceptable lubricants (EAL) under regulatory pressure and spill risk [4,245]. In practice this means fluids that meet biodegradability and low-toxicity criteria under EPA VGP (Environmental Protection Agency Vessel General Permit) and related frameworks [246,247]. Three technical basestocks dominate i.e. synthetic esters, polyalkylene glycols (PAG), and water-rich formulations, supported by seawater-tolerant greases [248]. Additionally, due to the fire restrictions at the offshore platform, the DRTS requires water-based hydraulic fluid. Their tribological value is governed as much by water management, additive chemistry, and elastomer compatibility as by nominal viscosity grade [249].

ISO 15380 formalizes biodegradable hydraulic fluid families as HETG (hydraulic environmental triglyceride) triglyceride esters, HEES

Table 12
Materials for seals in marine applications [12,53,60,71,89,114,153,206,208,210–212,215,219,222,223,226,229,244].

Seal material class	Representative materials	Strengths	Limitations	Application relevance
Elastomers	HNBR, FKM, EPDM	HNBR: good tear + abrasion resistance, compatible with many EALs. FKM: low permeability, oil & ozone resistance. EPDM: excellent seawater & steam resistance.	EPDM incompatible with hydrocarbons. Hydrolysis & compression set can limit life.	Dynamic rod/shaft seals in hydraulic actuators, pressure barriers in marine converters
Polyurethane (PU/TPU)	Polyether-based TPU	High tear strength and abrasion resistance. Resilient against particle cutting. Polyether-TPU resists hydrolysis in seawater.	Heat build-up at high sliding speed. Potential stiffness at low temperatures.	Wipers, scrapers, silt- and debris-excluding lips in offshore equipment
PTFE-based	Virgin or filled PTFE	Ultra-low friction, chemically inert. Stable in EALs and seawater. Filler grades improve wear and creep resistance.	Cold flow/creep if unfilled. Needs spring energizer for contact pressure.	Spring-energized rotary seals, piston scrapers, barrier-fluid seals
Mechanical face seal couples	SiC–SiC, WC–SiC, C–SiC	Extremely hard, abrasion- and corrosion-resistant. Stable in silt and seawater. Textured faces allow hydrodynamic lift.	Brittle failure modes. Carbon faces oxidize in hot aerated water.	Main tidal shafts, pump seals, critical zero-leakage locations
Advanced hybrids/composites	PTFE + PEEK step seals, laminated TPU/PTFE lips, DLC-coated faces	Combine wear toughness with low friction. High PV capacity (>20 MPa with water). DLC reduces mixed-regime friction, biofouling resistance.	Complex manufacturing. Higher cost, qualification needed.	High-load rod seals, advanced face seals in next-gen tidal/WEC converters

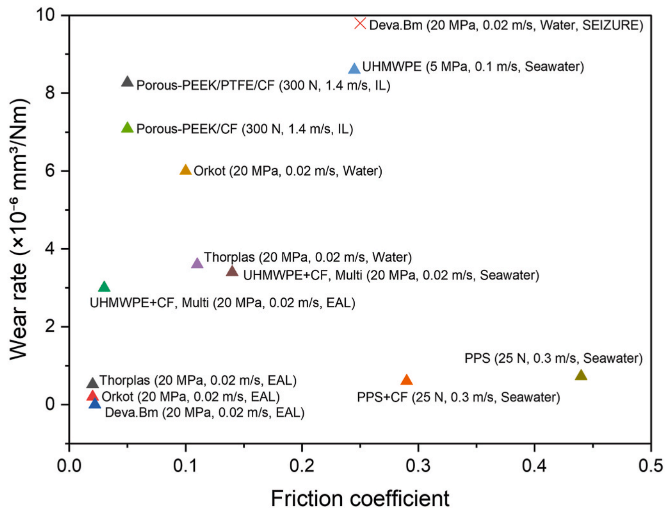

Fig. 21. Lubricated (seawater, EAL, ionic liquid) friction and wear rate for self-lubricating bearing materials. Data points are labelled with material, contact pressure and sliding speed [192,194,197,250–252].

(hydraulic environmental ester synthetic) synthetic esters, HEPG (hydraulic environmental polyalkylene glycol) polyalkylene glycols, and HEPR (hydraulic environmental polyalphaolefin and related hydrocarbons) polyalphaolefins with biodegradation enhancers [247]. Selection is constrained by seal compatibility, hydrolytic stability, and demulsibility targets in the standard.

Water contamination is the first-order life limiter. Micropitting, scuffing and bearing spall accelerate sharply at dissolved water levels that would be considered “trace” on land systems. In rolling contacts fed by oils with ~0.1 to 1.0 percent water by volume, micropitting growth rates and fatigue lives degrade by factors that remain significant even for modern AW/EP packages [253,254]. For gear oils, independent rig studies show micropitting severity rising markedly at 300 to 1000 ppm water and boundary film breakdown during transient load reversals. The mechanism is combined film collapse, hydrogen uptake, and additive deactivation [144].

Seawater as a lubricant is viable only for specific bearings and materials. For water-lubricated journal and polymer composite bearings, measured friction coefficients between 0.05 and 0.10 at modest unit loads are achievable in clean water [201,255,256]. Under silt loading, both COF and wear rates rise, and performance degrades strongly when abrasive fines embed in the softer counterface [110,257]. These observations are consistent across UHMWPE (multiscale) composites sliding against stainless shafts [194,258,259], and in legacy lignum-vitae bearings where low-speed COF can remain <0.1 in clean water but increases with particulate load [260].

Water-glycol hydraulic fluids behave as boundary-biased lubricants. With kinematic viscosities typically 32 to 46 mPas at 40 °C and ~35 to 40 percent water, they run in mixed to boundary regimes at the low sliding speeds common to PTO actuation [261]. Tribometer data show higher friction than mineral-oil baselines but acceptable wear when paired with polymeric or bronze tribo-pairs and corrosion-inhibitor packages tuned for chlorides [257,262]. Cavitation margins are smaller because of higher vapor pressure, and copper corrosion must be controlled with ashless inhibitors [261,263,264].

PAG (polyalkylene glycol) fluids split into two behaviors that matter offshore. Water-soluble PAGs (HEPG per ISO 15380) offer excellent boundary friction and very high Viscosity Index (VI) but are strongly hygroscopic [265]. They tolerate water without emulsifying and can maintain film thickness at low speed. However, they demand careful seal selection and are not miscible with hydrocarbons. Water-insoluble PAGs act more like synthetics with superior traction reduction relative to mineral oils. Both classes show low sludge tendency in wet environments and can reduce scuffing relative to mineral oils at equal viscosity [248,264].

Synthetic esters dominate EAL gear and hydraulic oils, offering strong lubricity, low-temperature flow, and compliance with biodegradation criteria, but their field implementation presents practical challenges. Many ester- and glycol-based EALs are more hygroscopic and hydrolytically sensitive than mineral oils [249], making them vulnerable to viscosity loss, additive depletion, hydrolysis, and acid formation under unavoidable seawater ingress or sustained bulk temperatures without robust antioxidant, antiwear, and water-control strategies [266]. Elastomer compatibility varies with ester structure and must be validated against the actual seal compounds [237], while oxidative stability over long maintenance intervals and the logistical difficulty of achieving complete oil changeovers on remote offshore platforms further constrain their effective use in submerged PTOs, gearboxes, and yaw systems.

Greases for wet bearings have converged on calcium sulfonate complex thickeners [267]. Compared with lithium and polyurea greases, calcium sulfonate complex greases exhibit superior mechanical stability, inherent EP performance, and corrosion resistance in the presence of water [143,268]. Shear tests show minimal softening when dry and maintain structure even when water contaminated, with no water separation observed in controlled studies [143,269]. This makes them highly suited for splines, slow bearings and exposed linkages on tidal devices [270].

Additive chemistry must shift with the base fluid and environment [4]. Conventional ZDDP and sulfurized EP chemistries are effective for scuffing but can be less compatible with certain EALs and may promote corrosive films under seawater ingress [261,271]. Modern ashless anti-wear (AW) additives, overbased sulfonates, and tailored corrosion inhibitors are used to balance tribofilm formation and chloride protection [4,148]. Recent work shows that overbased sulfonates can enhance anticorrosion and maintain rheology in wet conditions for calcium sulfonate greases [4,272].

Seal and material compatibility is non-negotiable. Water-soluble PAGs can extract plasticizers from some elastomers; certain HEES formulations swell NBR yet are acceptable with FKM (fluorelastomer) and HNBR (hydrogenated NBR) [153]. For water-glycols, polyurethane seal wear is a recurrent field failure mode unless surfaces are very smooth and hardness is controlled. These constraints need validation against the elastomer grade and surface finish of hydraulic pistons or ocean rods [205].

In practical terms, lubricant selection depends heavily on operating environment and service constraints. For near-surface wave energy converter WEC-PTO hydraulics with frequent start-stop operation, HEES or water-glycol systems are viable when water control is robust, and boundary additives are optimized [266]. Mixed-regime friction should be expected, and components should be designed with seal-friendly surfaces [206]. For submerged tidal gearboxes and bearings that cannot be frequently serviced, EAL gear oils based on HEES or water-insoluble PAGs offer lower scuffing risk at low speed and greater water tolerance than mineral oils [253,264]. However, micropitting risk rises significantly once water content exceeds a few 100 ppm, making it important to keep the system dry and control the air space above the oil [144]. For deep ocean-current devices, where pressure and temperature remain stable and access are minimal, water-compatible PAGs and calcium-sulfonate greases are recommended for their wet stability and corrosion resistance [143,267], provided seal and polymer compatibility are addressed during design. Table 13 lists the comparative summary of marine lubricants.

Additionally, the performance and longevity of a base oil are fundamentally engineered through a balanced package of chemical additives. These components are not mere supplements but are critical for managing the specific failure modes encountered in marine energy systems [4]. Key functionalities include the formation of protective tribofilms by anti-wear and extreme pressure additives (AW, EP) under

Table 13
Comparative summary of lubricant for marine tribology [4,143,144,148,153,205,206,237,248,249,254,257,260–267,269–273].

Lubricant class	Water handling	Corrosion control in chlorides	Strength	Typical failure trigger
HEES (synthetic esters; EAL hydraulic/gear)	Demulsibility varies by chemistry; intolerant of sustained free water; hydrolysis risk at elevated T and low pH	Strong with tuned inhibitor packs; acidic by-products if hydrolyzed can accelerate MIC	Very good lubricity, low-temp flow, EAL compliance	Hydrolysis with water ingress; seal swell for some NBR
HEPG (water-soluble PAGs; EAL)	Miscible with water; no stable emulsion; hygroscopic but tolerant to dissolved water	Good under wet conditions with proper inhibitors; low sludge tendency	Excellent wet stability; low sludge/varnish; good micropitting resistance at equal viscosity	Incompatibility with hydrocarbon oils; moisture absorbing from atmosphere increases water content
PAG (water-insoluble)	Does not absorb water; tends to separate it for removal; sensitive to dissolved water at contact	Good with ashless AW/EP; better micropitting resistance than mineral at same ISO VG	High VI, low friction, oxidative stability	Additive miscibility limits; cross-contamination with mineral oils
Water-glycol (HFC)	water-rich; cavitation margin smaller	Needs robust inhibitors	Fire resistance; inherently spill-benign	Vapor pressure and cavitation; copper corrosion without tailored inhibitors
HEPR (PAO-based EAL)	Good demulsibility; not water-tolerant long-term	Strong with modern AW/EP + anticorrosion; less prone to hydrolysis than esters	Balanced choice for sealed gearboxes with low wet exposure	Micropitting risk rises with ppm-level water; not ideal for wet housings
Calcium sulfonate complex greases	Water washout resistance; holds structure when wet	Excellent rust prevention due to overbased sulfonates	Wet stability, mechanical stability, corrosion protection	Over-thickening at low temps; oil bleed under shock loads if base oil too light
Seawater	Performance collapses with load	Requires corrosion-proof pairs	Zero spill risk; strong heat rejection	Corrosion/Tribocorrosion; Abrasive wear from slit to seals/bearings

high load; the reduction of parasitic losses by friction modifiers in boundary lubrication regimes; and the critical defense against the environment provided by corrosion inhibitors and demulsifiers [121,274]. The selection and compatibility of these additives, particularly within the constraints of EALs, are a primary determinant in the reliability of submerged and splash-zone tribological interfaces [249,261,273]. Table 14 details the key lubricant additives and their engineered functions for mitigating tribological failures in marine environments.

Based on experimental data from a hydrodynamic journal bearing test rig [193,250], Mccarthy et al. study compares the performance of three EALs: a saturated ester, a rapeseed base fluid, and a Propylene Glycol Dioleate (PGD) against three mineral turbine oils (ISO VG32, VG46, and VG68) under hydrodynamic conditions. The investigated lubricants and their respective viscosities at 40 °C are: VG32 mineral (27 mPa s), VG46 mineral (37 mPa s), VG68 mineral (56 mPa s), Synthetic ester (29 mPa s), Rapeseed oil (32 mPa s), and PGD (19 mPa s). Fig. 22 presents the comparative analysis of their performance.

It was noticed that the VG68 mineral oil, which has the highest base viscosity, exhibits the highest operating temperatures. The synthetic ester's temperature profile consistently falls between those of the VG32 and VG46 mineral oils, which aligns with its intermediate base viscosity. The PGD fluid, with the lowest base viscosity, demonstrates significantly superior thermal performance, recording the lowest temperatures of all tested lubricants. Fig. 22a shows the local fluid viscosity along the bearing centerline, calculated from the measured temperatures at 2000 rpm and 2 MPa. In the high-temperature, minimum film region, the VG46 mineral oil and synthetic ester show nearly identical viscosities despite their different base viscosities. However, in the cooler inlet zone (positions 15° to 45°), the synthetic ester's lower base viscosity results in reduced fluid friction. The environmentally acceptable lubricants (EALs), rapeseed oil and PGD, generally display effective viscosity characteristics that contribute to stable film formation. Fig. 22b plots the minimum oil-film thickness against applied load at a constant speed of 2000 rpm. As expected, film thickness decreases with increasing load for all lubricants. The VG68 mineral oil, with the highest base viscosity, consistently generates the thickest film. Rapeseed oil, despite a lower base viscosity than VG46, shows competitive film-building ability, highlighting the role of its high Viscosity Index. Fig. 22c illustrates the minimum oil-film thickness as a function of rotational speed under a constant 2 MPa load. Film thickness increases with speed for all fluids. The VG68 mineral oil again provides the greatest film thickness across all speeds. The synthetic ester and PGD show comparable performance at lower speeds, but the synthetic ester maintains a thicker film as speed increases, demonstrating the advantage of its tailored rheological properties.

These results highlight the critical role of both base viscosity and the viscosity index. Higher base viscosity generally leads to thicker films, while a higher VI helps maintain film strength under thermal stress. It should be noted that these values are comparative, as absolute measurements are influenced by factors not fully characterized in this study [193], such as thermal expansion and pressure-viscosity effects.

6.5. *Surface engineering and coating strategies*

To withstand multi-tribological demands simultaneously, surface engineering becomes indispensable. Current approaches integrate functional coatings and interfacial architectures that enhance surface performance while preserving base material ductility.

6.5.1. *Hard and wear-resistant coatings*

Thermal spray coatings (e.g., WC-CoCr, Cr_3C_2-NiCr) are commonly applied on cylinder rods, shaft sleeves, and impact-prone areas [115,188]. These offer excellent erosion and abrasive wear resistance, but their performance hinges on microstructural densification and pore sealing. Unsealed porosity permits chloride ingress, leading to subsurface corrosion, microcrack nucleation, and eventual spallation under mechanical load [9,34].

Amorphous metal coatings (e.g., Fe- and Zr-based metallic glasses) exhibit non-crystalline microstructures with high hardness, corrosion resistance, and fretting fatigue tolerance. Their homogeneous atomic structure mitigates crack initiation and offers superior pitting resistance in submerged, reciprocating components (e.g., hydrokinetic rotor bearings).

6.5.2. *Low-friction and chemically stable films*

PVD coatings, such as DLC, TiN, or CrN, provide ultra-low friction and high wear resistance. However, their application on polymeric or elastomeric substrates is limited by poor adhesion and brittle failure under impact or micropitting [277]. They are better suited for hard substrates with controlled surface preparation and compatible loading regimes.

Hydrophilic ceramic coatings (e.g., Al_2O_3-TiO_2, SiO_x-based films) show potential in promoting boundary water film retention, especially in water-lubricated sliding systems [278]. These coatings can reduce metal-to-metal contact by enhancing capillary wetting and hydrodynamic lift, particularly beneficial in mixed or boundary lubrication regimes.

Table 14
Primary lubricant additive classes, their molecular functions, and critical considerations for ocean tribological systems [4,121,249,261,273,275,276].

Additive class	Primary function	Mechanism of action	Key consideration for oceanic system
Anti-wear (AW) additives (e.g., ZDDP)	Prevent metal-to-metal contact under boundary lubrication.	Forms a protective, sacrificial tribofilm on metal surfaces via thermal decomposition and adsorption.	Effectiveness can be reduced by water ingress; must be compatible with EAL formulations.
Extreme Pressure (EP) Additives (e.g., Sulfur-Phosphorus)	Prevent seizure and welding under very high loads/shock.	Reacts chemically with the metal surface under high frictional heat to form a low-shear strength compound.	Can be corrosive to yellow metals; selection is critical for gearboxes. Must be "ashless" for many EALs.
Friction modifiers	Reduce friction in mixed/boundary lubrication regimes.	Physically or chemically adsorbs to surfaces to form a low-shear layer, reducing the coefficient of friction.	Crucial for improving efficiency in slow-moving, high-load components like WEC hinges and tidal pitch bearings.
Viscosity index improvers	Reduce the rate of viscosity change with temperature.	Long-chain polymers that uncoil as temperature increases, counteracting the natural thinning of the oil.	Mechanical shearing in gearboxes can permanently degrade polymers, leading to viscosity loss over time.
Corrosion & rust inhibitors	Protect ferrous and non-ferrous metal surfaces from corrosion.	Forms a protective monolayer on metal surfaces, blocking water and oxygen. Overbased detergents neutralize acids.	Critical for combating seawater ingress and salt-laden atmospheres. Overbased calcium sulfonates are highly effective.
Antioxidants	Retard oxidative degradation of the lubricant.	Radical Scavengers (e.g., amines) terminate free-chain reactions. Peroxide Decomposers (e.g., ZDDP, phenols) neutralize peroxides.	High operating temperatures and water contamination accelerate oxidation. Essential for extending oil life.
Detergents & dispersants	Keep contaminants suspended and surfaces clean.	Detergents (metallic soaps) neutralize acids and clean deposits. Dispersants (ashless) keep soot and sludge finely suspended.	Prevents sludge formation from oil oxidation and biofouling by-products. Vital for systems with water ingress.
Demulsifiers	Promote rapid separation of water from oil.	Changes the interfacial tension at the oil-water boundary, causing water droplets to coalesce and separate.	A primary defense against seawater emulsion, protecting components from corrosion and lubricant from hydrolysis.
Antifoam agents	Suppress foam formation.	Insoluble silicone or organic polymers that reduce surface tension, causing foam bubbles to collapse.	Essential in systems with high churning or air entrainment (e.g., gearboxes, hydraulic reservoirs).
Pour point depressants	Enable flow at low temperatures.	Modifies wax crystal formation in the oil, preventing them from interlocking and solidifying.	Important for systems in cold climates to ensure circulation at startup.

6.5.3. *Corrosion-resistant sacrificial systems*

Zinc-rich coatings and anodic overlays serve as sacrificial systems, protecting more critical tribo-interfaces from chloride-driven attack [279,280]. Their use in bolt assemblies, flange faces, and crevice-prone joints prevent galvanic corrosion and delays structural failure.

6.5.4. *Self-responsive and adaptive interfaces*

Self-healing coatings using dynamic covalent networks (e.g., disulfide linkages, Diels-Alder systems) or microencapsulated healing agents offer emerging pathways for damage tolerance [281,282]. In marine tribo-contacts, these could delay crack propagation, reduce maintenance frequency, and improve component lifetime.

Swell-tolerant elastomers, designed to accommodate volumetric expansion without inducing interfacial stress, are particularly valuable in sealing applications where water uptake would otherwise cause extrusion or debonding [283].

6.5.5. *Biofouling-resistant materials and interfaces*

From a regulatory perspective, conventional biocide-leaching coatings are effectively obsolete under the international maritime organization (IMO) treaty, and emerging frameworks under EU REACH are increasingly restrictive on nano-additives with unresolved ecotoxicity. This regulatory squeeze necessitates a shift away from biocide reliance towards structural, surface-engineered, and multifunctional solutions that combine tribological durability with biological passivity.

Conventional fouling-mitigation strategies rely on bio-inert materials (e.g., PTFE, silicone-based elastomers), which exhibit low surface energy to discourage biological adhesion [284]. While effective at reducing organism attachment, such materials lack the mechanical integrity required for load bearing or sliding contacts under marine operating conditions [7,37,158].

Recent advances have explored bio-inspired micro- and nano-topographies, such as those mimicking the dermal denticles of sharks (e.g., Sharklet patterns), lotus leaf structures, or cicada wings [285]. These surfaces function by reducing available adhesion area at the microbial scale [13,285], disrupting biofilm development through spatial patterning [37], and inducing self-cleaning hydrodynamic effects in flow environments [156–158].

In study [13,37] it was shown that increased roughness can improve mechanical interlocking, making surfaces more resistant to wear. However, this same roughness can also unintentionally promote the attachment of biofouling organisms, such as algae and barnacles, which interfere with lubrication. The effect of roughness on biofouling depends on how well it provides contact points for organisms to settle, with rougher surfaces often supporting greater attachment due to increased available area for adhesion [285]. For instance, bio-organisms tend to settle more readily on surfaces with higher roughness, as the increased contact area helps them anchor themselves more firmly. This is particularly evident with microscopic algae and barnacle larvae, which prefer surfaces with specific roughness patterns that mimic their ideal attachment sites. In some cases, the roughness pattern itself can guide the organism's choice of settlement site. However, this attachment is not solely governed by roughness and material properties also play a significant role [37].

While roughness can encourage biofouling, innovative surface treatments such as slippery liquid-infused surfaces (SLIPS) have shown promise in reducing fouling in laboratory environment. These surfaces maintain lubricity, which prevents organisms from settling, even on rough microstructures [286]. This hints that the positive effect of liquid-based lubricants such as oil or seawater may benefit. However, practical deployment in tribologically loaded systems is still limited. These surfaces typically lack the mechanical resilience to withstand contact pressures, abrasive loading, or frictional heating. Hybrid approaches, where bioinspired patterning is combined with wear-resistant coatings, are emerging but require significant optimization for marine tribo-systems [37].

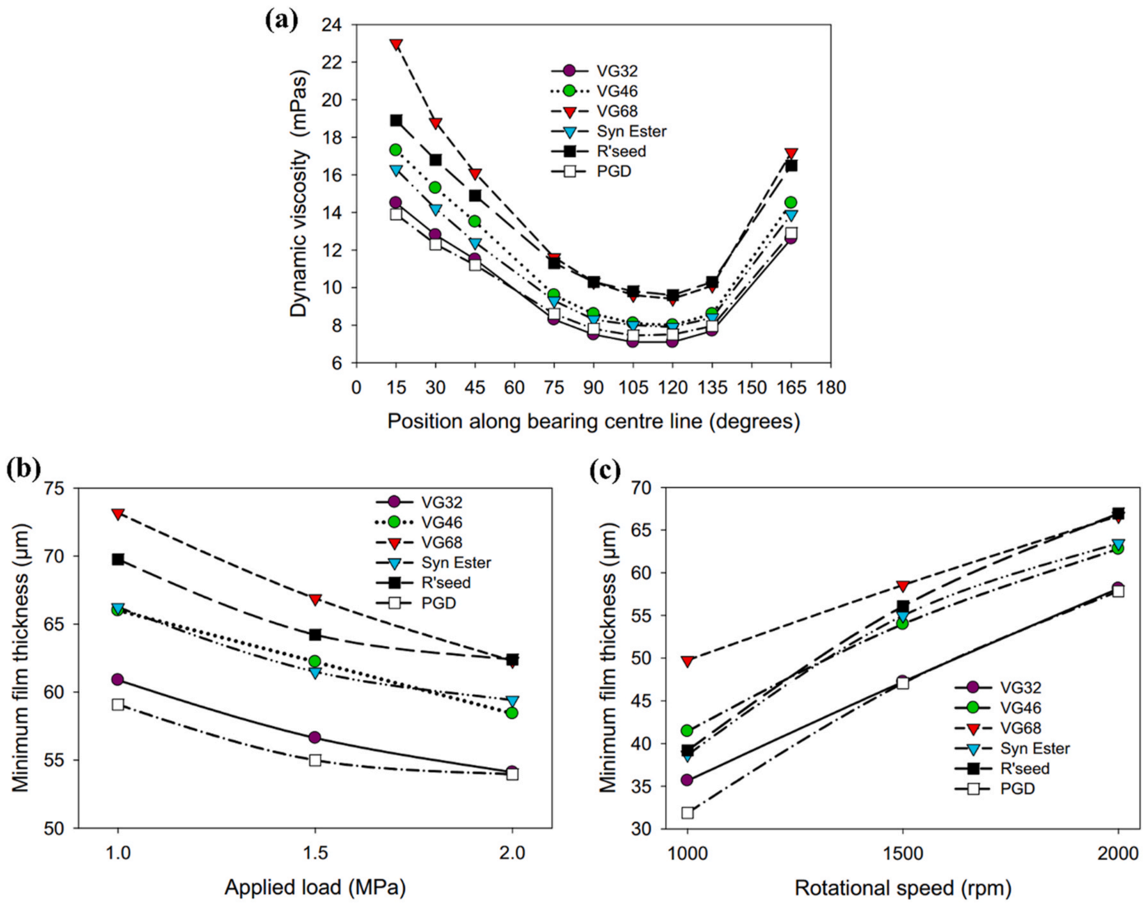

Fig. 22. Performance comparison of lubricants in a hydrodynamic journal bearing: (a) Local viscosity profile along the bearing centerline at 2000 rpm and 2 MPa, (b) Minimum film thickness versus applied load at 2000 rpm, and (c) Minimum film thickness versus rotational speed at 2 MPa. Reproduced with permission from Ref. [250].

6.6. Offshore repairability

Weldability (or repair) is a critical limiting factor in deploying high-performance alloys in ocean rods [287–289]. Duplex stainless steels, while offering superior strength and corrosion resistance, require stringent heat input control to maintain an optimal ferrite-austenite phase balance. Improper welding can result in sensitization, intermetallic precipitation (e.g., sigma phase), and pitting corrosion, severely

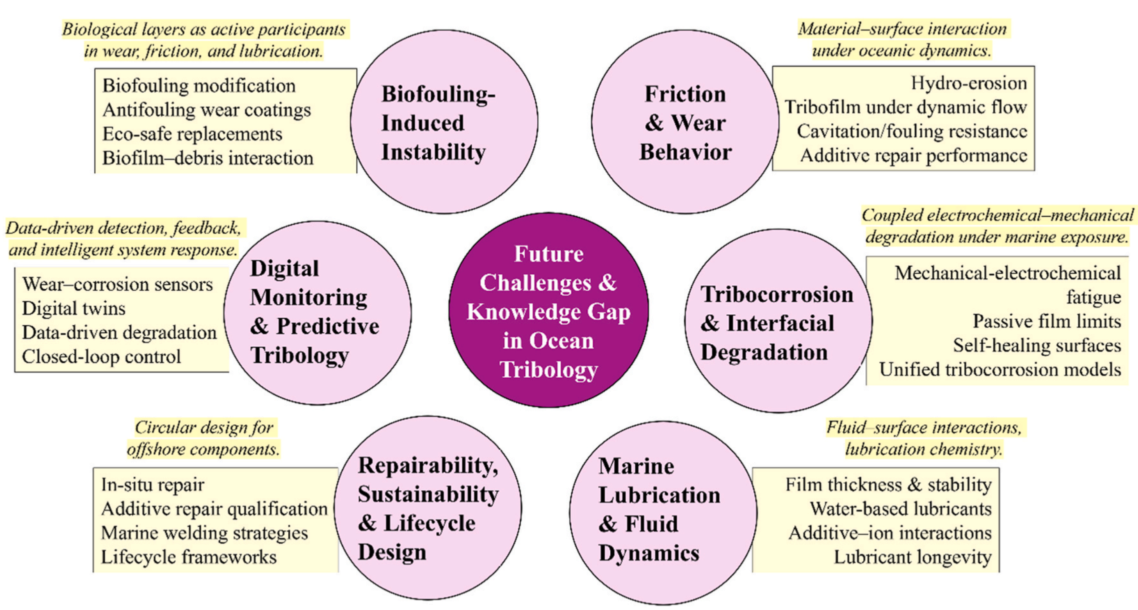

Fig. 23. Key areas of challenge and research gaps in marine renewable energy tribological systems.

compromising durability. Similarly, PH steels (e.g., 17-4 PH, 15-5 PH), demand post-weld heat treatments to restore mechanical properties and corrosion resistance [290,291]. These treatments are typically impractical in offshore settings due to their thermal, spatial, and procedural complexity [292]. The lack of in-situ heat treatment infrastructure effectively disqualifies many PH steels from direct field repair, limiting their use to modular or factory-prepared subassemblies.

On-site refurbishment using additive manufacturing, laser cladding or plasma transferred arc deposition offers pathways for in-situ rebuilding of worn surfaces, such piston rods [115,293,294]. However, standardization and field qualification for such repair works are still in early stages.

7. Future studies and research gaps

Advancement of ocean/marine tribology depends on resolving fundamental uncertainties across interacting phenomena rather than simply improving materials or coatings. Fig. 23 illustrates key areas of challenge and research gaps in MRE tribological systems. Tribocorrosion remains a central challenge. Several objectives should be answered such as, to what extent does tribocorrosion accelerate when abrasive ingress disrupts passive films, and can coatings be engineered to self-heal? To what extent do transient electrochemical gradients induced by wave and tidal fluctuations alter surface hardness or fatigue life in composite or coated materials? How do cavitation microjets influence passive film repair kinetics in duplex steels, can multi-layered coatings survive simultaneous chloride attack and cavitation stress, and what electrochemical feedback occur between corrosion debris and abrasive wear?

For biofouling or organic deposits, critical unknowns include how micro- and macro-fouling layers affect frictional contact, debris formation, and local hydrodynamics at bearing or seal interfaces. How does microbial colonization on seal lips alter lubrication regimes and frictional heat generation? Can these layers be engineered (using surface texturing, etc.) to promote self-lubricating boundary films rather than acting purely as a mechanical hindrance? What is the effect of biofouling layers on third-body film composition and wear particle dynamics.

From lubrication perspectives, several questions should be answered. Such as, how thick and stable are boundary or mixed lubrication films when using seawater versus advanced ionic liquids or hydrogel-infused surfaces at oscillatory low-speed, highly loaded contacts? How do additive interactions, dissolved salts, and debris generation modify film formation, and what limits film resilience over months or years in situ? Can nanoparticle-based additives form durable tribofilms in situ without washout? Furthermore, can engineered composites exploit seawater chemistry, such as Ca^{2+} and Mg^{2+} ions, to self-generate lubricating films in situ? What are the critical scales of hydrodynamic film thickness achievable in seawater at oscillatory low-speed contacts?

The mechanics of sliding wear and abrasion require further quantitative linking of micro-scale wear mechanisms to system-scale performance. How does periodic impact or particulate-laden flow accelerate micro-pitting or abrasive removal, and can surface textures or graded coatings mitigate this without sacrificing bearing stiffness or load capacity? Advanced seals raise similar challenges such as what is the tolerance window under abrasive particle intrusion before hydrodynamic lift collapses?

Erosion and cavitation effects in such systems are inadequately understood [113,285,295]. How does repeated cavitation bubble collapse influence coating delamination or initiate microcrack networks in advanced ceramics or polymer-metal hybrids? Can surfaces be engineered to divert erosive energy through controlled roughness or compliant microstructures? Additionally, the coupling between hydrodynamics, surface topography (biomimetic) [296], and fouling remains largely unexplored; what riblet or dimple geometries simultaneously minimize drag, manage debris transport, and resist microbial colonization in turbulent boundary layers?

The integration of digital tribology and predictive monitoring introduces open questions on data-driven control [297–300]. What sensor configurations and model fidelities are required to detect early tribocorrosion or lubrication failure before catastrophic wear occurs? How can modulating rotational speed, flow rates, or surface hydration be systematically validated to extend operational life in highly variable ocean environments?

Therefore, a critical barrier to bridging the TRL 4-9 gap is the lack of standardized (tribo-test) protocols that unify hydrodynamic duty cycles with bio-chemical synergy. Current IEC specifications lack methodologies for combining bio-organic fouling with mechanical sliding; in practice, barnacle excision on a reciprocating shaft can gouge seals and expose nascent metal to accelerated galvanic attack, a phenomenon not captured by standard salt-fog or pin-on-disk tests. Future experimental frameworks must transition to High-Fidelity Synergistic Rigs that replicate the stochastic PV load profiles of WECs/TECs (typically 0.1-20 MPa m/s). New experimental designs must quantify the "PV-Envelope Collapse," where the synergy of silt-abrasion and corrosion may reduce the operational PV tolerance of polymers and composites. This review advocates for: (1) In-situ Potentiodynamic-Tribometers replicating WEC-specific duty cycles (0.1-0.5 Hz) under cavitation; (2) Bio-Chemical Hybrid Rigs using "living" biofilms to measure lubrication regime shifts; and (3) Sensor-Integrated Bearings (measuring torque, acoustic emission, and surface hydration) to provide the high-fidelity data needed to validate predictive MTBF models and digital-twin validation.

8. Conclusions and outlook

Global decarbonization mandates have elevated ocean energy as a strategic contributor to future power systems, yet this review demonstrates that tribological degradation remains the dominant constraint on durability, availability, and cost competitiveness. A central finding of this work is that the persistent reliability gap in wave, tidal, and ocean-current energy systems is not primarily due to a lack of candidate materials, but to how tribological phenomena have been investigated and qualified to date.

This review reveals a clear imbalance in research focus: corrosion and tribocorrosion dominate the literature, while coupled (multi) degradation synergy particularly the interaction of wear, biofouling, or lubrication instability remain underrepresented. Likewise, the scarcity of test methodologies that integrate realistic motion spectra, PV regimes, electrochemical conditions, and biological activity prevents meaningful extrapolation from laboratory data to offshore performance. As a result, reported wear rates, friction coefficients, and corrosion metrics obtained under controlled conditions provide limited predictive value unless the coupled nature of these processes is preserved.

The performance limits of bearings, seals, and coatings in marine systems are governed less by nominal material properties than by the instability of lubrication and surface integrity under coupled loading. Seawater provides insufficient hydrodynamic support at low speeds and oscillatory motions, forcing most contacts into mixed or boundary regimes where small perturbations rapidly escalate wear. Alternative lubricants including oils (con: emulsify), biodegradable esters (con: hydrolyze with time), and water-compatible ionic liquids or zwitterionic surfactants systems remain unvalidated under biofilm-covered, particle-laden, and turbulent conditions. Polymer composites and ceramic-polymer hybrid bearings exhibit low wear under controlled environments, yet their reliance on transfer-layer formation renders them vulnerable to disruption by silt abrasion, fouling debris, and flow-induced shear. In sealing systems, textured and composite architectures extend tolerance to misalignment and particle ingress, but cavitation erosion and biofouling-driven frictional instabilities remain unresolved failure triggers. Metallic alloys with high pitting resistance retain corrosion performance only while passive films remain intact; once mechanically disrupted, tribocorrosion accelerates beyond repassivation kinetics.

Biofouling acts as an active tribological agent rather than a passive surface contaminant, modifying roughness spectra, altering lubrication regimes, and introducing biologically derived third bodies into sliding contacts. Existing antifouling or biomimetic coatings suppress biological adhesion but lack the mechanical resilience required for high contact pressures. The critical design frontier therefore lies in integrating antifouling chemistry with load-bearing tribological architectures, rather than optimizing either in isolation.

Materials selection must account for offshore repairability as a governing constraint rather than a secondary consideration. High-performance alloys commonly used in hydraulic and linear rods exhibit narrow processing tolerances that prevent reliable field repair, with duplex stainless steels sensitive to heat input–induced phase instability and PH steels requiring post-weld treatments impractical offshore. These constraints fundamentally limit lifecycle sustainability, irrespective of initial corrosion or wear resistance.

Taken together, the field of ocean tribology is at a threshold. Specific laboratory studies show opportunities for low-wear composites, hybrid bearings, and advanced coatings and lubricants, while monitoring technologies offer the possibility of predictive maintenance. Yet, without targeted advances in offshore repairability, multi-degradation simulation, and component-level offshore qualification, the gap between controlled lab results and offshore feasibility will persist. The path forward requires treating tribology not as an afterthought of materials or hydrodynamics, but as the integrating science of sustainability in marine energy systems.

Declaration of competing interest

The authors declare that they have no known competing financial interests or personal relationships that could have appeared to influence the work reported in this paper.

Acknowledgement

This research is funded by the Slovenian Research Agency ARIS under the Research Core Funding Programme No. P2-0231 and Marie-Sklodowska Curie COFUND - Seal of Excellence No. 5100- 237/2023-7 (February 5, 2024). The author is grateful to the Ocean Tribology Center (OTC) and the COST Action Programme CA23155 for their engagement in fostering transnational knowledge exchange in the field.

Data availability

No data was used for the research described in the article.

References

[1] Rehman, S., Alhems, L.M., Alam, M.M., Wang, L., Toor, Z., 2023. A review of energy extraction from wind and ocean: technologies, merits, efficiencies, and cost. Ocean. Eng. 267, 113192. https://doi.org/10.1016/J.OCEANENG.2022.113192.

[2] Dickson, M., Pennock, S., Todalshaug, J., Rebenius, K., 2025. Results and lessons learned from CorPower ocean's full Scale C4 wave energy converter first ocean deployment period. In: Proceedings of the 16th European Wave and Tidal Energy Conference, Funchal, p. 958. https://doi.org/10.36688/ewtec-2025958, 1.

[3] Shao, X., Ringsberg, J.W., Yao, H.D., Gowda, U.R.S.L., Khedkar, H.N., Todalshaug, J.H., 2024. Hydrodynamic interactions and enhanced energy harnessing amongst many WEC units in large-size wave parks. J. Mar. Sci. Eng. 12, 730. https://doi.org/10.3390/JMSE12050730, 12 (2024) 730.

[4] Carter, B.H., Green, D., 2010. Marine Lubricants, Chemistry and Technology of Lubricants, third ed., pp. 389–409. https://doi.org/10.1023/B105569_13

[5] Wood, R.J.K., 2017. Marine wear and tribocorrosion. Wear 376–377, 893–910. https://doi.org/10.1016/J.WEAR.2017.01.076.

[6] Johnson, R., Von Der Ohe, C.B., 2011. Tribocorrosion in marine environments. Ttiubocorros. Pass. Metal Coat. 441–474. https://doi.org/10.1533/9780857093738.3.441.

[7] Birchon, D., 1970. Use and abuse of materials in ocean engineering. Proc. Inst. Mech. Eng. 241–271. https://doi.org/10.1243/PIME_PROC_1970_185_034_02.

[8] Magagna, D., Uihlein, A., 2015. Ocean energy development in Europe: current status and future perspectives. Int. J. Mar. Energy 11, 84–104. https://doi.org/10.1016/J.IJOME.2015.05.001.

[9] Von Der Ohe, C.B., Johnsen, R., Espallargas, N., 2010. Hydraulic cylinders for offshore splash zone operation: a review of piston rod failure cases and alternative concepts. Proc. Int. Conf. Offshore Mech. Arctic Eng. OMAE 6, 1–14. https://doi.org/10.1115/OMAE2009-79039.

[10] Wood, R.J.K., Bahaj, A.S., Turnock, S.R., Wang, L., Evans, M., 2010. Tribological design constraints of marine renewable energy systems. Philos. Trans. R. Soc. A Math. Phys. Eng. Sci. 368, 4807–4827. https://doi.org/10.1098/RSTA.2010.0192.

[11] Beaubien, L.A., Wolock, I., Buchanan, C.L., Whitman, C.L., 1972. Behavior of materials in a subsurface ocean environment. https://apps.dtic.mil/sti/tr/pdf/AD0747245.pdf. (Accessed 5 August 2025).

[12] Lindén, J.B., Andersson, K.-Å., Harnden, R., Bonel, A., Fonseca, G., Vinagre, P.A., Pinori, E., 2022. Marine Biofouling, Corrosion, and Wear Protection of Power Take off Rods for Wave Energy Conversion - Laser Cladding and Scraping, pp. 1–15. https://doi.org/10.5006/C2022-17891.

[13] Scardino, A.J., Guenther, J., de Nys, R., 2008. Attachment point theory revisited: the fouling response to a microtextured matrix. Biofouling 24, 45–53. https://doi.org/10.1080/08927010701784391.

[14] Smith, W.V., Schneider, L.G., 1963. Lubrication in a sea water environmen, naval engineers journal. SAE Tech. Pap. 75, 841–854. https://doi.org/10.4271/630225.

[15] Vizentin, G., Vukelic, G., 2020. Degradation and damage of composite materials in marine environment. Mater. Sci. 26, 337–342. https://doi.org/10.5755/J01.MS.26.3.22950.

[16] Dhandapani, A., Krishnasamy, S., Thiagamani, S.M.K., Periasamy, D., Muthukumar, C., Sundaresan, T.K., Ali, S., Kurniawan, R., 2024. Evolution, prospects, and predicaments of polymers in marine applications: a potential successor to traditional materials. Recycling 9, 8. https://doi.org/10.3390/RECYCLING9010008, 9 (2024) 8.

[17] Fronek, A., Nosonovsky, M., Barger, B., Avdeev, I., 2012. Tribological and mechanical design considerations for wave energy collecting devices. Green Energy Technol. 49, 607–619. https://doi.org/10.1007/978-3-642-23681-5_21/FIGURES/6.

[18] Vanegas-Cantarero, M.M., Pennock, S., Bloise-Thomaz, T., Jeffrey, H., Dickson, M.J., 2022. Beyond LCOE: a multi-criteria evaluation framework for offshore renewable energy projects. Renew. Sustain. Energy Rev. 161, 112307. https://doi.org/10.1016/J.RSER.2022.112307.

[19] Ocean Energy - European Commission, (n.d.). https://research-and-innovation.ec.europa.eu/research-area/energy/ocean-energy_en (accessed March 1, 2025).

[20] Zappa, W., Junginger, M., van den Broek, M., 2019. Is a 100% renewable European power system feasible by 2050? Appl. Energy 233–234, 1027–1050. https://doi.org/10.1016/j.apenergy.2018.08.109.

[21] European Commission, 2023. Delivering on the EU Offshore Renewable Energy Ambitions, p. 668. https://eur-lex.europa.eu/legal-content/EN/TXT/?uri=COM:2020:741:FIN&qid=1605792629666. (Accessed 18 July 2024).

[22] Tapoglou, E., Tattini, J., Schmitz, A., Georgakaki, A., Długosz, M., Letout, S., Kuokkanen, A., Mountraki, A., Ince, E., Shtjefni, D., Joanny, O.G., Eulaerts, O., Grabowska, M., 2023. Clean Energy Technology Observatory: Ocean Energy in the European Union - 2023 Status Report on Technology Development. Trends, Value Chains and Markets. https://doi.org/10.2760/82978.

[23] Kluger, J.M., Haji, M.N., Slocum, A.H., 2023. The power balancing benefits of wave energy converters in offshore wind-wave farms with energy storage. Appl. Energy 331, 120389. https://doi.org/10.1016/J.APENERGY.2022.120389.

[24] Tatum, S.C., Frost, C.H., Allmark, M., O'Doherty, D.M., Mason-Jones, A., Prickett, P.W., Grosvenor, R.I., Byrne, C.B., O'Doherty, T., 2016. Wave–current interaction effects on tidal stream turbine performance and loading characteristics. Int. J. Mar. Energy 14, 161–179. https://doi.org/10.1016/J.IJOME.2015.09.002.

[25] Milne, I.A., Day, A.H., Sharma, R.N., Flay, R.G.J., 2016. The characterisation of the hydrodynamic loads on tidal turbines due to turbulence. Renew. Sustain. Energy Rev. 56, 851–864. https://doi.org/10.1016/J.RSER.2015.11.095.

[26] Mason-Jones, A., O'Doherty, D.M., Morris, C.E., O'Doherty, T., 2013. Influence of a velocity profile & support structure on tidal stream turbine performance. Renew. Energy 52, 23–30. https://doi.org/10.1016/J.RENENE.2012.10.022.

[27] Wood, R.J.K., 2006. Erosion–corrosion interactions and their effect on marine and offshore materials. Wear 261, 1012–1023. https://doi.org/10.1016/J.WEAR.2006.03.033.

[28] Wood, R.J.K., Speyer, A.J., 2004. Erosion-corrosion of candidate HVOF aluminium-based marine coatings. Wear 256, 545–556. https://doi.org/10.1016/S0043-1648(03)00564-7.

[29] Quaranta, E., Davies, P., 2022. Emerging and innovative materials for hydropower engineering applications: turbines, bearings, sealing, dams and waterways, and ocean power. Engineering 8, 148–158. https://doi.org/10.1016/J.ENG.2021.06.025.

[30] Blavette, A., O'Sullivan, D.L., Lewis, A.W., Egan, M.G., 2011. Grid integration of wave and tidal energy. Proc. Int. Conf. Offshore Mech. Arctic Eng. OMAE 5, 749–758. https://doi.org/10.1115/OMAE2011-49953.

[31] von der Ohe, C.B., Johnsen, R., Espallargas, N., 2010. Modeling the multi-degradation mechanisms of combined tribocorrosion interacting with static and cyclic loaded surfaces of passive metals exposed to seawater. Wear 269, 607–616. https://doi.org/10.1016/J.WEAR.2010.06.010.

[32] Wood, R.J.K., 2007. Tribo-corrosion of coatings: a review. J. Phys. D Appl. Phys. 40, 5502–5521. https://doi.org/10.1088/0022-3727/40/18/S10.

[33] Kumar, R., Kalin, M., Emami, N., 2026. Sliding-speed effects on self-lubricating marine composites: a comparative assessment of tribological, mechanical, and thermal performance. Tribol. Int. 216, 111593. https://doi.org/10.1016/J.TRIBOINT.2025.111593.
[34] Von Der Ohe, C.B., Johnsen, R., Espallargas, N., 2009. Premature failure of riser tensioner piston rods exposed to offshore splash zone operation-status and review of critical multi-degradation factors. In: Proceedings of the CORROSION 2009. CORROSION. AMPP, Atlanta, GA, pp. 1–23. https://doi.org/10.5006/C2009-09199, 2009.
[35] Singh, R., Tiwari, S.K., Mishra, S.K., 2012. Cavitation erosion in hydraulic turbine components and mitigation by coatings: current status and future needs. J. Mater. Eng. Perform. 21, 1539–1551. https://doi.org/10.1007/S11665-011-0051-9/FIGURES/10.
[36] Chen, Y.M., Mongis, J., 2005. Cavitation wear in plain bearing: case study. Mech. Ind. 6, 195–201. https://doi.org/10.1051/MECA:2005020.
[37] Xiao, L., 2014. Influence of Surface Topography on Marine Biofouling. Ruprecht-Karls University of Heidelberg, Germany. https://doi.org/10.11588/heidok.00016523. Doctoral Dissertation.
[38] von der Ohe, C.B., Johnsen, R., Espallargas, N., 2011. The effect of cyclic and static tensile stresses on the tribocorrosion behavior of austenitic and duplex stainless steels in marine environment. In: NACE - International Corrosion Conference Series. OnePetro, Texas, 11408.
[39] Marsh, G., 2009. Wave and tidal power — an emerging new market for composites. Reinforc Plast 53, 20–24. https://doi.org/10.1016/s0034-3617(09)70220-6.
[40] Syrek-Gerstenkorn, B., Paul, S., 2024. Metallic coatings in offshore wind sector—a mini review. npj Mater. Degrad. 8, 1–11. https://doi.org/10.1038/S41529-024-00480-8.
[41] Sternhell, G., Taylor, P.D., Itzhak, D., 2002. Galvanic effects of various metallic couples on marine biofouling in a coral reef environment. In: NACE - International Corrosion Conference Series 2002-April, pp. 1–11. https://doi.org/10.5006/C2002-02183/51359.
[42] Poon, C., O'Halloran, S.M., Connolly, A., Barrett, R.A., Leen, S.B., 2023. Fretting wear and fatigue in submarine power cable conductors for floating offshore wind energy. Tribol. Int. 186, 108598. https://doi.org/10.1016/J.TRIBOINT.2023.108598.
[43] ASTM(1) G48-11, Standard Test Methods for Pitting and Crevice Corrosion Resistance of Stainless Steels and Related Alloys by Use of Ferric Chloride Solution, (n.d.).
[44] ASTM(1) G61-86, Standard Test Method for Conducting Cyclic Potentiodynamic Polarization Measurements for Localized Corrosion Susceptibility of iron-, nickel-, or Cobalt-based Alloys, (n.d).
[45] ASTM(1) D1141-98, Standard Practice for the Preparation of Substitute Ocean Water, (n.d).
[46] Glavatskih, S., Höglund, E., 2008. Tribotronics—towards active tribology. Tribol. Int. 41, 934–939. https://doi.org/10.1016/J.TRIBOINT.2007.03.001.
[47] Ritchie, H., Rosado, P., Roser, M., 2024. Energy Mix, our World in Data. https://ourworldindata.org/energy-mix. (Accessed 18 July 2024).
[48] Ahamed, R., McKee, K., Howard, I., 2020. Advancements of wave energy converters based on power take off (PTO) systems: a review. Ocean. Eng. 204. https://doi.org/10.1016/j.oceaneng.2020.107248.
[49] Wave Energy Technology – Corpower Ocean, (n.d). https://corpowerocean.com/wave-energy-technology/(accessed October 23, 2025).
[50] Aquamarine power : EMEC: European marine energy centre, (n.d). https://www.emec.org.uk/about-us/wave-clients/aquamarine-power/(accessed October 23, 2025).
[51] Pelamis Wave Power : EMEC: european marine energy centre, (n.d). https://www.emec.org.uk/about-us/wave-clients/pelamis-wave-power/(accessed August 21, 2025).
[52] Guo, B., Wang, T., Jin, S., Duan, S., Yang, K., Zhao, Y., 2022. A review of point absorber wave energy converters. J. Mar. Sci. Eng. 10. https://doi.org/10.3390/JMSE10101534.
[53] Solutions, T., 2022. Hydraulic seals–linear. http://www.may-isc.co.il/wp-content/uploads/2015/11/slydring_gb_en.pdf. (Accessed 18 May 2025).
[54] Du, C., Bai, X., Yuan, C., 2021. Fretting tribocorrosion behaviors of marine mooring chain steel 22MnCrNiMo in artificial seawater. J. Tribol. 143. https://doi.org/10.1115/1.4048774/1088419.
[55] Chen, M., Ouyang, M., Guo, H., Zou, M., Zhang, C., 2023. A coupled hydrodynamic–structural model for flexible interconnected multiple floating bodies. J. Mar. Sci. Eng. 11. https://doi.org/10.3390/JMSE11040813.
[56] Minesto | Renewable energy. From the ocean., (n.d). https://minesto.com/(accessed October 23, 2025).
[57] IHI and toshiba to research ocean turbine system - offshore energy, (n.d). https://www.offshore-energy.biz/ihi-and-toshiba-to-research-ocean-turbine-system/(accessed October 23, 2025).
[58] Thornhill, J., 2015. The challenge of stern tube bearings and seals. In: SNAME 14th Propeller and Shafting Symposium, PSS 2015. https://doi.org/10.5957/PSS-2015-013.
[59] jing Gu, Y., gang Lin, Y., kun Xu, Q., wei Liu, H., Li, W., 2018. Blade-pitch system for tidal current turbines with reduced variation pitch control strategy based on tidal current velocity preview. Renew. Energy 115, 149–158. https://doi.org/10.1016/J.RENENE.2017.07.034.
[60] Wang, R.Y., Wang, C.H., Wang, Y., Zhang, W.F., 2023. Synergistic effects of multiple environmental factors on degradation of silicone rubber seals under marine atmosphere. Materials 16, 7013. https://doi.org/10.3390/MA16217013, 7013 16 (2023.
[61] Ding, H., Zhou, G., Dai, Z., Bu, Y., Jiang, T., 2009. Corrosion wear behaviors of 2024Al in artificial rainwater and seawater at fretting contact. Wear 267, 292–298. https://doi.org/10.1016/J.WEAR.2008.11.031.
[62] Zhou, Z., Benbouzid, M., Charpentier, J.F., Scuiller, F., Tang, T., 2017. Developments in large marine current turbine technologies – a review. Renew. Sustain. Energy Rev. 71, 852–858. https://doi.org/10.1016/J.RSER.2016.12.113.
[63] Song, W., Yang, C., Cui, W., Lei, Y., Hong, J., Wang, Z., Hu, Z., 2022. Study of pressure-balanced oil-filled (PBOF) technology. Ocean. Eng. 260, 111757. https://doi.org/10.1016/J.OCEANENG.2022.111757.
[64] Ma, K., Shu, H., Smedley, P., L'Hostis, D., Duggal, A., 2013. A Historical Review on Integrity Issues of Permanent Mooring Systems. https://doi.org/10.4043/24025-MS.
[65] Kim, I.C., Lee, N.J., Wata, J., Hyun, B.S., Lee, Y.H., 2016. Experiments on the magnetic coupling in a small scale counter rotating marine current turbine. IOP Conf. Ser. Mater. Sci. Eng. 129, 012047. https://doi.org/10.1088/1757-899X/129/1/012047.
[66] Sangal, S., Singhal, M.K., Saini, R.P., 2018. Hydro-abrasive erosion in hydro turbines: a review. Int. J. Green Energy 15, 232–253. https://doi.org/10.1080/15435075.2018.1431546.
[67] Lewis, M., Neill, S.P., Robins, P., Hashemi, M.R., Ward, S., 2017. Characteristics of the velocity profile at tidal-stream energy sites. Renew. Energy 114, 258–272. https://doi.org/10.1016/J.RENENE.2017.03.096.
[68] Kawai, H., 1998. A brief history of recognition of the Kuroshio. Prog. Oceanogr. 41, 505–578. https://doi.org/10.1016/S0079-6611(98)00024-X.
[69] Chang, L.Y., Chen, F., Tseng, K.T., 2016. Dynamics of a marine turbine for deep ocean currents. J. Mar. Sci. Eng. 4, 59. https://doi.org/10.3390/JMSE4030059, 4 (2016) 59.
[70] Cowie, P.R., 2010. Biofouling patterns with depth. Biofouling 87–99. https://doi.org/10.1002/9781444315462.CH6.
[71] Titah-Benbouzid, H., Benbouzid, M., 2015. Marine Renewable Energy Converters and Biofouling: a Review on Impacts and Prevention, A Review on Impacts and Prevention. EWTEC. https://doi.org/10.34894/VQ1DJA. Paper 09P1-4-2.
[72] Zhang, B., Li, B., Fu, S., Mao, Z., Ding, W., 2022. Vortex-induced vibration (VIV) hydrokinetic energy harvesting based on nonlinear damping. Renew. Energy 195, 1050–1063. https://doi.org/10.1016/J.RENENE.2022.06.102.
[73] Zhang, H.C., Xu, D.L., Liu, C.R., Wu, Y.S., 2016. Wave energy absorption of a wave farm with an array of buoys and flexible runway. Energy 109, 211–223. https://doi.org/10.1016/J.ENERGY.2016.04.107.
[74] Uihlein, A., Magagna, D., 2016. Wave and tidal current energy - a review of the current state of research beyond technology. Renew. Sustain. Energy Rev. 58, 1070–1081. https://doi.org/10.1016/j.rser.2015.12.284.
[75] Li, G., Jiang, Y., Yu, D., Dong, Z., 2024. A mixed stochastic waves model for analyzing offshore structures considering engineering characteristics correlation of wind-generated-wave and swell. Ocean. Eng. 314. https://doi.org/10.1016/J.OCEANENG.2024.119671.
[76] Barber, N.F., Ursell, F., 1948. The generation and propagation of ocean waves and swell. I. Wave periods and velocities. Philos. Trans. R. Soc. Lond., Ser. A Math. Phys. Sci. 240, 527–560. https://doi.org/10.1098/RSTA.1948.0005.
[77] Henderson, R., 2006. Design, simulation, and testing of a novel hydraulic power take-off system for the pelamis wave energy converter. Renew. Energy 31, 271–283. https://doi.org/10.1016/j.renene.2005.08.021.
[78] Lin, J., liang Lin, B., Sun, J., ling Chen, Y., 2016. Modelling hydrodynamic processes in tidal stream energy extraction. J. Hydrodyn. B 28, 1058–1064. https://doi.org/10.1016/S1001-6058(16)60711-4.
[79] Dexter, S.C., Dalrymple, R.A., KobayashI, N., 1988. Mar. Envrion. 28, 35–87. https://doi.org/10.1016/B978-0-12-341828-9.50008-5.
[80] Muraoka, J.S., 1967. Deep-Ocean Biodeterioration of Materials. U.S. Naval Civil Engineering Laboratory. https://doi.org/10.5962/bhl.title.47743.
[81] Grossart, H.P., Gust, G., 2009. Hydrostatic pressure affects physiology and community structure of marine bacteria during settling to 4000 m: an experimental approach. Mar. Ecol. Prog. Ser. 390, 97–104. https://doi.org/10.3354/MEPS08201.
[82] Cloern, J.E., 1996. Phytoplankton bloom dynamics in coastal ecosystems: a review with some general lessons from sustained investigation of San Francisco Bay, California. Rev. Geophys. 34, 127–168. https://doi.org/10.1029/96RG00986.
[83] Manasrah, R., Abu-Hilal, A., Rasheed, M., 2019. Physical and Chemical Properties of Seawater in the Gulf of Aqaba and Red Sea, pp. 41–73. https://doi.org/10.1007/978-3-319-99417-8_3.
[84] Wang, J., Gao, B., Cui, W., 2023. A method for improving the hydrostatic pressure testing of the compressive strength of solid buoyancy materials used at full ocean depth. Ocean. Eng. 286, 115673. https://doi.org/10.1016/J.OCEANENG.2023.115673.
[85] Johnson, A.A., Lewenstein, T., Imbembo, E.A., 1969. The effects of the hydrostatic pressure in a deep ocean on the mechanical behaviour of metals. Ocean. Eng. 1, 201–232. https://doi.org/10.1016/0029-8018(69)90022-5.
[86] Liu, R., Liu, L., Wang, F., 2022. The role of hydrostatic pressure on the metal corrosion in simulated deep-sea environments — a review. J. Mater. Sci. Technol. 112, 230–238. https://doi.org/10.1016/J.JMST.2021.10.014.
[87] Myan, F.W.Y., Walker, J., Paramor, O., 2013. The interaction of marine fouling organisms with topography of varied scale and geometry: a review. Biointerphases 8, 1–13. https://doi.org/10.1186/1559-4106-8-30/133892.
[88] Liang, P., Li, X., Guo, F., Cao, Y., Zhang, X., Jiang, F., 2022. Influence of sea wave shock on transient start-up performance of water-lubricated bearing. Tribol. Int. 167, 107332. https://doi.org/10.1016/J.TRIBOINT.2021.107332.

[89] Yang, L., Moan, T., 2010. Numerical modeling of wear damage in seals of a wave energy converter with hydraulic power take-off under random loads. Tribol. Trans. 54, 44–56. https://doi.org/10.1080/10402004.2010.518340.
[90] Grotz, L., Kirane, K., 2024. Characterizing compressive failure mechanisms and their transitions in woven composites under on and off-axis loading. Compos. Struct. 330. https://doi.org/10.1016/j.compstruct.2023.117848.
[91] Subba Rao, T., Murthy, P.S., Veeramani, P., Narayanan, D.S., Ramesh, R., Jyothi, B.N., Muthukumaran, D., Murugesan, M., Vadivelan, A., Dharani, G., Santhanakumar, J., Ramadass, G.A., 2021. Assessment of biogrowth assemblages with depth in a seawater intake system of a coastal power station. Biofouling 37, 506–520. https://doi.org/10.1080/08927014.2021.1933457.
[92] Agostini, V.O., Macedo, A.J., Muxagata, E., Pinho, G.L.L., 2019. Surface coatings select their micro and macrofouling communities differently on steel. Environ. Pollut. 254. https://doi.org/10.1016/J.ENVPOL.2019.113086.
[93] Lindén, J.B., Andersson, K.Å., Pinori, E., Harnden, R., Bonel, A., 2022. Biofouling and corrosion defense on wave energy converters. Mater. Perform. 61, 32–36. https://doi.org/10.5006/MP2022_61_9-32.
[94] Li, G., Zhu, W., 2022. A review on up-to-date gearbox technologies and maintenance of tidal current energy converters. Energies 15, 9236. https://doi.org/10.3390/EN15239236, 15 (2022) 9236.
[95] Khalil, Touimi, 2020. Design Optimization of a Gearbox Driven Tidal Stream Turbine. Université de Bretagne. https://theses.hal.science/tel-03269393v1. (Accessed 21 August 2025).
[96] Elasha, F., Mba, D., Togneri, M., Masters, I., Teixeira, J.A., 2017. A hybrid prognostic methodology for tidal turbine gearboxes. Renew. Energy 114, 1051–1061. https://doi.org/10.1016/J.RENENE.2017.07.093.
[97] Hurtado Molina, E., Long, H., 2025. Fretting wear in raceway-ball contact under wind turbine pitch bearing operating conditions. Wear 564–565, 205696. https://doi.org/10.1016/J.WEAR.2024.205696.
[98] He, P., Hong, R., Wang, H., Lu, C., 2019. Pitch bearing/raceway fretting: influence of contact angle. Proc. Inst. Mech. Eng. C J. Mech. Eng. Sci. 233, 1734–1749. https://doi.org/10.1177/0954406218776033.
[99] Evangelisti, A., Agati, G., Borello, D., Mazzotta, L., Capobianchi, P., Venturini, P., 2025. Numerical prediction of cavitation for a horizontal axis tidal turbine. Flow Turbul. Combust. 114, 887–912. https://doi.org/10.1007/S10494-024-00615-6/FIGURES/15.
[100] Neill, S.P., Litt, E.J., Couch, S.J., Davies, A.G., 2009. The impact of tidal stream turbines on large-scale sediment dynamics. Renew. Energy 34, 2803–2812. https://doi.org/10.1016/J.RENENE.2009.06.015.
[101] Rasool, G., Sharifi, S., Johnstone, C., Stack, M.M., 2016. Mapping synergy of erosion mechanisms of tidal turbine composite materials in sea water conditions. J. Bio Tribocorros. 2, 1–15. https://doi.org/10.1007/S40735-016-0040-5/TABLES/3.
[102] Yang, G., Mao, Z., Zhang, T., Li, B., Tian, W., 2024. Research on the hydrodynamic performance of a small ocean current turbine with deflectable blades. Energy Convers. Manag. 302, 118060. https://doi.org/10.1016/J.ENCONMAN.2024.118060.
[103] Tian, W., Mao, Z., Ding, H., 2018. Design, test and numerical simulation of a low-speed horizontal axis hydrokinetic turbine. Int. J. Nav. Archit. Ocean Eng. 10, 782–793. https://doi.org/10.1016/j.ijnaoe.2017.10.006.
[104] Wu, D., Guan, Z., Cheng, Q., Guo, W., Tang, M., Liu, Y., 2020. Development of a friction test apparatus for simulating the ultra-high pressure environment of the deep ocean. Wear 452–453, 203294. https://doi.org/10.1016/J.WEAR.2020.203294.
[105] Apolinario, M., Coutinho, R., 2009. Understanding the biofouling of offshore and deep-sea structures. Advances in Marine Antifouling Coatings and Technologies, pp. 132–147. https://doi.org/10.1533/9781845696313.1.132.
[106] Zhang, H., Cao, W., Wu, Z., Song, X., Wang, J., Yan, T., 2015. Biofouling on deep-sea submersible buoy systems off Xisha and Dongsha Islands in the northern South China Sea. Int. Biodeterior. Biodegrad. 104, 92–96. https://doi.org/10.1016/J.IBIOD.2015.05.003.
[107] Little, B., Ray, R., Wagner, P., Lewandowski, Z., Lee, W.C., Characklis, W.G., Mansfeld, F., 1991. Impact of biofouling on the electrochemical behaviour of 304 stainless steel in natural seawater. Biofouling 3, 45–59. https://doi.org/10.1080/08927019109378161.
[108] Ashkenazy, Y., Gildor, H., Solodoch, A., 2025. Statistical analysis of ocean currents in the eastern Mediterranean. Ocean Sci. 21, 1641–1661. https://doi.org/10.5194/OS-21-1641-2025.
[109] Pan, Y.C., Dai, Z., Ma, H., Zheng, J., Leng, J., Xie, C., Yuan, Y., Yang, W., Yalikun, Y., Song, X., Han, C.B., Shang, C., Yang, Y., 2024. Self-powered and speed-adjustable sensor for abyssal ocean current measurements based on triboelectric nanogenerators. Nat. Commun. 15 (1), 1–10. https://doi.org/10.1038/s41467-024-50581-w, 15 (2024).
[110] Toro, A., Sinatora, A., Tanaka, D.K., Tschiptschin, A.P., 2001. Corrosion–erosion of nitrogen bearing martensitic stainless steels in seawater–quartz slurry. Wear 251, 1257–1264. https://doi.org/10.1016/S0043-1648(01)00765-7.
[111] Fong, M., 1993. Microbiologically influenced corrosion on high strength low alloyed steel: AISI 8630. https://search.proquest.com/openview/f0a3f7a2ee455efba84b05459422f287/1?pq-origsite=gscholar&cbl=18750&diss=y. (Accessed 12 August 2025).
[112] Bromaghin, A., Ali, M., Ravens, T., Petersen, T., Hoffman, J., 2014. Experimental study of abrasion characteristics for critical sliding components for use in hydrokinetic devices. Renew. Energy 66, 205–214. https://doi.org/10.1016/J.RENENE.2013.11.069.
[113] Wang, Z., Dai, Z., Wu, S., Zhang, B., Cao, J., Ye, R., 2023. Combined effect of cavitation and multi-scale texture on the bearing properties of seawater-lubricated friction pair. Phys. Fluids 35, 87129. https://doi.org/10.1063/5.0160229.
[114] Qiao, Z., Guo, Y., Zhang, Z., Wang, X., Wang, D., 2025. Fretting behavior of hydrogenated nitrile rubber for sealing application of ultra-deep well. Tribol. Int. 202, 110328. https://doi.org/10.1016/J.TRIBOINT.2024.110328.
[115] Tuominen, J., Näkki, J., Pajukoski, H., Miettinen, J., Peltola, T., Vuoristo, P., N€, J., Pajukoski, H., Miettinen, J., Peltola, T., Vuoristo, P., 2015. Wear and corrosion resistant laser coatings for hydraulic piston rods. J. Laser Appl. 27, 22009. https://doi.org/10.2351/1.4914503.
[116] Huang, Q., Liu, H., Ding, Z., 2022. Impact factors on friction induced vibration of shaft-bearing system considering stick-slip behavior. Mar. Struct. 84, 103226. https://doi.org/10.1016/J.MARSTRUC.2022.103226.
[117] James, M.N., Hattingh, D.G., 2015. Case studies in marine concentrated corrosion. Eng. Fail. Anal. 47, 1–15. https://doi.org/10.1016/J.ENGFAILANAL.2014.08.013.
[118] Ding, X., Wang, L., Fan, X., Liu, X., Zhang, Z., Xue, B., 2025. The synergistic effects of material aging and surface texture on the performance and reliability of marine sealing systems. Ocean. Eng. 330, 121227. https://doi.org/10.1016/J.OCEANENG.2025.121227.
[119] Kumar, R., Antonov, M., Klimczyk, P., Mikli, V., Gomon, D., 2022. Effect of cBN content and additives on sliding and surface fatigue wear of spark plasma sintered Al2O3-cBN composites. Wear 494–495, 204250. https://doi.org/10.1016/J.WEAR.2022.204250.
[120] Chen, L., Lam, W.H., 2015. A review of survivability and remedial actions of tidal current turbines. Renew. Sustain. Energy Rev. 43, 891–900. https://doi.org/10.1016/J.RSER.2014.11.071.
[121] Wang, W., Ku, P., Stevenson, L.M., Kumara, C., Meyer, I. Harry M., Luo, H., Mathews, T.J., Qu, J., 2025. Marine toxicity, biodegradability, and rolling-sliding tribological performance of ionic liquid-enhanced environmentally-acceptable lubricants for tidal turbomachinery. ACS Sustain. Chem. Eng. 13, 12482–12495. https://doi.org/10.1021/ACSSUSCHEMENG.5C03399.
[122] Stammler, M., Ellerbrok, H., Pasaribu, R., Rieper, U., 2024. Short-term influence of water ingress on wear in pitch bearings of wind turbines. Lubricants 12, 310. https://doi.org/10.3390/LUBRICANTS12090310, 12 (2024) 310.
[123] Mischler, S., 2008. Triboelectrochemical techniques and interpretation methods in tribocorrosion: a comparative evaluation. Tribol. Int. 41, 573–583. https://doi.org/10.1016/J.TRIBOINT.2007.11.003.
[124] Kim, W.S., Yun, I.H., Lee, J.J., Jung, H.T., 2010. Evaluation of mechanical interlock effect on adhesion strength of polymer–metal interfaces using micro-patterned surface topography. Int. J. Adhesion Adhes. 30, 408–417. https://doi.org/10.1016/J.IJADHADH.2010.05.004.
[125] Heiser, J., Soo, P., 1995. Corrosion of barrier materials in seawater environments. https://inis.iaea.org/records/5qcz1-bpk05. (Accessed 17 October 2025).
[126] LaCoursiere, M.P., Aidun, D.K., Morrison, D.J., 2017. Slow strain rate testing for hydrogen embrittlement susceptibility of alloy 718 in substitute ocean water. J. Mater. Eng. Perform. 26, 2337–2345. https://doi.org/10.1007/S11665-017-2675-X/FIGURES/11.
[127] Kain, R.M., 2002. Seawater crevice corrosion resistance of stainless steels coated with silane and antifouling paint systems. In: NACE - International Corrosion Conference Series 2002-April, pp. 1–16. https://doi.org/10.5006/C2002-02187.
[128] Arango, D., Liu, J., 2024. Investigation of the initiation and propagation of filiform corrosion on aluminum alloys by electrochemical techniques. Can. Metall. Q. 63, 84–96. https://doi.org/10.1080/00084433.2022.2160898.
[129] Maurya, H.S., Kumar, R., Kumar, S.A., Tarraste, M., Hussain, A., Rahmani, R., Juhani, K., Sergejev, F., Prashanth, K.G., 2025. Sliding wear and debris evolution in LPBFed ceramic-reinforced steel composites under variable loads and temperatures. Mater. Chem. Phys. 345, 131195. https://doi.org/10.1016/J.MATCHEMPHYS.2025.131195.
[130] Uhlig, H.H., 1954. Mechanism of fretting corrosion. J. Appl. Mech. 21, 401–407. https://doi.org/10.1115/1.4010940.
[131] Abi-Akl, R., Ledieu, E., Enke, T.N., Cordero, O.X., Cohen, T., 2019. Physics-based prediction of biopolymer degradation, cite this. Soft Matter 15, 4098. https://doi.org/10.1039/c9sm00262f.
[132] Hao, Z., Zhang, Z., Zhou, W., Zhang, S., Ma, T., Wei, H., Wang, G., Wang, Q., Wang, L., Li, R., 2025. Progress of material degradation: metals and polymers in deep-sea environments. Corrosion Rev. 43, 315–334. https://doi.org/10.1515/CORRREV-2024-0009/MACHINEREADABLECITATION/RIS.
[133] Gant, A.J., Gee, M.G., May, A.T., 2004. The evaluation of tribo-corrosion synergy for WC–Co hardmetals in low stress abrasion. Wear 256, 500–516. https://doi.org/10.1016/J.WEAR.2003.04.001.
[134] Wu, J., Gao, J., Zhang, D., Tan, F., Yin, J., Wang, Y., Sun, Y., Li, E., 2020. Microbial communities present on mooring chain steels with different copper contents and corrosion rates. J. Oceanol. Limnol. 38, 378–394. https://doi.org/10.1007/S00343-019-8366-8/METRICS.
[135] Shi, X.B., Yan, W., Yan, M.C., Wang, W., Yang, Z.G., Shan, Y.Y., Yang, K., 2017. Effect of Cu addition in pipeline steels on microstructure, mechanical properties and microbiologically influenced corrosion. Acta Metall. Sin. 30, 601–613. https://doi.org/10.1007/S40195-017-0545-Z/FIGURES/14.
[136] Javed, M.A., Ivanovich, N., Messinese, E., Liu, R., Astorga, S.E., Yeo, Y.P., Idapalapati, S., Lauro, F.M., Wade, S.A., 2024. The role of metallurgical features in the microbially influenced corrosion of carbon steel: a critical review. Microorganisms 12, 892. https://doi.org/10.3390/MICROORGANISMS12050892, 12 (2024) 892.
[137] Zhao, T., Liu, Z., Xu, X., Li, Y., Du, C., Liu, X., 2019. Interaction between hydrogen and cyclic stress and its role in fatigue damage mechanism. Corros. Sci. 157, 146–156. https://doi.org/10.1016/J.CORSCI.2019.05.028.

[138] Cassagne, T., Marchebois, H., Mesquita, T., 2021. A Review of Hydrogen Embrittlement of Nickel-based Alloys for Oil and Gas Applications. (Accessed 19 October 2025).
[139] The Performance, Wear, and Environmental Impact of Lubrication Systems Used in Marine Engines, (n.d).
[140] Tamayo, J.G.Z., Glavatskih, S., 2023. Lubrication of offshore mechanical components: towards sustainable & reliable power production. Proc. Eur. Wave Tidal Energy Conf. 15, 259–260. https://doi.org/10.36688/EWTEC-2023-259.
[141] Rostek, E., Babiak, M., Wróblewski, E., 2017. The influence of oil pressure in the engine lubrication system on friction losses. Procedia Eng. 192, 771–776. https://doi.org/10.1016/J.PROENG.2017.06.133.
[142] Chiu, Y.P., 1974. An analysis and prediction of lubricant film starvation in rolling contact systems. Asle Trans. 17, 22–35. https://doi.org/10.1080/05698197408981435.
[143] Zhou, Y., Bosman, R., Lugt, P.M., 2019. On the shear stability of dry and water-contaminated calcium sulfonate complex lubricating greases. Tribol. Trans. 62, 626–634. https://doi.org/10.1080/10402004.2019.1588445.
[144] Qin, H., Doll, G.L., 2023. Effects of water contamination on micropitting and rolling contact fatigue of bearing steels. J. Tribol. 145. https://doi.org/10.1115/1.4055181/1145389.
[145] Xue, Q., Liu, W., 1994. Tribochemistry and the development of AW and EP oil additives — a review. Lubric. Sci. 7, 81–92. https://doi.org/10.1002/LS.3010070107.
[146] Tse, J.S., Song, Y., Liu, Z., 2007. Effects of temperature and pressure on ZDDP. Tribol. Lett. 28, 45–49. https://doi.org/10.1007/S11249-007-9246-5/FIGURES/2.
[147] Wu, Y., Li, W., Zhang, M., Wang, X., 2013. Oxidative degradation of synthetic ester and its influence on tribological behavior. Tribol. Int. 64, 16–23. https://doi.org/10.1016/J.TRIBOINT.2013.02.002.
[148] Cen, H., Morina, A., Neville, A., Pasaribu, R., Nedelcu, I., 2012. Effect of water on ZDDP anti-wear performance and related tribochemistry in lubricated steel/steel pure sliding contacts. Tribol. Int. 56, 47–57. https://doi.org/10.1016/J.TRIBOINT.2012.06.011.
[149] Chokelarb, W., Sriprom, P., Permana, L., Assawasaengrat, P., 2024. Assessment of overall remaining useful life of lubricants by integrating oil quality and performance. Heliyon 10, e37486. https://doi.org/10.1016/J.HELIYON.2024.E37486.
[150] Rodiouchkina, M., 2022. Tribology of self-lubricating Polymer Composites for Hydropower Applications. Luleå University of Technology. https://urn.kb.se/resolve?urn=urn%3Anbn%3Ase%3Altu%3Adiva-90197.
[151] Summer, F., Grün, F., Ravenhill, E.R., 2020. Friction and wear performance of various polymer coatings for journal bearings under stop start sliding. Lubricants 8, 1. https://doi.org/10.3390/LUBRICANTS8010001, 8 (2019) 1.
[152] Penchaliah, R., 2020. Tribological Effects of Diesel Engine Oil Contamination on Steel and Hybrid Sliding Contacts, pp. 279–296. https://doi.org/10.1007/978-3-030-47451-5_15.
[153] Ismail, A.R., Arshad, A.M., Rahman, A.T.A., Ismail, N.J., 2018. Elastomer compatibility study of oil-based and ester-based drilling fluids. AIP Conf. Proc. 2030, 20213. https://doi.org/10.1063/1.5066854/832741.
[154] Torbacke, M., Johansson, A., 2005. Seal material and base fluid compatibility: an overview. J. Synth. Lubric. 22, 123–142. https://doi.org/10.1002/JSL.2005.22.2.123.
[155] Wang, B., Li, X., Liao, Y., Li, Y., Peng, X., Chen, Y., 2025. Sealing characteristics and control strategies of hydraulically controllable rod seal for deep-sea hydraulic manipulators. Proc. Inst. Mech. Eng. C J. Mech. Eng. Sci. 239, 6833–6849. https://doi.org/10.1177/09544062251344523.
[156] Hunsucker, J.T., Hunsucker, K.Z., Gardner, H., Swain, G., 2016. Influence of hydrodynamic stress on the frictional drag of biofouling communities. Biofouling 32, 1209–1221. https://doi.org/10.1080/08927014.2016.1242724.
[157] Chang, T., Panhwar, F., Zhao, G., 2020. Flourishing self-healing surface materials: recent progresses and challenges. Adv. Mater. Interfac. 7, 1901959. https://doi.org/10.1002/ADMI.201901959;WGROUP:STRING:PUBLICATION.
[158] Schoefs, F., Bakhtiari, A., Ameryoun, H., 2022. Evaluation of hydrodynamic force coefficients in presence of biofouling on marine/offshore structures, a review and new approach. J. Mar. Sci. Eng. 10, 558. https://doi.org/10.3390/JMSE10050558, 10 (2022) 558.
[159] Núñez, P., Misic, C., Cutroneo, L., Capello, M., Medina, R., Besio, G., 2023. Biofilm-induced effect on the buoyancy of plastic debris: an experimental study. Mar. Pollut. Bull. 193, 115239. https://doi.org/10.1016/J.MARPOLBUL.2023.115239.
[160] Dobson, T., Yunnie, A., Kaloudis, D., Larossa, N., Coules, H., 2024. Biofouling and corrosion rate of welded nickel aluminium bronze in natural and simulated seawater. Biofouling 40, 193–208. https://doi.org/10.1080/08927014.2024.2326067.
[161] Singh, A.K., 2020. Microbially induced corrosion and its mitigation. https://doi.org/10.1007/978-981-15-8019-2.
[162] Sanders, P.F., Sturman, P.J., 2014. Biofouling in the oil industry. Petrol. Micribiol. 171–198. https://doi.org/10.1128/9781555817589.CH9;CTYPE:STRING:BOOK.
[163] Han, Y., Zhao, W., Zheng, Y., Wang, H., Sun, Y., Zhang, Y., Luo, J., Zhang, H., 2021. Self-adhesive lubricated coating for enhanced bacterial resistance. Bioact. Mater. 6, 2535–2545. https://doi.org/10.1016/J.BIOACTMAT.2021.01.028.
[164] Islam, M.A., Alam, T., Farhat, Z.N., Mohamed, A., Alfantazi, A., 2015. Effect of microstructure on the erosion behavior of carbon steel. Wear 332–333, 1080–1089. https://doi.org/10.1016/J.WEAR.2014.12.004.
[165] Walczak, M., Sharifi, S., Stack, M.M., 2020. On a multiphysics approach to modelling the erosion–enhanced corrosion of low–alloy carbon steel in chloride containing environments. Corros. Sci. 176, 109045. https://doi.org/10.1016/J.CORSCI.2020.109045.
[166] Habibi, P., Abad, F., Dai, S., Mehmanparast, A., Lotfian, S., 2025. Failure analysis of tidal turbine blades: understanding erosion mechanisms and their impact on structural integrity. Eng. Fail. Anal. 182, 110045. https://doi.org/10.1016/J.ENGFAILANAL.2025.110045.
[167] Bello, J.O., Wood, R.J.K., Wharton, J.A., 2007. Synergistic effects of micro-abrasion–corrosion of UNS S30403, S31603 and S32760 stainless steels. Wear 263, 149–159. https://doi.org/10.1016/J.WEAR.2006.12.044.
[168] Jiang, J., Stack, M.M., Neville, A., 2002. Modelling the tribo-corrosion interaction in aqueous sliding conditions. Tribol. Int. 35, 669–679. https://doi.org/10.1016/S0301-679X(02)00058-0.
[169] Sedillot, F., Stevenson, A., 1983. Laminated rubber articulated joint for the deep water gravity tower. J. Energy Resour. Technol. 105, 480–486. https://doi.org/10.1115/1.3230957.
[170] Zhang, T.C., Jiang, X.X., Li, S.Z., 1996. Acceleration of corrosive wear of duplex stainless steel by chloride in 69% H3PO4 solution. Wear 199, 253–259. https://doi.org/10.1016/0043-1648(96)06982-7.
[171] Cao, S., Mischler, S., 2018. Modeling tribocorrosion of passive metals – a review. Curr. Opin. Solid State Mater. Sci. 22, 127–141. https://doi.org/10.1016/J.COSSMS.2018.06.001.
[172] Prithiraj, A., Otunniyi, I.O., Osifo, P., van der Merwe, J., 2019. Corrosion behaviour of stainless and carbon steels exposed to sulphate – reducing bacteria from industrial heat exchangers. Eng. Fail. Anal. 104, 977–986. https://doi.org/10.1016/J.ENGFAILANAL.2019.06.042.
[173] Javed, M.A., Neil, W.C., Stoddart, P.R., Wade, S.A., 2016. Influence of carbon steel grade on the initial attachment of bacteria and microbiologically influenced corrosion. Biofouling 32, 109–122. https://doi.org/10.1080/08927014.2015.1128528.
[174] Ashton, S.A., King, R.A., Miller, J.D.A., 1973. Protective film formation on ferrous metals in semicontinuous cultures of nitrate-reducing bacteria. Br. Corrosion J. 8, 132–136. https://doi.org/10.1179/000705973798322215.
[175] Cai, Z., Xu, J., Wei, B., Sun, C., 2022. A comparative study of sulfate-reducing Desulfovibrio desulfuricans induced corrosion behaviors in Q235, X65, X70, and X80 pipeline steels. Int. J. Pres. Ves. Pip. 195, 104599. https://doi.org/10.1016/J.IJPVP.2021.104599.
[176] Liu, Z., Cui, T., Chen, Y., Dong, Z., 2023. Effect of Cu addition to AISI 8630 steel on the resistance to microbial corrosion. Bioelectrochemistry 152, 108412. https://doi.org/10.1016/J.BIOELECHEM.2023.108412.
[177] Wang, Y., Wu, J., Zhang, D., Li, E., Zhu, L., 2021. The inhibition effects of Cu and Ni alloying elements on corrosion of HSLA steel influenced by Halomonas titanicae. Bioelectrochemistry 141, 107884. https://doi.org/10.1016/J.BIOELECHEM.2021.107884.
[178] Shi, X., Yan, W., Xu, D., Yan, M., Yang, C., Shan, Y., Yang, K., 2018. Microbial corrosion resistance of a novel Cu-bearing pipeline steel. J. Mater. Sci. Technol. 34, 2480–2491. https://doi.org/10.1016/J.JMST.2018.05.020.
[179] Yang, K., Shi, X., Yan, W., Zeng, Y., Shan, Y., Ren, Y., 2020. Novel Cu-bearing pipeline steels: a new strategy to improve resistance to microbiologically influenced corrosion for pipeline steels. Ams.Org.Cn 56, 385–399. https://doi.org/10.11900/0412.1961.2019.00372.
[180] Mansouri, H., Alavi, S.A., Fotovat, M., 2015. Microbial-influenced corrosion of corten steel compared with carbon steel and stainless steel in oily wastewater by Pseudomonas aeruginosa. J. Occup. Med. 67, 1594–1600. https://doi.org/10.1007/S11837-015-1429-1/FIGURES/8.
[181] Nesterova, E.V., Вячеславовна, Н.Е., Verevkin, A.G., Григорьевич, В.А., Prokhorova, N.V., ВладиМировна, П.Н., 2021. The influence of carbon steel chemical composition on the biochemical activity of sessile sulfate-reducing bacteria. Samara J. Sci. 10, 87–92. https://doi.org/10.17816/snv2021104113.
[182] Walsh, D.W., 1999. The implications of thermomechanical processing for microbiologically influenced corrosion. In: NACE - International Corrosion Conference Series 1999-April, pp. 1–16. https://doi.org/10.5006/C1999-99188/50370.
[183] Guo, Z., Chai, Z., Liu, T., Gao, S., Hui, X., Zhang, C., Guo, N., Dong, L., 2022. Pseudomonas aeruginosa-accelerated corrosion of Mo-bearing low-alloy steel through molybdenum-mediating chemotaxis and motility. Bioelectrochemistry 144, 108047. https://doi.org/10.1016/J.BIOELECHEM.2021.108047.
[184] Cochella, G., 1999. Correlation of polarization resistance measurements to microbiologically induced corrosion. https://search.proquest.com/openview/523cb710bbf6dab4defda70e67f42195/1?pq-origsite=gscholar&cbl=18750&diss=y. (Accessed 12 August 2025).
[185] Francis, R., Byrne, G., 2021. Duplex stainless steels—alloys for the 21st century. Metals 11, 836. https://doi.org/10.3390/MET11050836, 11 (2021) 836.
[186] Von der Ohe, C.B., Johnsen, R., Espallargas, N., 2012. Multi-degradation behavior of austenitic and super duplex stainless steel – the effect of 4-point static and cyclic bending applied to a simulated seawater tribocorrosion system. Wear 288, 39–53. https://doi.org/10.1016/J.WEAR.2012.02.016.
[187] Kumar, R., Antonov, M., Berglund, T., Pampori, T.H., Maurya, H.S., Viljus, M., 2025. Wear mechanisms of PM-HIP tool steels under low and high-stress abrasion: role of carbide type and content. J. Mater. Res. Technol. https://doi.org/10.1016/J.JMRT.2025.04.317.
[188] Kumar, R., Torres, H., Aydinyan, S., Antonov, M., Varga, M., Hussainova, I., Rodriguez Ripoll, M., 2023. Tribological behavior of Ni-based self-lubricating claddings containing sulfide of nickel, copper, or bismuth at temperatures up to 600 °C. Surf. Coat. Technol. 456, 129270. https://doi.org/10.1016/J.SURFCOAT.2023.129270.

[189] Kumar, R., Hussainova, I., Antonov, M., Maurya, H.S., Rodríguez Ripoll, M., 2024. Temperature-induced wear micro-mechanism transition in additively deposited nickel alloys with different solid lubricants. Wear 552–553, 205452. https://doi.org/10.1016/J.WEAR.2024.205452.
[190] Kumar, R., Hussainova, I., Rahmani, R., Antonov, M., 2022. Solid lubrication at high-Temperatures—A review. Materials 15, 1695. https://doi.org/10.3390/MA15051695, 15 (2022) 1695.
[191] Ukonsaari, J., 2004. Tribology of journal bearings under environmentally adapted lubrication with shaft oscillation. https://urn.kb.se/resolve?urn=urn:nbn:se:ltu:diva-26550. (Accessed 16 October 2025).
[192] Somberg, J., 2024. Graphene as Solid Lubricant in Polymer Composites with Application in Hydropower Bearings. Luleå University of Technology. https://urn.kb.se/resolve?urn=urn%3Anbn%3Ase%3Altu%3Adiva-104606. (Accessed 16 October 2025).
[193] Mccarthy, D.M.C., 2008. Sliding bearings for hydropower applications : novel materials, surface texture and EALs. https://urn.kb.se/resolve?urn=urn:nbn:se:ltu:diva-18105. (Accessed 16 October 2025).
[194] Gangwani, P., 2025. Water-lubricated high-performance polymers. https://repozitorij.uni-lj.si/IzpisGradiva.php?id=174609. (Accessed 16 October 2025).
[195] Rodiouchkina, M., Lind, J., Pelcastre, L., Berglund, K., Rudolphi, Å.K., Hardell, J., 2021. Tribological behaviour and transfer layer development of self-lubricating polymer composite bearing materials under long duration dry sliding against stainless steel. Wear 484–485, 204027. https://doi.org/10.1016/J.WEAR.2021.204027.
[196] Lin, L., Schlarb, A.K., 2016. Effect of the varied load conditions on the tribological performance and the thermal characteristics of PEEK-based hybrid composites. Tribol. Int. 101, 218–225. https://doi.org/10.1016/J.TRIBOINT.2016.04.025.
[197] Berglund, K., Shi, Y., 2017. Friction and wear of self-lubricating materials for hydropower applications under different lubricating conditions. Lubricants 5, 24. https://doi.org/10.3390/LUBRICANTS5030024, 5 (2017) 24.
[198] Long, R., Pan, Z., Jin, Z., Zhang, Y., Sun, S., Wang, Y., Wang, Y., Li, M., 2021. Tribological behavior of grooves textured thrust cylindrical roller bearings under dry wear. Adv. Mech. Eng. 13, 1–14. https://doi.org/10.1177/16878140211067284.
[199] Zhang, Y., Deng, J., Meng, Y., Yue, H., 2020. Tribological performance of steel guideway with biomimetic hexagonal micro-textures. Surf. Eng. 36, 1–9. https://doi.org/10.1080/02670844.2020.1742469.
[200] Litwin, W., 2015. Properties comparison of rubber and three layer PTFE-NBR-bronze water lubricated bearings with lubricating grooves along entire bush circumference based on experimental tests. Tribol. Int. 90, 404–411. https://doi.org/10.1016/J.TRIBOINT.2015.03.039.
[201] Zhang, Z., Ouyang, W., Liang, X., Yan, X., Yuan, C., Zhou, X., Guo, Z., Dong, C., Liu, Z., Jin, Y., Xiao, J., 2024. Review of the evolution and prevention of friction, wear, and noise for water-lubricated bearings used in ships. Friction 12, 1–38. https://doi.org/10.1007/S40544-022-0707-5.
[202] Li, X., Guo, Z., Huang, Q., Yuan, C., 2022. Application of bionic tribology in water-lubricated bearing: a review. J. Bionic Eng. 19, 902–934. https://doi.org/10.1007/S42235-022-00177-1.
[203] Monkova, K., Urban, M., Monka, P.P., Kozak, D., 2021. Study of the influence of surface treatment on the wear development under quasi-static loading of the levers of a newly designed thrust bearing. Eng. Fail. Anal. 124, 105383. https://doi.org/10.1016/j.engfailanal.2021.105383.
[204] Kumar, P., Bin Yaqub, T., Kumar, R., Nadeem, I., Morina, A., Kalin, M., 2026. Electro-stimulated tribological behavior of DLC coatings under unlubricated sliding conditions. Tribol. Int. 215, 111451. https://doi.org/10.1016/J.TRIBOINT.2025.111451.
[205] Lee, S.J., Kim, C.L., 2023. Influence of surface structure on friction and wear characteristics of silicone rubber for hydraulic rod seals. RSC Adv. 13, 33595–33602. https://doi.org/10.1039/D3RA06485A.
[206] Minet, C., Brunetire, N., Tournerie, B., 2011. A deterministic mixed lubrication model for mechanical seals. J. Tribol. 133. https://doi.org/10.1115/1.4005068/468693.
[207] Lovrec, D., Kalb, R., Tič, V., 2024. Ionic hydraulic fluids and seal-material compatibility. Appl. Sci. 14, 2187. https://doi.org/10.3390/APP14052187, 14 (2024) 2187.
[208] Korobchuk, M.V., 2022. Elastomer materials for application in equipment of subsea production systems, inorganic materials. Appl. Res. 13, 1161–1172. https://doi.org/10.1134/S2075113322050215/TABLES/8.
[209] Zhang, Z., Jia, X., Guo, F., Wang, Y., 2021. Effect of vulcanization on the tribological behavior and sealing performance of EPDM seals: experimentation and simulation. Tribol. Int. 164, 107219. https://doi.org/10.1016/J.TRIBOINT.2021.107219.
[210] Wang, Z., Wang, J., Wu, H.N., Zhang, R., yu Zhang, G., Zhang, F., Mariani, S., 2025. Investigation of the microstructure, mechanical properties and thermal degradation kinetics of EPDM under thermo-stress conditions used for joint sealing of floating prefabricated concrete platform of offshore wind power. Constr. Build. Mater. 485, 141897. https://doi.org/10.1016/J.CONBUILDMAT.2025.141897.
[211] Kass, M.D., Janke, C.J., Connatser, R.M., Lewis, S., 2021. Compatibility of biologically derivable alcohols, alkanes, esters, ketones, and an ether as diesel blendstocks with fuel system elastomers. Energy Fuels 35, 4979–4996. https://doi.org/10.1021/ACS.ENERGYFUELS.0C04357/ASSET/IMAGES/LARGE/EF0C04357_0034.JPEG.
[212] Sârbu, F.A., Arnăuţ, F., Deaconescu, A., Deaconescu, T., 2024. Theoretical and experimental research concerning the friction forces developed in hydraulic cylinder coaxial sealing systems made from polymers. Polymers 16, 157. https://doi.org/10.3390/POLYM16010157, 16 (2024) 157.
[213] Zhang, Y., Yang, X., Wang, S., Lv, G., Gao, Y., Chen, K., Yang, H., 2023. Research status and prospect of wear and aging on hydraulic rubber sealing materials. Plast, Rubber Compos. 52, 249–266. https://doi.org/10.1080/14658011.2023.2197677.
[214] Rubber Seal Compatibility Chart, (n.d). https://www.thelubricantstore.com/rubber-seal-compatibility-chart (accessed August 20, 2025).
[215] Dhanumalayan, E., Joshi, G.M., 2018. Performance properties and applications of polytetrafluoroethylene (PTFE)—a review. Adv. Compos. Hybrid Mater. 1 (2), 247–268. https://doi.org/10.1007/S42114-018-0023-8, 1 (2018).
[216] Deaconescu, A., Deaconescu, T., 2020. Tribological behavior of hydraulic cylinder coaxial sealing systems made from PTFE and PTFE compounds. Polymers 12, 155. https://doi.org/10.3390/POLYM12010155, 12 (2020) 155.
[217] Sui, H., Pohl, H., Schomburg, U., Upper, G., Heine, S., 1999. Wear and friction of PTFE seals. Wear 224, 175–182. https://doi.org/10.1016/S0043-1648(98)00306-8.
[218] Kumar, R., Malaval, B., Antonov, M., Zhao, G., 2020. Performance of polyimide and PTFE based composites under sliding, erosive and high stress abrasive conditions. Tribol. Int. 147, 106282. https://doi.org/10.1016/J.TRIBOINT.2020.106282.
[219] Huang, T.C., Tsai, J.W., Liao, K.C., 2022. Wear and leakage assessments of canted coil spring–energized polytetrafluoroethylene seals under ultra-high cycle operations. Eng. Fail. Anal. 135, 106110. https://doi.org/10.1016/J.ENGFAILANAL.2022.106110.
[220] Huang, T.C., Lin, C.Y., Liao, K.C., 2023. Experimental and numerical investigations of the wear behavior and sealing performance of PTFE rotary lip seals based on the elasto-hydrodynamic analysis with considerations of the asperity contact. Tribol. Int. 187. https://doi.org/10.1016/j.triboint.2023.108747.
[221] Hillery, F.E., 1992. Application and Design of Spring-Energized Plastic Seals, pp. 1–24. https://doi.org/10.5006/C1992-92067.
[222] Ramasubramanian, K., Nikhil, C., Rao, S., Mandal, S., Ganguly, R., Rao, M.S.R., Arunachalam, N., 2024. Tribological behavior of diamond coated reaction-bonded silicon carbide under dry and seawater environment. Surf. Coat. Technol. 476, 130204. https://doi.org/10.1016/J.SURFCOAT.2023.130204.
[223] Flitney, R., 2014. Materials, Seals and Sealing Handbook, pp. 369–435. https://doi.org/10.1016/B978-0-08-099416-1.00005-X.
[224] Huebner, M., 2016. Barrier and buffer fluid selection and considerations for mechanical seals. https://doi.org/10.21423/R1WC7S.
[225] Warda, H.A., Wahba, E.M., Selim, E.A., 2015. Integral pumping devices for dual mechanical seals: experiments and numerical simulations. J. Eng. Gas Turbines Power 137. https://doi.org/10.1115/1.4028384/373858.
[226] Dingui, K., Brunetière, N., Bouyer, J., Adjemout, M., 2020. Surface texturing to reduce temperature in mechanical seals. Tribol. Online 15, 222–229. https://doi.org/10.2474/TROL.15.222.
[227] Meng, X., Bai, S., Peng, X., 2014. Lubrication film flow control by oriented dimples for liquid lubricated mchanical seals. Tribol. Int. 77, 132–141. https://doi.org/10.1016/j.triboint.2014.04.020.
[228] Shi, L., Wei, W., Wang, T., Zhang, Y., Zhu, W., Wang, X., 2020. Experimental investigation of the effect of typical surface texture patterns on mechanical seal performance. J. Braz. Soc. Mech. Sci. Eng. 42, 1–12. https://doi.org/10.1007/S40430-020-02318-1/FIGURES/10.
[229] Guo, D., Cai, N., Wu, G., Xie, F., Tan, S., Jiang, N., Li, H., 2020. Improving pressure–velocity limit of mechanical seal with polycrystalline diamond coating. Appl. Sci. 10, 6090. https://doi.org/10.3390/APP10176090, 10 (2020) 6090.
[230] Kariminejad, A., Kumar, R., Antonov, M., Hussainova, I., Klimczyk, P., 2025. Erosive wear of spark plasma sintered Al2O3 - cBN ceramic composites. Diam. Relat. Mater. 155, 112328. https://doi.org/10.1016/J.DIAMOND.2025.112328.
[231] Hollman, P., Björkman, H., Alahelisten, A., Hogmark, S., 1998. Diamond coatings applied to mechanical face seals. Surf. Coat. Technol. 105, 169–174. https://doi.org/10.1016/S0257-8972(98)00481-2.
[232] Papatheodorou, T., 2005. Influence of hard chrome plated rod surface treatments on sealing behavior of hydraulic rod seals. Seal. Technol. 2005, 5–10. https://doi.org/10.1016/S1350-4789(05)00600-8.
[233] Rendón, J., Olsson, M., 2009. Abrasive wear resistance of some commercial abrasion resistant steels evaluated by laboratory test methods. Wear 267, 2055–2061. https://doi.org/10.1016/J.WEAR.2009.08.005.
[234] Kumar, R., Torres, H., Aydinyan, S., Antonov, M., Varga, M., Rodriguez Ripoll, M., Hussainova, I., 2022. Microstructure and high temperature tribological behaviour of self-lubricating Ti-TiBx composite doped with NiBi. Surf. Coat. Technol. 447, 128827. https://doi.org/10.1016/J.SURFCOAT.2022.128827.
[235] Embury, P., Armour, J., 2004. Influence of elastomer compound design on the performance of rotary shaft lip seals. Seal. Technol. 2004, 7–10. https://doi.org/10.1016/S1350-4789(04)00304-6.
[236] Duhring, B., Iversen, G., 1999. The application of plastics in dynamic seals. Proc. IME J. J. Eng. Tribol. 213, 227–237. https://doi.org/10.1243/1350650991542965.
[237] van der Waal, G., 1985. The relationship between the chemical structure of ester base fluids and their influence on elastomer seals, and wear characteristics. J. Synth. Lubric. 1, 280–301. https://doi.org/10.1002/JSL.3000010404.
[238] Donnet, P.C., Morina, P.A., 2023. Investigation of the Detergent Activity in a Fully Formulated Lubricant for DLC-involving Contact : Control of Friction by load-induced Detergent Structure Modification, p. 255. https://doi.org/10.34894/VQ1DJA.

[239] Equey, S., Roos, S., Mueller, U., Hauert, R., Spencer, N.D., Crockett, R., 2008. Reactions of zinc-free anti-wear additives in DLC/DLC and steel/steel contacts. Tribol. Int. 41, 1090–1096. https://doi.org/10.1016/J.TRIBOINT.2008.03.004.
[240] Pichumani, P., 2012. Wear and tribofilm formation with zinc-free antiwear additives. https://mavmatrix.uta.edu/context/materialscieng_theses/article/1075/type/native/viewcontent. (Accessed 20 August 2025).
[241] Li, B., Li, M., Fan, C., Ren, M., Wu, P., Luo, L., Wang, X., Liu, X., 2015. The wear-resistance of composite depending on the interfacial interaction between thermoplastic polyurethane and fluorinated UHMWPE particles with or without oxygen. Compos. Sci. Technol. 106, 68–75. https://doi.org/10.1016/J.COMPSCITECH.2014.11.005.
[242] hu Yin, M., chao Zhang, Y., min Zhou, R., yang Zhai, Z., lei Wang, J., hui Cui, Y., shui Li, D., 2022. Friction mechanism and application of PTFE coating in finger seals. Tribol. Trans. 65, 260–269. https://doi.org/10.1080/10402004.2021.1949512.
[243] Chen, L., Sun, Z.R., Li, C.J., Yang, G.J., 2024. Response of NiCrAl-bentonite abradable seal coatings to thermal/salt corrosion. Corros. Sci. 233, 112111. https://doi.org/10.1016/J.CORSCI.2024.112111.
[244] Mofidi, M., 2009. Tribology of Elastomeric Seal Materials, Doctoral Thesis. Luleå University of Technology.
[245] Standard guide for selection of environmentally acceptable lubricants for the U.S. environmental protection agency (EPA) vessel general permit. https://doi.org/10.1520/D8324-21, 2021.
[246] Sniderman, D., 2017. VGP 2013: propelling marine lubricants, STLE. https://www.stle.org/files/TLTArchives/2017/05_May/Feature.aspx. (Accessed 16 August 2025).
[247] HEPG, HEES and HEPR, 2023. ISO 15380:2023 - lubricants, industrial oils and related products (class L) — family H (Hydraulic systems) — specifications for hydraulic fluids in categories HETG. https://www.iso.org/standard/82967.html (accessed August 16, 2025).
[248] Shi, Y., Minami, I., Grahn, M., Björling, M., Larsson, R., 2014. Boundary and elastohydrodynamic lubrication studies of glycerol aqueous solutions as green lubricants. Tribol. Int. 69, 39–45. https://doi.org/10.1016/j.triboint.2013.08.013.
[249] Aspnes, M.G., Espallargas, N., 2019. Formulation and testing of new environmentally acceptable lubricants (EAL) for use in maritime gear components. https://ntnuopen.ntnu.no/ntnu-xmlui/handle/11250/2623259. (Accessed 16 August 2025).
[250] McCarthy, D.M.C., Glavatskih, S.B., Byheden, Å., 2009. Influence of oil type on the performance characteristics of a two-axial groove journal bearing. Lubric. Sci. 21, 366–377. https://doi.org/10.1002/LS.98.
[251] Yuan, W., Yao, X., Guo, Q., Li, C., Chi, B., Yu, J., 2024. Tribological performance of shaft and surface pairs with PPS and its composites in seawater under cyclic loading. Tribol. Lett. 72, 1–20. https://doi.org/10.1007/S11249-024-01901-0/FIGURES/22.
[252] Huang, X., Wu, J., Lu, X., Feng, X., Shi, Y., 2017. Tribological properties of porous PEEK composites containing ionic liquid under dry friction condition. Lubricants 5, 19. https://doi.org/10.3390/LUBRICANTS5020019, 5 (2017) 19.
[253] Cantley, R.E., 1977. The effect of water in lubricating oil on bearing fatigue life. ASLE Trans. 20, 244–248. https://doi.org/10.1080/05698197708982838.
[254] Soltanahmadi, S., Morina, A., van Eijk, M.C.P., Nedelcu, I., Neville, A., 2017. Tribochemical study of micropitting in tribocorrosive lubricated contacts: the influence of water and relative humidity. Tribol. Int. 107, 184–198. https://doi.org/10.1016/J.TRIBOINT.2016.11.031.
[255] Wang, J.Z., Yan, F.Y., Xue, Q.J., 2009. Tribological behaviors of some polymeric materials in sea water. Chin. Sci. Bull. 54, 4541–4548. https://doi.org/10.1007/S11434-009-0578-4/METRICS.
[256] Mens, J.W.M., de Gee, A.W.J., 1991. Friction and wear behaviour of 18 polymers in contact with steel in environments of air and water. Wear 149, 255–268. https://doi.org/10.1016/0043-1648(91)90378-8.
[257] Liu, X., Deng, Y., Zhou, X., Huang, J., Guo, X., Li, B., 2025. Study on friction and wear properties of water lubricated bearing material in different watersheds. Wear 570, 205999. https://doi.org/10.1016/J.WEAR.2025.205999.
[258] Yang, T., Duan, H., Cai, T., Zhan, S., Ma, L., Jin, Y., Li, J., Jia, D., 2026. Synergistic modification strategy of UHMWPE with enhanced tribological properties in seawater. Tribol. Int. 214, 111307. https://doi.org/10.1016/J.TRIBOINT.2025.111307.
[259] Chen, S., Li, J., Wei, L., Jin, Y., Shang, H., Hua, M., Duan, H., 2017. Tribological properties of polyimide-modified UHMWPE for bushing materials of seawater lubricated sliding bearings. Tribol. Int. 115, 470–476. https://doi.org/10.1016/J.TRIBOINT.2017.06.011.
[260] Friedrich, K., Akpan, E.I., Wetzel, B., 2021. On the tribological properties of extremely different wood materials. Eur. J. Wood Wood Prod. 79, 977–988. https://doi.org/10.1007/S00107-020-01654-2.
[261] Iversen, J., Brink, A., 2016. Formulation of Enhanced Water-Glycol Lubricants for Offshore Components - the Influence of Thickeners in Environmentally Acceptable Lubricants on the Wear of a Steel Piston Cylinder, p. 109. https://ntnuopen.ntnu.no/ntnu-xmlui/handle/11250/2406355. (Accessed 16 August 2025).
[262] Singh, T., Jain, M., Ganguli, D., Ravi, K., 2006. Evaluation of water glycol hydraulic fluids: a tribological approach. J. Synth. Lubric. 23, 177–184. https://doi.org/10.1002/jsl.20.
[263] Wang, J., Wang, J., Li, C., Zhao, G., Wang, X., 2011. A high-performance multifunctional lubricant additive for water-glycol hydraulic fluid. Tribol. Lett. 43, 235–245. https://doi.org/10.1007/S11249-011-9799-1.
[264] Gong, P., Wen, X., Bai, P., Yue, L., Ding, J., Tian, Y., Li, L., 2024. Influence of low concentration seawater on the friction corrosion performance of water–glycol fire-resistant hydraulic fluid. J. Bio Tribocorros. 10, 1–9. https://doi.org/10.1007/S40735-024-00855-Z.
[265] Hofmann, S., Lohner, T., Stahl, K., 2024. Influence of water evaporation on elastohydrodynamic lubrication with water-containing polyalkylene glycols. Friction 12, 2370–2388. https://doi.org/10.1007/S40544-024-0916-1.
[266] Boyde, S., 2000. Hydrolytic stability of synthetic ester lubricants. J. Synth. Lubric. 16, 297–312. https://doi.org/10.1002/JSL.3000160403.
[267] Liu, D., Zhao, G., Wang, X., 2012. Tribological performance of lubricating greases based on calcium carbonate polymorphs under the boundary lubrication condition. Tribol. Lett. 47, 183–194. https://doi.org/10.1007/S11249-012-9976-X.
[268] Shekhawat, D., Jain, A., Vashishtha, N., Singh, A.P., Kumar, R., 2025. Tribological performance comparison of lubricating greases for electric vehicle bearings. Lubricants 13, 108. https://doi.org/10.3390/LUBRICANTS13030108, 13 (2025) 108.
[269] Rezasoltani, A., Khonsari, M.M., 2016. An engineering model to estimate consistency reduction of lubricating grease subjected to mechanical degradation under shear. Tribol. Int. 103, 465–474. https://doi.org/10.1016/J.TRIBOINT.2016.07.012.
[270] Cyriac, F., Lugt, P.M., Bosman, R., Venner, C.H., 2016. Impact of water on EHL film thickness of lubricating greases in rolling point contacts. Tribol. Lett. 61. https://doi.org/10.1007/S11249-016-0642-6.
[271] Canter, N., 2019. Zddp's Uncertain Future. STLE. https://www.stle.org/files/TLTArchives/2019/09_September/Tech_Beat.aspx. (Accessed 16 August 2025).
[272] Zheng, M., Ren, G., Wang, S., Li, Y., Xing, M., 2024. Investigating the effect of overbased sulfonates on calcium sulfonate complex grease: enhancements in physicochemical, rheological, and tribological properties. RSC Adv. 14, 32992–33006. https://doi.org/10.1039/D4RA04307C.
[273] Ademi, K., Wijanarko, W., Espallargas, N., 2025. Toward cost-effective environmentally acceptable lubricants: influence of synthetic ester and low-viscosity polyalphaolefin blend type on additive performance. Tribol. Lett. 73, 1–18. https://doi.org/10.1007/S11249-025-01991-4/FIGURES/9.
[274] Wang, W., Qu, J., 2025. Current and candidate additives for environmentally acceptable lubricants—A review. Friction 13. https://doi.org/10.26599/FRICT.2025.9440988.
[275] Morina, A., Neville, A., Priest, M., Green, J.H., 2006. ZDDP and MoDTC interactions and their effect on tribological performance - tribofilm characteristics and its evolution. Tribol. Lett. 24, 243–256. https://doi.org/10.1007/S11249-006-9123-7.
[276] Neville, A., Morina, A., Haque, T., Voong, M., 2007. Compatibility between tribological surfaces and lubricant additives—How friction and wear reduction can be controlled by surface/lube synergies. Tribol. Int. 40, 1680–1695. https://doi.org/10.1016/J.TRIBOINT.2007.01.019.
[277] Marian, M., Zambrano, D.F., Rothammer, B., Waltenberger, V., Boidi, G., Krapf, A., Merle, B., Stampfl, J., Rosenkranz, A., Gachot, C., Grützmacher, P.G., 2023. Combining multi-scale surface texturing and DLC coatings for improved tribological performance of 3D printed polymers. Surf. Coat. Technol. 466, 129682. https://doi.org/10.1016/J.SURFCOAT.2023.129682.
[278] Ge, D., Deng, J., Duan, R., Li, X., Liu, Y., Yue, H., 2019. Effect of surface wettability on tribological properties of Al2O3/TiC ceramic under wet lubrication. Ceram. Int. 45, 24554–24563. https://doi.org/10.1016/J.CERAMINT.2019.08.184.
[279] Qi, C., Weinell, C.E., Dam-Johansen, K., Wu, H., 2023. Assessment of anticorrosion performance of zinc-rich epoxy coatings added with zinc fibers for corrosion protection of steel. ACS Omega 8, 1912–1922. https://doi.org/10.1021/ACSOMEGA.2C03738.
[280] Qi, C., Dam-Johansen, K., Weinell, C.E., Bi, H., Wu, H., 2022. Enhanced anticorrosion performance of zinc rich epoxy coatings modified with stainless steel flakes. Prog. Org. Coating 163, 106616. https://doi.org/10.1016/J.PORGCOAT.2021.106616.
[281] Han, Y., Cao, Y., Lei, H., Han, Y., Cao, Y., Lei, H., 2022. Dynamic covalent hydrogels: strong yet dynamic. Gels 8, 577. https://doi.org/10.3390/GELS8090577, 8 (2022) 577.
[282] Son, D.H., Kim, G.Y., Jeong, J.E., Lee, S.H., Il Park, Y., Kong, H., Cheong, I.W., Kim, J.C., 2021. Influence of material properties on the damage-reporting and self-healing performance of a mechanically active dynamic network polymer in coating applications. Molecules 26, 2468. https://doi.org/10.3390/MOLECULES26092468, 26 (2021) 2468.
[283] Lavielle, N., Asker, D., Hatton, B.D., 2021. Lubrication dynamics of swollen silicones to limit long term fouling and microbial biofilms. Soft Matter 17, 936–946. https://doi.org/10.1039/D0SM01039A.
[284] Wen, T., Guo, F., Huang, Y., Zhu, S., Jia, X., 2020. Analysis of static sealing rules of foamed silicone rubber based on a porous media model. Cell. Polym. 39, 101–116. https://doi.org/10.1177/0262489319890076.
[285] Kumar, R., Rezapourian, M., Rahmani, R., Maurya, H.S., Kamboj, N., Hussainova, I., 2024. Bioinspired and multifunctional tribological materials for sliding, erosive, machining, and energy-absorbing conditions: a review. Biomimetics 9, 209. https://doi.org/10.3390/BIOMIMETICS9040209, 9 (2024) 209.
[286] Epstein, A.K., Wong, T.S., Belisle, R.A., Boggs, E.M., Aizenberg, J., 2012. Liquid-infused structured surfaces with exceptional anti-biofouling performance. Proc. Natl. Acad. Sci. U. S. A 109, 13182–13187. https://doi.org/10.1073/pnas.1201973109.

[287] Chandrasekaran, S., Jain, A.K., 2017. Ocean Structures: Construction, Materials, and Operations. CRC Press. https://doi.org/10.1201/9781315366692.

[288] Fu, Y., Guo, N., Zhou, C., Wang, G., Feng, J., 2021. Investigation on in-situ laser cladding coating of the 304 stainless steel in water environment. J. Mater. Process. Technol. 289, 116949. https://doi.org/10.1016/J.JMATPROTEC.2020.116949.

[289] Kumar, R., Antonov, M., Varga, M., Hussainova, I., Rodriguez Ripoll, M., 2023. Synergistic effect of Ag and MoS2 on high-temperature tribology of self-lubricating NiCrBSi composite coatings by laser metal deposition. Wear 532–533, 205114. https://doi.org/10.1016/J.WEAR.2023.205114.

[290] Chen, H., Du, Y., Liang, Q., Ma, W., Tu, J., 2025. Effect of double aging treatment on the tribological properties of 15-5PH coating on 17-4PH stainless steel by laser cladding. J. Mater. Res. Technol. 35, 4378–4389. https://doi.org/10.1016/J.JMRT.2025.02.104.

[291] Sarkar, S., Mukherjee, S., Kumar, C.S., Kumar Nath, A., 2020. Effects of heat treatment on microstructure, mechanical and corrosion properties of 15-5 PH stainless steel parts built by selective laser melting process. J. Manuf. Process. 50, 279–294. https://doi.org/10.1016/J.JMAPRO.2019.12.048.

[292] Tavares, S.S.M., Corte, J.S., Pardal, J.M., 2016. Failure of 17-4 PH Stainless Steel Components in Offshore Platforms, Handbook of Materials Failure Analysis with Case Studies from the Oil and Gas Industry, pp. 353–370. https://doi.org/10.1016/B978-0-08-100117-2.00019-4.

[293] Sun, G., Wang, Z., Lu, Y., Chen, M., Yang, K., Ni, Z., 2022. Underwater laser welding/cladding for high-performance repair of marine metal materials: a review. Chin. J. Mech. Eng. 35, 1–19. https://doi.org/10.1186/s10033-021-00674-0.

[294] Kumar, R., Antonov, M., Beste, U., Goljandin, D., 2020. Assessment of 3D printed steels and composites intended for wear applications in abrasive, dry or slurry erosive conditions. Int. J. Refract. Metals Hard Mater. 86, 105126. https://doi.org/10.1016/J.IJRMHM.2019.105126.

[295] Romero, R., Teran, L.A., Coronado, J.J., Ladino, J.A., Rodríguez, S.A., 2019. Synergy between cavitation and solid particle erosion in an ultrasonic tribometer. Wear 428–429, 395–403. https://doi.org/10.1016/J.WEAR.2019.04.007.

[296] Kumar, R., Antonov, M., Holovenko, Y., Surzenkov, A., 2020. Erosive wear resistance of nature-inspired flexible materials. Tribol. Lett. 68, 1–8. https://doi.org/10.1007/S11249-020-01296-8.

[297] Zhu, X., Zhong, C., Zhe, J., 2017. Lubricating oil conditioning sensors for online machine health monitoring – a review. Tribol. Int. 109, 473–484. https://doi.org/10.1016/J.TRIBOINT.2017.01.015.

[298] Zhu, J., He, D., Bechhoefer, E., 2013. Survey of lubrication oil condition monitoring, diagnostics, and prognostics techniques and systems. J. Chem. Sci. Technol. 2, 100–115.

[299] Liu, L., Shao, W., Yan, Y., Liu, D., Zhang, J., 2025. Intelligent self-adaption of marine engine degradation based on a digital-twin model. Energy Convers. Manag. 341, 119995. https://doi.org/10.1016/J.ENCONMAN.2025.119995.

[300] Chen, S., Cheng, G., Guo, F., Jia, X., Wen, X., 2025. Integrating friction noise for in situ monitoring of polymer wear performance: a machine learning approach in tribology. J. Tribol. 147. https://doi.org/10.1115/1.4066947.